A THESIS

FOR THE DEGREE OF DOCTOR OF PHILOSOPHY

Improvement of glucose homeostasis by Ishophloroglucin A and Diphlorethohydroxycarmalol from *Ishige okamurae* in diabetic zebrafish model

HYE-WON YANG

Department of Marine Life Sciences

GRADUATE SCHOOL

JEJU NATIONAL UNIVERSITY

February, 2020

Improvement of glucose homeostasis by Ishophloroglucin A and Diphlorethohydroxycarmalol from *Ishige okamurae* in diabetic zebrafish model

Hye-Won Yang

(Supervised by Professor You-Jin Jeon)

A thesis submitted in partial fulfillment of the requirement

for the degree of DOCTOR OF PHILOSOPHY

2020. 02.

This thesis has been examined and approved by

Thesis director, Gi-Young Kim, Professor of Marine Life Science

Choon Bok Song, Professor of Marine Life Science

BoMi Ryu, Research Professor of Marine Life Science

Jae-Young Oh, Research Professor of Marine Life Science

You-Jin Jeon, Professor of Marine Life Science

2020.02

Date

Department of Marine Life Science

GRADUATE SCHOOL

JEJU NATIONAL UNIVERSITY

CONTENTS

국문초록

항상성은 외부 조건의 변화에 대하여 인체 내부 기작이 작동하여 물질대사가 진행될 수 있도록 정해진 환경을 유지하는 것으로, 이러한 기작들은 세포, 조직, 기관, 유기체 전체 수준에서 일어난다. 우리 몸은 음식물을 섭취해서 영양소를 공급받고 이를 체내에서 소화, 흡수 과정을 거쳐 온몸의 세포에 전달하여 에너지원으로 포도당이 사용된다. 사람의 혈액에는 일정한 양의 포도당이 존재하며, 체내에서 포도당이 정상적으로 이용되지 않을 경우 항상성이 깨지고 결과적으로 체내 혈당이 정상보다 높은 상태로 지속되며 이를 당뇨병이라고 한다. 포도당 항상성은 혈당을 유지시키기 위해 인슐린과 글루카곤의 균형을 통해 유지된다. 이는 주로 뇌, 췌장, 간, 또한 근육 조직으로부터 방출되는 다양한 호르몬과 신경 펩티드의 네트워크에 의해 수행된다. 특히, 본 연구에서는 포도당 항상성을 위해 포도당이 근육으로 어떻게 흡수되고 어떻게 조절되는지에 대하여 알아보고자 한다. 이전 연구에서 세포내 칼슘 레벨이 증가하면 membrane으로 이동하는 당 수송체 중 하나인 Glucose transporter 4 (Glut4)가 memebrane으로 이동하게 되고 이를 포도당이 근육으로 흡수된다고 보고되었다. 또한, 건강한 근육에서는 외부 자극이 주어졌을 때 세포내 칼슘 레벨이 증가하는 반면, 당뇨병에서의 근육에서는 외부 자극이 주어졌을 때 세포내 칼슘 레벨이 증가하나 그 양이 건강한 근육에 비해 적다는 것이 보고되었다. 이는, 실제로 근육 세포내 칼슘이 혈당조절에 관여함을 보여준다.

해조류 중 패는 이전연구에서 당뇨모델인 *db/db* 마우스 및 hyperglycemic zebrafish 모델에서 혈당 조절을 통해 항당뇨 효능이 입증되었다. 더불어, 패에서 분리된 물질인 Ishophloroglucin A (IPA) 와 Diphlorethohydroxycarmalol (DPHC) 는 혈당조절을 위한 기능성소재로서 잠재적 가치가 있다고 보고되었다. 그러나, 패 추출물 및 유래 물질인 IPA 와 DPHC가 근육에서의 포도당 항상성 유지 및 에너지 대사에 대한 연구는 아직 보고되지 않았다. 따라서, 본 연구에서는 혈당조절을 위해 근육세포 및 zebrafish 모델에서 패 추출물, IPA, 그리고 DPHC 처리에 따른 세포내 칼슘 변화, 포도당 항상성, 및 에너지 대사에 대한 작용을 확인하고자 하였다.

먼저, 근육세포에서 인슐린없이 패 추출물 처리에 의해 glucose uptake가 증가하는 것을 통해 hyperglycemic zebrafish 모델에서 평가한 결과, 혈당조절능이 있음을 확인하였다. 패 추출물에 의해 혈당 조절이 됨에 따라, 패 추출물이 어떻게 근육 내로 포도당 흡수를 자극 시킬 수 있는지에 대하여 살펴보았다. 이전 연구에서는 외부의 자극에 의하여 세포내 칼슘이 증가하고 이를 통해 Glut4가 translocation이 되면서 포도당이 근육으로 흡수된다고 보고되었다. 이를 통해 패 추출물을 근육 세포에 처리하였을 때 세포내 칼슘 레벨 변화에 대하여 확인하였다.

근육 세포내 칼슘은 패 추출물 처리에 의해 현저하게 증가하지만 칼슘 chelator인 BAPTA-AM을 처리하였을 때는 세포내 칼슘 변화가 없음을 확인하였다. 이러한 세포내 칼슘 변화가 어떤 기전을 통해 자극이 되는지 살펴보았다. 이전 연구에

따르면, 세포내 칼슘 증가 경로는 칼슘 channel을 통한 칼슘 influx와 근소포체 안에 있는 칼슘이 세포질 내로 방출되는 경로가 있다고 보고되었다. 패 추출물 처리에 따른 세포내 칼슘 증가가 어떤 경로와 관련 있는지 확인하고자 세포 외 칼슘의 유무에 따른 세포내 칼슘 레벨을 측정하였다. 그 결과 세포 외 칼슘의 유무에 관계없이 패 추출물 처리에 따른 세포내 칼슘 레벨 변화가 없음을 확인함으로써 패 추출물에 의한 세포내 칼슘 레벨 변화는 근소포체에서 세포 내로 칼슘 방출과 관련이 있음을 시사할 수 있다. 더불어, 패 유래 물질인 IPA와 DPHC 처리에 따른 세포내 칼슘 레벨 변화를 확인한 결과 근소포체에서 세포 내로 칼슘 방출함으로써 세포내 칼슘을 증가시키는 것을 확인하였다.

그리고 IPA 와 DPHC가 glucose uptake를 증가시켜 hyperglycemic zebrafish 모델에서 혈당 조절이 되는 것을 확인하였다. 이를 통해 zebrafish 모델에서 세포내 칼슘 변화에도 영향을 주는지 확인하였고 그 결과, IPA와 DPHC를 처리한 zebrafish 에서 세포내 칼슘 레벨이 증가하였으나, BAPTA-AM을 처리한 군에서는 변화가 없음을 확인하였다. 이는 패 유래 물질인 IPA와 DPHC가 zebrafish에서 세포내 칼슘 레벨을 증가시키며, zebrafish가 세포 내 칼슘 레벨 변화를 확인하는데 있어 동물모델로서의 적용가능함을 시사할 수 있다.

더 나아가, IPA와 DPHC가 세포내 칼슘을 증가시킴으로써 혈당조절에 도움을 줄 수 있는지 확인하기 위해 hyperglycemic zebrafish 모델 에서 IPA와 DPHC 그리고 BAPTA-AM을 주입시킨 뒤, 혈당을 측정하였다. 그 결과, IPA와 DPHC만을 주입한 군에서는 혈당조절이 가능하나, BAPTA-AM과 IPA 또는 DPHC를 주입한 군에서는 혈

당조절이 되지 않았다. 이를 통해 세포 내 칼슘 증가에 따라 혈당조절이 가능하다는 것을 시사할 수 있다. 세포내 칼슘 레벨 변화에 따라 혈당 조절하는데 있어 작용하는 관련 단백질 인자의 변화를 확인하였다. 관련 단백질인 AMPK와 Glut4가 zebrafish 근육 조직에서 IPA와 DPHC에 의해 증가하는 것을 확인하였다. 이를 통해 IPA 와 DPHC는 근소포체에 있는 칼슘을 세포 내로 방출시켜 세포내 칼슘 레벨을 증가시키고 이후, AMPK와 Glut4를 자극하게 되어 세포 외의 포도당을 세포 내로 흡수시키는 것을 확인하였다. 결과적으로 IPA와 DPHC에 의해 혈당조절이 가능함을 확인하였다.

더 나아가 포도당 항상성에 문제가 생겼을 때, glucose intolerance 에서도 어떠한 영향을 주는지 확인하기 위해 4% high cholesterol diet (HCD)를 한 zebrafish 모델을 사용하였다. 우선, HCD의 식이 기간에 따른 혈당 변화 및 Glut4 발현을 통해 당뇨 연구를 위한 모델로서의 적용 가능성을 확인하였다. 5주동안 HCD를 식이하고, 매주마다 IPGTT를 통해 혈당 변화를 관찰하였다. 그 결과, 식이 기간이 증가함에 따라 non cholesterol diet (NCD)군에 비해 혈당 조절이 되지 않으며, 특히, 공복 및 식후 혈당이 증가하는 것을 확인하였다. 또한, Glut4 발현을 통해 당수송체에도 기능장애가 발생하는 것을 확인하였다. 따라서, 당뇨연구를 위한 모델로서 HCD zebrafish 모델의 적용 가능성을 시사할 수 있다.

패 추출물, IPA, 그리고 DPHC가 포도당 항상성을 조절할 수 있는지 확인하기 위해 3주동안 HCD를 식이하고 2주동안 HCD에 각각의 시료를 혼합하여 식이하였다. 5주 이후, IPGTT를 통해 혈당 변화를 관찰하였으며, 근육 조직에서 당수송체인

Glut4 발현 변화를 관찰하였다. 그 결과, HCD만을 식이한 군에서는 혈당 조절이 되지 않으며, 공복, 식후 혈당 및 Glut4의 발현이 NCD 군에 비해 감소하는 것을 확인하였다. 감소한 공복, 식후 혈당 및 Glut4의 발현이 패 추출물, IPA, 그리고 DPHC를 식이한 군에서 개선되는 것을 확인하였다. 이를 통해, 패 추출물 그리고 유래 물질인 IPA와 DPHC가 HCD에 의해 손상된 glucose tolerance 를 개선시키는 것을 확인하였다. 이를 통해 패 추출물과 유래 물질인 IPA와 DPHC의 식이가 포도당 항상성을 유지시키는데 도움을 준다는 것을 시사할 수 있다.

이전 연구에 따르면, 근육 세포내 칼슘 레벨이 증가하였을 때, 근수축이 발생하게 된다. 이를 통해, IPA와 DPHC에 의해 증가된 근육 세포내 칼슘 레벨이 결과적으로 근수축에 영향을 주는지 대해 확인하고자 하였다. Troponin C는 칼슘이 결합하는 부위이며, Troponin I 는 근육이 이완되었을 때 교차 다리를 억제하는 부위이다. 우선, HCD의 식이 기간에 따른 근수축 기능을 면역형광 및 조직학적 변화를 통해 확인한 결과, 식이 기간에 따라서 Troponin C의 발현은 감소하고 Troponin I의 발현은 증가하였다. 이를 통해, HCD 식이에 따라 근수축 기능 장애를 유도 시킬 수 있음을 확인하였다.

HCD 식이에 의해 유도된 근수축 기능 장애를 IPA와 DPHC가 개선시킬 수 있는지에 대한 효능평가를 면역형광 및 조직학적 변화를 통해 확인하였다. IPA와 DPHC를 식이한 군에서 HCD 군보다 Troponin C 의 발현은 증가하고 Troponin I의 발현은 감소하는 것을 확인하였다. 게다가, Metformin을 식이한 군보다 IPA와 DPHC 식이를 한 군에서 근수축 기능 장애가 개선되는 것을 확인하였다.

또한, 근수축 관련 인자인 CaMKII의 발현을 확인하였으며 그 결과 IPA와 DPHC를 식이한 군에서 발현이 증가하였다. 이를 통해 HCD 식이에 의한 근수축 기능 장애를 IPA와 DPHC 식이에 의해 개선되는 것을 확인하였다.

더 나아가, IPA와 DPHC가 근육 세포내 칼슘 증가로 인해 발생된 근수축을 통해 세포내로 흡수된 포도당이 어떻게 에너지를 발생하게 되는지 확인하였다. Zebrafish 근육 조직에서 세포내로 흡수된 포도당은 해당과정을 통해 ATP를 발생하는 것을 확인하였다. 이렇게 발생된 ATP는 다시 근수축을 유도하게 된다. IPA와 DPHC의 처리에 따른 에너지 소비를 확인한 결과 처리 1시간 뒤에 급격하게 증가하는 것을 확인하였다.

이 모든 결과를 종합해 볼 때, 패 추출물 및 유래 물질인 IPA 와 DPHC가 근육 세포내 칼슘 레벨을 증가시켜 세포외 포도당이 세포내로 흡수되어 결과적으로 혈당 조절을 하는 것을 확인하였다. 포도당 항상성 연구를 위해 HCD zebrafish 모델을 구축하였으며, 이 모델을 이용하여 패 추출물, IPA, 그리고 DPHC의 glucose intolerance를 개선시키는 것을 확인하였다. 더 나아가, IPA와 DPHC에 의한 근수축을 통해 발생되는 변화 및 포도당을 이용하여 발생되는 에너지 대사를 조절하는 것을 확인하였다. 이를 통해, 패 추출물, IPA, 그리고 DPHC는 항당뇨 소재로서 잠재적인 기능성 식품 및 천연의학 소재로서 충분한 가능성이 있으며, HCD zebrafish 모델이 당뇨를 비롯하여 다양한 대사성질환 연구에 있어 널리 이용 되어질 것이라 사료되어진다.

LIST OF FIGURES

of IO extract or BAPTA-AM was also monitored. $^{***}p<0.001$ compared with the PSS group.

Fig. 1-4. Detection of cytosolic Ca^{2+} levels by IO extract using the Fluo-4 Ca^{2+} indicator in the skeletal myotubes. Myotubes were loaded with Fluo4 in PSS (A) in the presence or absence of Ca^{2+} and treated with control (PSS only), 100 μg/ml of IO extract or BAPTA-AM. (B) Box plots representation of the cytosolic Ca^{2+} levels in myotubes responses after 100 μg/ml of IO extract or BAPTA-AM treatment as presented in (A). No significance; N.S compared with the IO extract in the presence or absence of extracellular Ca^{2+}.

Fig. 1-5. Determination of cell viability by the MTT assay and glucose uptake by 2-NBDG in the skeletal myotubes. The skeletal muscle cells were incubated with the indicated concentrations of (A) IPA and (C) DPHC for 24. Differentiated skeletal muscle cells were starved in low glucose media and incubated for 24 h with (B) IPA (0.75, 2.5, and 7.5 μM), (D) DPHC (3, 10, and 30 μM) and 2-NBDG (50 μM). Data are expressed as the mean ± SE (n = 3 for each group). * Values having different superscript are significantly different at $^{*}p<0.05$ and $^{***}p<0.001$ compared with the non-treated group. No significance; N.S.

Fig. 1-6. Detection of cytosolic Ca^{2+} levels by IPA and DPHC in the absence of extracellular Ca^{2+} using the Fluo-4 Ca^{2+} indicator in the myotubes. (A) Traces and (B) box plot representation of Ca^{2+} levels in response to addition of IPA (0.75, 2.5, and 7.5 μM) or BAPTA-AM in myotubes. (D) Traces and (E) box plot representation of Ca^{2+} levels in response to addition of DPHC (3, 10, and 30 μM) or BAPTA-AM in myotubes. The fluorescence levels

of single myotubes after addition of (C) IPA or (F) DPHC or BAPTA-AM was also monitored. $^{***}p<0.001$ compared with the PSS group.

Fig. 1-7. Detection of cytosolic Ca^{2+} levels by IPA and DPHC using the Fluo-4 Ca^{2+} indicator in the skeletal myotubes. Myotubes were loaded with Fluo4 in PSS in the presence or absence of Ca^{2+} and treated with control (PSS only), (A) 7.5 μM of IPA or (C) 30 μM of DPHC or BAPTA-AM. (B) and (D) Box plots representation of the cytosolic Ca^{2+} levels in myotubes responses after 7.5 μM of IPA or 30 μM of DPHC or BAPTA-AM treatment as presented in (A) and (C). No significance; N.S compared with the IPA or DPHC in the presence or absence of extracellular Ca^{2+}.

Fig. 1-8. Toxicity of IPA and DPHC by assessment of survival rate in zebrafish. The zebrafish were treated with various of concentrations of IPA and DPHC. (A) Survival curves of zebrafish embryos after exposure to (A) IPA (0.3, 1.5, 3, and 5 μM) and (B) DPHC (1.2, 6, 12, and 20 μM) (n = 15 for each group). Data are expressed as the mean ± SE (n = 4 for each group). * Values having different superscript are significantly different at $^{*}p<0.05$ compared with the no sample-treated group.

Fig. 1-9. Regulation of blood glucose level by IPA and DPHC in hyperglycemic zebrafish model. The zebrafish exposed to 0.6% glucose and then injected with (A) IPA (0.03, 0.1, and 0.3 μg/g body weight), or DPHC (0.03, 0.1, and 0.3 μg/g), or Metformin (5 μg/g) for 90 min. Data are expressed as the mean ± SE, n = 4 per group. * and $^{\#}$ Values having different superscript

are significantly different at $^{###}p<0.001$ compared with the non-treated group; $^{**}p<0.01$ and $^{***}p<0.001$ compared with the no sample-treated group.

Fig. 1-10. Detection of cytosolic Ca^{2+} images by IPA and DPHC using the Fluo-4 in zebrafish larvae. Zebrafish larvae were stimulated with only (A) IPA (0.3, 1.5, and 3 μM) and (C) DPHC (1.2, 6, and 12 μM), compared with Fluo-4 exposed group (F). Zebrafish larvae were stimulated with (B) IPA or (D) DPHC in Fluo-4 and compared with/without Fluo-4 groups. Changes in cytosolic Ca^{2+} levels were measured by changes in fluorescence intensity of Fluo-4 using Image J. Experiments were performed in triplicate and the data are expressed as the mean ± SE, n = 4 per group. * and $^{\#}$ Values having different superscript are significantly different at $^{##}p<0.01$ compared with the non-treated group; $^{**}p<0.01$ compared with the no sample-treated group.

Fig. 1-11. Regulation of blood glucose level by IPA and DPHC in hyperglycemic zebrafish model. Zebrafish were injected with BAPTA-AM (3 μg/g body weight) for 1 h, after which the zebrafish were injected with (A) IPA (0.3 μg/g body weight) or (B) DPHC (0.3 μg/g body weight) for 90 min. Experiments were performed in triplicate and the data are expressed as mean ± SE, n = 4 per group. * and $^{\#}$ Values having different superscript are significantly different at $^{###}p<0.001$ compared with non-treated group; $^{**}p<0.05$, and $^{***}p<0.001$ compared with the no sample-treated group. No significance; N.S compared with BAPTA-AM treated group.

Fig. 1-12. Effect of IPA on Glut4 expression increase of skeletal muscle in hyperglycemic zebrafish model. Representative Glut4 immunofluorescence images by (A) IPA and (C) DPHC in skeletal muscle of hyperglycemic zebrafish model. Quantitative graph was show level of Glut4 expression by (B) IPA and (D) DPHC from representative images and Image J software was used for measurement. Scale bar = 100 μm, Data are expressed as mean ± SE. * and $^{\#}$ Values having different superscript are significantly different at $^{\#\#}p$ <0.01 compared with non-treated group; $^{*}p$<0.05, compared with the no sample-treated group. No significance; N.S compared with BAPTA-AM treated group.

Fig. 1-13. Improvement of glucose transport pathway by IPA and DPHC in zebrafish muscle tissues. The zebrafish exposed to 0.6% glucose and then injected with IPA (0.3 μg/g) or DPHC (0.3 μg/g) or Metformin (5 μg/g) for 90 min. Zebrafish were pre-injected with BAPTA-AM (3 μg/g) for 1 h. Tissues were analyzed (A) AMPK, and (B) Glut4 by western blotting and signal intensity were evaluated by the Fusion FX7 acquisition system (Vibert Lourmat, Eberhardzell, Germany). Data expressed as the mean ± SE, n = 4 per group. $^{\#\#}p$ <0.01 and $^{\#\#\#}p$ <0.001; compared to non-treated group, $^{*}p$<0.05, $^{**}p$ <0.01, and $^{***}p$ <0.001; compared to control.

Fig. 2-1. Change of blood glucose level in HCD zebrafish for 5 weeks. Zebrafish receiving HCD for 5 weeks and induced impaired glucose tolerance. (A) intraperitoneal glucose tolerance tests (IPGTT) were performed and calculated (B) area under the curve (AUC) from the GTT in all zebrafish groups at each time point. Data are expressed as the mean ± SE (n = 4 for each group). * Values having different superscript are significantly different at $^{**}p$<0.01 and

$^{***}p<0.001$ compared with the NCD group.

Fig. 2-2. Fasting and postprandial glucose levels in HCD zebrafish for 5 weeks. Zebrafish receiving HCD for 5 weeks measured (A) fasting and (B) postprandial glucose levels at each point time point. Data are expressed as the mean ± SE (n = 4 for each group). * Values having different superscript are significantly different at $^{**}p<0.01$ and $^{***}p<0.001$ compared with the NCD group.

Fig. 2-3. Evaluation of Glut4 expression level in skeletal muscle of HCD zebrafish at each time point. (A) Representative Glut4 immunofluorescence images of skeletal muscle in HCD zebrafish at each point time. (B) Quantitative graph was show level of Glut4 expression by HCD from representative images and Image J software was used for measurement. Scale bar = 100 μm, Data are expressed as mean ± SE. * Values having different superscript are significantly different at $^{*}p<0.05$, $^{**}p<0.01$, and $^{***}p<0.001$ compared with the NCD group.

Fig. 2-4. Effect of IO extract supplementation on glucose intolerance in HCD zebrafish. Zebrafish were fed HCD supplemented IO extract (1, 3, and 5%, HCD/IO) and Metformin (1%, HCD/Met) for 2 weeks followed by additional 3 weeks of HCD. After 5 weeks, zebrafish were intraperitoneally injected with glucose (0.3 mg/g body weight). (A) intraperitoneal glucose tolerance tests (IPGTT) were performed and calculated (B) area under the curve (AUC) from the GTT in all zebrafish group at each time point. Data are expressed as the mean ± SE (n = 4 for each group). * and $^{\#}$ Values having different superscript are significantly different at

$^{###}p<0.001$ compared with the NCD group; $^{**}p<0.01$ and *** $p<0.001$ compared with the HCD/Saline group.

Fig. 2-5. Effect of IO extract supplementation on fasting and postprandial glucose levels in HCD zebrafish. After 5 weeks, zebrafish were intraperitoneally injected with glucose (0.3 mg/g body weight), and then measured (A) fasting and (B) postprandial glucose levels in all zebrafish group. Data are expressed as the mean ± SE (n = 4 for each group). * and $^{\#}$ Values having different superscript are significantly different at $^{###}p<0.001$ compared with the NCD group; $^{**}p<0.01$ and *** $p<0.001$ compared with the HCD/Saline group.

Fig. 2-6. Evaluation of Glut4 expression level by IO extract supplementation in skeletal muscle of HCD zebrafish. (A) Representative Glut4 immunofluorescence images of skeletal muscle in all zebrafish groups after 5 weeks. (B) Quantitative graph was show level of Glut4 expression by IO extract from representative images and Image J software was used for measurement. Scale bar = 100 μm, Data are expressed as mean ± SE. * and $^{\#}$ Values having different superscript are significantly different at $^{###}p<0.001$ compared with the NCD group; $^{*}p<0.05$ and *** $p<0.001$ compared with the HCD/Saline group.

Fig. 2-7. Effect of IPA supplementation on glucose intolerance in HCD zebrafish. Zebrafish were fed HCD supplemented IPA (0.0003, 0.001, and 0.003%, HCD/IPA) and Metformin (1%, HCD/Met) for 2 weeks followed by additional 3 weeks of HCD. After 5 weeks, zebrafish were intraperitoneally injected with glucose (0.3 mg/g body weight). (A) intraperitoneal glucose

tolerance tests (IPGTT) were performed and calculated (B) area under the curve (AUC) from the GTT in all zebrafish group at each time point. (C) fasting and (D) postprandial glucose levels were in all zebrafish group. Data are expressed as the mean ± SE (n = 4 for each group). * and $^{\#}$ Values having different superscript are significantly different at $^{\#\#\#}p<0.001$ compared with the NCD group; $^{**}p<0.01$ and $^{***}p<0.001$ compared with the HCD/Saline group.

Fig. 2-8. Effect of DPHC supplementation on glucose intolerance in HCD zebrafish. Zebrafish were fed HCD supplemented DPHC (0.0003, 0.001, and 0.003%, HCD/DPHC) and Metformin (1%, HCD/Met) for 2 weeks followed by additional 3 weeks of HCD. After 5 weeks, zebrafish were intraperitoneally injected with glucose (0.3 mg/g body weight). (A) intraperitoneal glucose tolerance tests (IPGTT) were performed and calculated (B) area under the curve (AUC) from the GTT in all zebrafish group at each time point. (C) fasting and (D) postprandial glucose levels were in all zebrafish group. Data are expressed as the mean ± SE (n = 4 for each group). * and $^{\#}$ Values having different superscript are significantly different at $^{\#\#\#}p<0.001$ compared with the NCD group; $^{**}p<0.01$ and $^{***}p<0.001$ compared with the HCD/Saline group.

Fig. 2-9. Evaluation of Glut4 expression level by IPA and DPHC supplementation in skeletal muscle of HCD zebrafish. Zebrafish were fed HCD supplemented IPA (0.0003, 0.001, and 0.003%, HCD/IPA), DPHC (0.0003, 0.001, and 0.003%, HCD/DPHC) and Metformin (1%, HCD/Met) for 2 weeks followed by additional 3 weeks of HCD. Representative Glut4 immunofluorescence images of (A) IPA and (C) DPHC in skeletal muscle of all zebrafish groups after 5 weeks. Quantitative graph was show level of Glut4 expression by (B) IPA and

(D) DPHC from representative images and Image J software was used for measurement. Scale bar = 100 μm, Data are expressed as mean ± SE. * and $^{\#}$ Values having different superscript are significantly different at $^{\#\#\#}p<0.001$ compared with the NCD group; $^{*}p<0.05$ and $^{***}p<0.001$ compared with the HCD group.

Fig. 3-1. Measurement of Troponin C & I intensity in skeletal muscle of HCD zebrafish. Zebrafish were fed HCD for 5 weeks. Representative (A) Troponin C and (C) Troponin I immunofluorescence images of skeletal muscle in HCD zebrafish at each time point. Quantitative graph was show level of (B) Troponin C and (D) Troponin I intensity from representative images and Image J software was used for measurement at each time point. Scale bar = 100 μm, Data are expressed as mean ± SE. * Values having different superscript are significantly different at $^{*}p<0.05$, $^{**}p<0.01$ and $^{***}p<0.001$ compared with NCD group.

Fig. 3-2. Effect of IPA on Troponin C and I intensity increase of skeletal muscle in HCD zebrafish. Representative (A) Troponin C and (C) Troponin I immunofluorescence images of skeletal muscle in HCD zebrafish model. Quantitative graph was show level of (B) Troponin C and (D) Troponin I intensity by IPA from representative images and Image J software was used for measurement. Scale bar = 100 μm, Data are expressed as mean ± SE. * and $^{\#}$ Values having different superscript are significantly different at $^{\#\#\#}p<0.001$ compared with NCD group; $^{*}p<0.05$, and $^{**}p<0.01$, and $^{***}p<0.001$ compared with HCD group.

Fig. 3-3. Histological changes of skeletal muscle by IPA supplementation in HCD

zebrafish. Representative histological changes of skeletal muscle by IPA supplementation in HCD zebrafish model using H&E staining. Scale bar = 100 μm.

Fig. 3-4. Effect of DPHC on Troponin C and I intensity increase of skeletal muscle in HCD zebrafish. Representative (A) Troponin C and (C) Troponin I immunofluorescence images of skeletal muscle in HCD zebrafish model. Quantitative graph was show level of (B) Troponin C and (D) Troponin I intensity by DPHC from representative images and Image J software was used for measurement. Scale bar = 100 μm, Data are expressed as mean ± SE. * and $^{\#}$ Values having different superscript are significantly different at $^{\#\#\#}p$ <0.001 compared with NCD group; $^{*}p$ <0.05, $^{**}p$ <0.01, and $^{***}p$ <0.001 compared with HCD group.

Fig. 3-5. Histological changes of skeletal muscle by DPHC supplementation in HCD zebrafish. Representative histological changes of skeletal muscle by DPHC supplementation in HCD zebrafish model using H&E staining. Scale bar = 100 μm.

Fig. 3-6. The CaMKII expression level by IPA and DPHC in hyperglycemic zebrafish muscle tissues. The zebrafish exposed to 0.6% glucose and then injected with (A) IPA (0.3 μg/g) or (B) DPHC (0.3 μg/g) or Metformin (5 μg/g) for 90 min. Zebrafish were pre-injected with BAPTA-AM (3 μg/g) for 1 h. Tissues were analyzed CaMKII by western blotting and signal intensity were evaluated by the Fusion FX7 acquisition system (Vibert Lourmat, Eberhardzell, Germany). Data expressed as the mean ± SE, n = 4 per group. $^{\#\#\#}p$<0.001; compared to non-treated group, $^{**}p$<0.01, and $^{***}p$<0.001; compared to control. N.S; No

Significant.

Fig. 3-7. The CaMKII expression level by IPA and DPHC in HCD zebrafish muscle tissues. Zebrafish were fed HCD supplemented (A) IPA (0.0003, 0.001, and 0.003%, HCD/IPA), (B) DPHC (0.0003, 0.001, and 0.003%, HCD/DPHC) and Metformin (1%, HCD/Met) for 2 weeks followed by additional 3 weeks of HCD. Tissues were analyzed CaMKII by western blotting and signal intensity were evaluated by the Fusion FX7 acquisition system (Vibert Lourmat, Eberhardzell, Germany). Data are expressed as mean ± SE. * and $^{\#}$ Values having different superscript are significantly different at $^{\#\#\#}p<0.001$ compared with the NCD group; $^{***}p<0.001$ compared with the HCD/Saline group. N.S; No Significant.

Fig. 3-8. Measurement of ATP levels in an alloxan-induced hyperglycemia zebrafish muscle tissues. Zebrafish were injected with BAPTA-AM (3 μg/g body weight) for 1 h, after which the zebrafish were injected with (A) IPA (0.3 μg/g body weight) or (B) DPHC (0.3 μg/g body weight) for 90 min. Experiments were performed in triplicate and the data are expressed as mean ± SE, n = 3 per group. * and $^{\#}$ Values having different superscript are significantly different at $*p<0.05$ compared with the no sample-treated group; $^{\#\#\#}$ $p<0.0001$ compared with the non-treated group.

Fig. 3-9. Measurement of ATP levels in HCD zebrafish muscle tissues. Zebrafish were fed 4% HCD supplemented (A) IPA (0.3 μg/g body weight) or (B) DPHC (0.3 μg/g body weight) for 2 weeks followed by additional 3 weeks of HCD. Experiments were performed in triplicate

and the data are expressed as mean ± SE, n = 3 per group. * and $^{\#}$ Values having different superscript are significantly different at $^{**}p<0.01$ and $^{***}p<0.001$ compared with HCD group; $^{\#\#\#}$ $p<0.001$ compared with NCD group.

Fig. 3-10. Detection of energy expenditure IPA and DPHC using Alamar blue. The larvae were exposed to IPA (0.3, 1.5, and 3 μM), and DPHC (1.2, 6, and 12 μM) with Alamar blue. Energy expenditure was measured from relative change in Fluorescence in response to addition of (A) IPA and (C) DPHC. Area under the curve (AUC) from the energy expenditure in all zebrafish groups at each time point. Data are expressed as the mean ± SE (n = 4 for each group). * Values having different superscript are significantly different at $^{***}p<0.001$ compared with the non-treated group.

Fig. 3-11. Mechanism of glucose homeostasis in skeletal muscle

INTRODUCTION

Diabetes mellitus is a chronic metabolic disorder caused by the inadequate balance of glucose homeostasis [1]. Glucose homeostasis is maintained by the tight regulation of blood glucose by insulin and glucagon [2].

Glucose is stored as glycogen in the skeletal muscle, a major site of glucose uptake that is critical to whole-body glucose metabolism in humans. Previous studies have shown that genetic activation of glycolytic metabolism in the skeletal muscle leads to an improvement in whole-body glucose homeostasis in mice [3]. Indeed, elevation in blood glucose levels results in increased glycolytic metabolism, which may represent an important aspect of the adaptive response in skeletal muscle [4]. Overall, glucose metabolites are major energy sources for skeletal muscle contraction [5].

Glucose uptake can also be induced through the activation of muscle contraction by signaling pathways that cross talk with the classic insulin regulatory mechanisms of glucose uptake [6]. Muscle contraction is a highly effective prophylactic against the hyperglycemia associated with the diabetes mellitus and induce glucose uptake by signaling pathways that the initiation of contraction-stimulated glucose transport and glucose transporter 4 (GLUT4) translocation [6,7]. GLUT with substrate specificities that dictate their functional roles regulate glucose level both outside and inside of the cell [8]. Also, some of the signaling mechanisms that mediate an increase in the expression of Glut4 in response to exercise have been identified to be driven by a rise in cytosolic Ca^{2+} levels due to increased release of Ca^{2+} from the sarcoplasmic reticulum (SR) [9,10]. These studies showed that an increase in glucose uptake during muscle contractions does not require membrane depolarization but only a release of Ca^{2+} to the cytoplasm [11]. Cytosolic Ca^{2+} in the skeletal muscle regulates several signaling pathways and

metabolic events related to contraction and relaxation [12].

Glucose transport activity and glucose metabolism was stimulated to muscle contraction and Glut4 overexpression [13]. In addition, AMPK as an energy sensor can increase ATP production, which is reported as a potential treatment for metabolic disease by reducing the blood glucose level and promoting fatty acid oxidation in skeletal muscle [14]. ATP which is energy source is immediately activated during muscle contraction [15]. Cells were known to cause metabolic disease such as obesity and diabetes by breaking the mechanisms involved in controlling metabolism by suppressing energy consumption when energy is lacking [3].

Energy metabolism requires the coordinated regulation of energy intake, storage, and expenditure [16]. Previous studies have shown that diabetes mellitus is commonly linked with a decreased efficient to use energy in skeletal muscle [17,18]. In skeletal muscle, increasing glucose uptake is derived from muscle contractile activity resulting in prevention diabetes [19]. During muscle contraction, energy expenditure is conducted by the molecular motors, the myosin heads or cross-bridges, and by ion pumps, mainly the SR Ca^{2+} pumps which is the major energy consumers [15,20].

Most of the current drugs for the treatment of diabetes aim to improve insulin production and metabolic regulation. Furthermore, previous studies have focused on the prevention of diabetes for both type 1 and type 2 diabetes [21,22]. In addition, the improper balance of glucose homeostasis can be prevented or reduced by functional foods. Therefore, there has recently been much interest in the use of natural products as a source of stronger and safer antidiabetic therapies [23-25].

Seaweeds contain bioactive substances, such as polysaccharides, proteins, lipids, and polyphenols, and have been reported to have nutraceutical and pharmaceutical potential in

functional foods [26,27]. *Ishige okamurae* (IO), an edible seaweed, possesses bioactive substances, such as ishophloroglucin A (IPA), diphlorethohydroxycarmalol (DPHC), and fucoxanthin, as well as other secondary metabolites [28]. In our previous studies, we demonstrated that the marine alga *Ishige okamurae* shows anti-diabetic associated responses through the modulation of blood glucose levels as well as inhibition of carbohydrate-digestive enzymes [29]. In addition, DPHC, a phlorotannin isolated from *Ishige okamurae*, was revealed to have potential anti-diabetic activity via prominent inhibitory effects against the α-glucosidase and α-amylase enzymes [30]. In additional, we identified IPA to standardize anti-diabetic activity potency of IO extract. However, regulating glucose homeostasis and the underlying mechanisms of glucose uptake in skeletal muscle cells and diabetic zebrafish model by IO extract, DPHC, and IPA treatment to control blood glucose levels have not yet been examined. Moreover, zebrafish (*Danio rerio*), as an animal model, have a number of features to study on metabolic syndrome such as cardiovascular disorders, kidney disorders, obesity and diabetes [31,32]. Previous studies were reported that alloxan, streptozotocin, and high-fat diet are used to induce diabetic zebrafish model [33,34].

Therefore, in the present study, we explored the effects of IO extract, DPHC, and IPA on cytosolic Ca^{2+} levels in the skeletal muscle and the underlying signaling mechanisms in *in vitro* and *in vivo* models. In addition, the correlation of IO extract and its components with glucose homeostasis was evaluated in a diabetic zebrafish model. Data from this study suggest a related mechanistic pathway following treatment with IO extract and its components on glucose homeostasis, and further shed light on strategies to improve glucose homeostasis to help ameliorate metabolic disorders in diabetic patients in the future.

Part I.

Regulation of blood glucose level by cytosolic Ca^{2+} level in skeletal muscle cell and hyperglycemic zebrafish model

1. ABSTRACT

In our previous study, *Ishige okamurae* (IO) extract and their component, Ishophloroglucin A (IPA) and Diphlorethohydroxycarmalol (DPHC) has been known to possess anti-diabetic activity. However, the molecular mechanisms responsible for this controlling activity and how IPA and DPHC exerts potential beneficial effects on glucose transport into the skeletal muscle cells to control glucose homeostasis remains largely unexplored. The change of cytosolic Ca^{2+} induced by IO extract and IPA and DPHC as component of IO extract for glucose utilization was studied in myotubes and in muscle of hyperglycemic zebrafish. In this paper, we examined the effect of IPA and DPHC as the component of IO on glucose homeostasis underlying glucose transport pathway. Myotubes were treated IO extract, which induced to elevate the cytosolic Ca^{2+} resulting in increasing the glucose uptake. In addition, it was observed that IPA and DPHC controlled blood glucose level upon hyperglycemic zebrafish model and improved glucose homeostasis through glucose transport pathway. Our results suggest that IO extract and its components can stimulate glucose homeostasis through the elevation of cytosolic Ca^{2+} level in myotubes. IO extract containing IPA and DPHC might be used as marine-derived nutraceuticals for the prevention of diabetes.

2. MATERIALS AND METHODS

2.1. Chemicals and reagents

Fluo-4 Direct^{tm} Calcium Assay kit was purchased from Invitrogen by Thermo Fisher Scientific (Whaltham, MA, USA). 3-(4,5-dimethylthiazol-2-yl)-2,5-diphenylte-trazolium bromide (MTT), 2-Deoxy-2-[(7-nitro-2,1,3-benzoxadiazol-4-yl)amino]-D-glucose (2-NBDG), 1,2-Bis(2-aminophenoxy)ethane-N,N,N′,N′-tetraacetic acid tetrakis(acetoxymethyl ester) (BAPTA-AM), D-(+)-Glucose (Glucose), 2,4,5,6(1H,3H)-Pyrimidinetetrone (Alloxan monohydrate), and 1,1-Dimethylbiguanide hydrochloride (Metformin) were purchased from Sigma-Aldrich (St. Louis, MO, USA). Antibodies against phospho-AMP-activated protein kinase (Thr172), AMPK and p-Akt (Ser473), Akt, Glut4, and GAPDH were obtained from Cell Signaling Technology (Bedford, MA, USA) and anti-rabbit secondary antibodies were purchased from Santa Cruz Biotechnology (Santa Cruz, CA, USA).

2.2. Preparation of IO extract, IPA, and DPHC

Ishige okamurae was collected in April 2016 in Seongsan in Jeju Island, South Korea. Preparation of IO extract and isolation of IPA were carried out according to the previously described method [14]. Briefly, 50% ethanolic extract of IO was fractionated through centrifugal partition chromatography (CPC 240, Tokyo, Japan) and further purified by semipreparative HPLC column (YMC-Pack ODS-A, 10×250 mm, 5 m) to obtain IPA. The identity of IPA (99% of purity) was verified by MS fragmentation of m/z 1986.26 at an ultrahigh resolution Q-TOF LC-MS/MS coupled with an electrospray ionization (ESI) resource

(maXis-HD, Bruker Daltonics, Breman, Germany) at Korea Basic Science Institute (KBSI) in Ochang, South Korea. According to the validated method of previous study [35], IO extract in this study have 1.8 % of IPA. In addition, Diphlorethohydroxyt carmalol (DPHC) was isolated as previously described by Heo et al [36].

2.3. C2C12 cell culture, differentiation and cell viability assay

C2C12 skeletal muscle cells (American Type Culture Collection) were maintained in DMEM with 10% FBS and antibiotics, at 37 °C in a humidified incubator of 5% CO_2. When the cells reached 80% confluence, C2C12 cells were differentiated into skeletal myotubes in DMEM-low glucose with 2% horse serum for 5 days. Viability levels of C2C12 cells were determined by the ability of mitochondria to convert MTT to insoluble formazan product. Cells were maintained in 96-well plates at a density of 3×10^4 cells/well, and subsequently subjected to different concentrations of IO extract (10, 30, 100, and 300 μg/ml), IPA (025, 0.75, 2.5, and 7.5 μM), and DPHC (0.1, 2, 10 and 30 μM) for 24 h. Cells were pretreated with MTT solution (2 mg/ml) for 3 h. Subsequently, cell density was determined by measuring optical density (OD) at 540 nm using a microplate reader (Gen5 version 2.05, BioTek, Winooski, Vermont, U.S.).

2.4. Glucose uptake assay

Differentiated cells, skeletal muscle cells were maintained in serum free and low glucose DMEM for 6 h before treatment with IO extract, IPA, and DPHC. After incubation, cells were treated with IO extract, IPA, and DPHC in glucose free media. Subsequently, 2-NBDG at 50 μM final concentration was added for 24 h at 37°C. Then, cells were washed twice with PBS,

serum-free medium was added and the fluorescence intensity immediately measured in a microplate reader at an excitation wavelength of 485 nm and an emission wavelength of 530 nm. After being taken up by the cells, 2-NBDG is converted into a non-fluorescent derivative (2-NBDG metabolite). The overall glucose uptake was obtained by quantifying the diminution in the fluorescence.

2.5. Cytosolic Ca^{2+} level by Fluo-4 in skeletal myotubes

Cytosolic Ca^{2+} level was detected using the Ca^{2+}-sensitive probe Fluo-4 in 1X PSS (Phosphate-buffered saline, comprised of 140 mM NaCl, 5.9 mM KCl, 1.8 mM $MgCl_2$, 10 mM HEPES, 11.5 mM Glucose, 1.2 mM NaH_2PO_4, 5 mM $NaHCO_3$). Skeletal muscle cells were incubated in 1X Fluo-4 for 30 minutes at 37 ˚C, washed with PBS and added 1X PSS with 0.1% BSA. After recording basal fluorescence for 10 sec at interval time of 1 sec, cells were directly added 1X PSS or IO extract (15, 45, and 100 μg/ml) or IPA (0.75, 2.5, and 7.5 μM) or DPHC (3, 10, and 30 μM) in 0.1% BSA. After recording fluorescence for 55 sec at interval time of 1 sec, reflecting cytosolic Ca^{2+} levels was obtained to the microscope (Gen 5 version 3.03, BioTek, Winooski, Vermont, U.S.).

2.6. Experimental animals

2.6.1. Maintenance of parental zebrafish and collection of embryos

Adult zebrafish was obtained from a commercial dealer (Jeju aquarium, Jeju, Korea). Fifteen fishes were kept in 3.5 L acrylic tank according to the conditions; 28.5 ± 1 ˚C, fed two times a day (Tetra GmgH D-49304 Melle Made in Germany) with a 14/10 light/dark cycle. Embryos

were mated, and spawning was stimulated by setting of light, after breeding 1 female and 2 males interbreed. Embryos were collected within 30 min and transferred to Petri dishes containing embryo media. The zebrafish experiment received approval from the Animal Care and Use Committee of the Jeju National University (Approval No. 2017-0001).

2.6.2. Toxicity of IO extract, IPA, and DPHC in zebrafish embryos

From approximately 4 hours post-fertilization (hpf), embryos (*n*=15) were transferred to individual wells of 12-well plates containing 950 µl embryo media with 50 µl of IO extract (10, 30, and 100 µg/ml), IPA (0.3, 1.5, 3, and 5 µM), and DPHC (1.2, 6, 12, and 20 µM). Percent survival of zebrafish embryos exposed to DPHC up to 168 hpf was measured.

2.6.3. Cytosolic Ca^{2+} level measurement in zebrafish larvae

The cytosolic Ca^{2+} level of zebrafish larvae was detected using the Ca^{2+}-sensitive probe Fluo-4. Zebrafish larvae were incubated in the 2X Fluo-4 for 30 minutes at 28.5 ± 1 ˚C and subsequently treated with IPA (0.3, 1.5, and 3 µM) and DPHC (1.2, 6, and 12 µM). As a control, to ensure if Ca^{2+} signal was completely blocked by chelation of cytosolic Ca^{2+} with BAPTA-AM, we pre-incubated fish with 0.1 mM BAPTA-AM for 1 h before loading the Fluo-4. The images were captured using the microscope (Gen 5 version 3.03, BioTek, Winooski, Vermont, U.S.). The intensity of the immunofluorescence staining, Image J software was used.

2.6.4. Blood glucose level

Wild-type zebrafish were exposed to 2 mg/ml alloxan for 1 h and transferred to 1% glucose for another 1 h. The media was then changed to water for 1 h, and zebrafish were injected with saline, IO extract, or IPA, or DPHC, or Metformin, with or without BAPTA-AM for 90 min. Adult zebrafish were divided into six groups: normal, alloxan-treated group, IO extract (10, 30, and 100 μg/g body weight), IPA (0.03, 0.1, and 0.3 μg/g body weight), DPHC (0.03, 0.1, and 0.3 μg/g body weight), Metformin (5 μg/g body weight), BAPTA-AM (3 μg/g body weight), and BAPTA-AM (3 μg/g body weight) with IPA or DPHC (0.3 μg/g body weight).

2.6.5. Tissue preparation

Zebrafish muscle tissue was fixed in Bouin's solution for approximately 24 h and subsequently transferred to 70% ethanol for storage. After dehydration and embedding in paraffin, the tissue block was sliced to 7 μm.

2.6.6. Immunofluorescence staining assay

Paraffin-sectioned slides were deparaffinized twice with xylene for 5 min, and hydrated in graded ethanol, and then incubated in antigen-retrieval solution for 5 min in the microscope. The slides were washed in running water for 5 min and then incubated in blocking solution for 1 h. After three washes in phosphate-buffered saline (PBS), the slides were incubated for overnight at 4 °C with primary antibody; glucose transporter type 4 (GLUT4). The primary antibody was diluted to 1:400 with blocking solution. The slides were washed with PBS, and then incubated with 488-fluorescent anti-rabbit secondary antibody for 2 h. The secondary antibody was diluted to 1:200 with blocking solution. After incubation for 2 h, the slides were

washed with PBS, and mounted by mounting medium. The images were captured using the microscope (Gen 5 version 3.03, BioTek, Winooski, Vermont, U.S.). The intensity of the immunofluorescence staining, Image J software was used.

2.6.7. Western blot analysis

Zebrafish muscle tissue were homogenized in lysis buffer using a homogenizer and then incubated for 10 min at 4 °C. The homogenates were centrifuged at 14,000 rpm for 15 min at 4 °C. The protein was quantified by using BCA^{TM} protein assay kit and equal amount of proteins (30 μg) were separated using 10% SDS-polyacrylamide gel. The separated proteins were transferred to nitrocellulose membranes (GE Healthcare Life Science) and blocked for 3 h with nonfat dry milk at room temperature. Membranes were incubated for overnight at 4 °C with primary antibodies; phosphorylated and/or total AMP-activated protein kinase (AMPK), protein kinase B (Akt), glucose transporter type 4 (GLUT4), and Glyceraldehyde 3-phosphate dehydrogenase (GAPDH). And then, membranes incubated with the secondary antibodies at 1:3000 dilutions for 2 h, protein bands were detected with chemiluminescence reagent (Maximum sensitivity substrate, Thermo Scientific). The images were captured using Fusion Solo apparatus (Vilber Lourmat) and measured using image J software.

2.7. Statistical analysis

All of data were presented as means ± standard deviation (S.D). The mean values were calculated based on data from at least three independent experiments which were conducted on separate days using freshly prepared reagents. All the experiments were statistically analyzed

using one-way analysis of variance (one-way ANOVA) and Dunnet (in GraphPad Prism Version 5.03). A p-value of less than 0.05 ($^{\#}p<0.05$, $^{\#\#}p<0.01$, and $^{\#\#\#}p<0.001$) was considered statistically significant and compared with non-treated group. A p-value of less than 0.05 ($^{*}p<0.05$, $^{**}p<0.01$, and $^{***}p<0.001$) was considered statistically significant and compared with no sample-treated group.

3. RESULTS

3.1. Measurement of cell viability and glucose uptake by IO extract in skeletal myotubes

As glucose uptake by skeletal muscles is the key step in glucose homeostasis [37], we examined the effect of IO extract on glucose uptake in differentiated myocytes. Initially, the cells were treated with IO extract (10, 30, 100, and 300 μg/ml for 24 h and cell viability was assessed using an MTT assay. As shown in Fig. 1-1A, cells treated with IO extract did not show a significant difference in cell viability compared to those of the control group. Therefore, it was confirmed that these concentrations of IO extract were non-toxic, and were used for further *in vitro* experiments.

Glucose uptake following IO extract treatment in skeletal myotubes was evaluated without insulin stimulation (Fig. 1-1B). The myotubes were treated with various concentrations (15, 45, and 100 μg/ml) of IO extract. Glucose uptake was significantly increased by IO extract treatment. These data suggested that IO extract treatment can induce glucose uptake in the absence of insulin in skeletal myotubes.

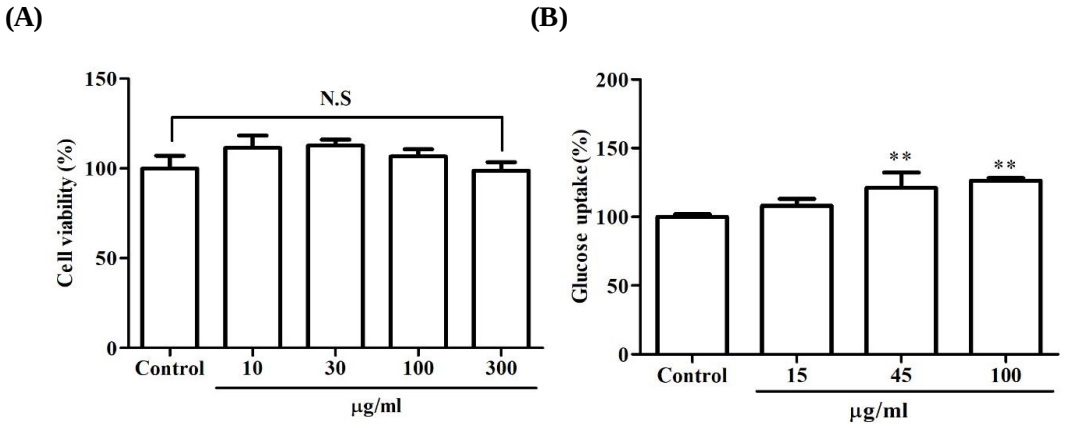

Fig. 1-1. Determination of cell viability by the MTT assay and glucose uptake by 2-NBDG in the skeletal myotubes. (A) The skeletal muscle cells were incubated with the indicated concentrations of IO extract for 24. (B) Differentiated skeletal muscle cells were starved in low glucose media and incubated for 24 h with IO extract (15, 45, and 100 μg/ml) and 2-NBDG (50 μM). Data are expressed as the mean ± SE (n = 3 for each group). * Values having different superscript are significantly different at $^{**}p<0.01$ compared with the non-treated group. No significance; N.S

3.2. Regulation of blood glucose level by IO extract in hyperglycemic zebrafish model

To assess whether blood glucose levels are influenced by IO extract, we used an alloxan-induced hyperglycemic zebrafish model [33]. This model is an acute hyperglycemic model for short-term experiments [38]. Initially, to evaluate the toxicity of IO extract zebrafish embryos were exposed to IO extract (10, 30, and 100 μg/ml) in the embryo media for 168 hpf. As shown in Fig. 1-2A, 97%, 83 %, and 77% of the zebrafish respectively survived after treatment with 10, 30, and 100 μg/ml IO extract, compared to that observed in the control group.

Zebrafish treated with 2 mg/ml alloxan showed pancreatic islet damage, leading to reduced glucose-mediated insulin secretion, resulting in a diabetic condition. Blood glucose levels of zebrafish in the 0.6% glucose group increased 2-fold compared to those in the normal group (Fig. 1-2B), which were comparable to the blood glucose levels in a hyperglycemic mouse model [39]. Zebrafish was injected with saline, or IO extract (10, 30, and 100 μg/g body weight), or Metformin (5 μg/g body weight) as positive control of blood glucose level controlling in diabetes [40], for 90 min. In Fig. 1-4A, blood glucose level of control group was significantly increased to 206% compared to normal group. In particular, IO extract- and Metformin-injected groups were observed the levels to 163%, 156%, and 155% of IO extract and 158% of Metformin compared to control group. These results suggest IO extract can be controlled blood glucose level in zebrafish model of hyperglycemia. However, the correlation between diabetes and glucose homeostasis through glucose transport pathway have not been reported. Thus, we hypothesized that glucose homeostasis can be improved by IO through Ca^{2+}-dependent signaling pathways in muscle resulting in controlling blood glucose level.

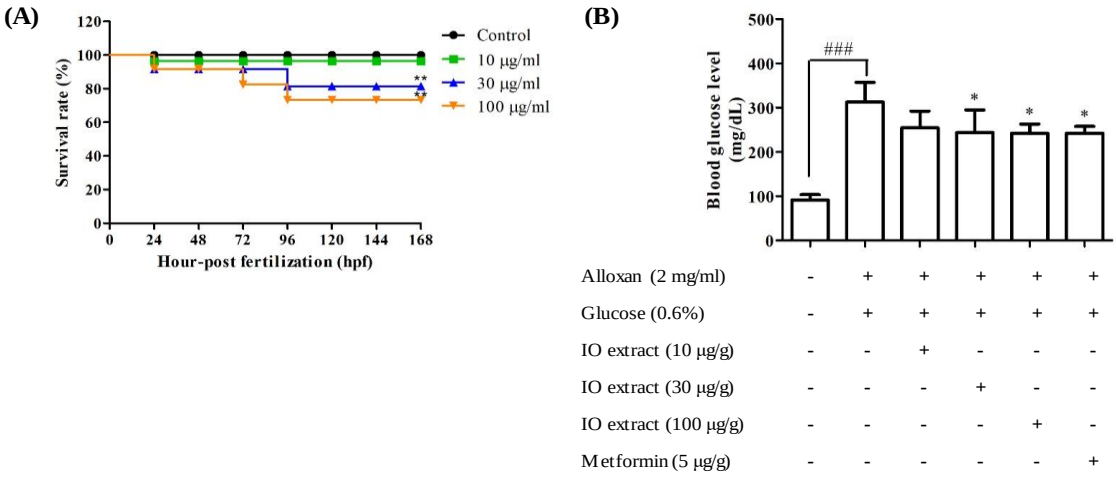

Fig. 1-2. Evaluation of toxicity of IO extract by assessment of survival rate and measurement of blood glucose level in zebrafish. The zebrafish were treated with various of concentrations of IO extract. (A) Survival curves of zebrafish embryos after exposure to IO extract (n = 15 for each group). (B) Blood glucose level of zebrafish injected with IO extract or Metformin for 90 min. Data are expressed as the mean ± SE (n = 4 for each group). * and $^{\#}$ Values having different superscript are significantly different at $^{\#\#\#}p<0.001$ compared with the non-treated group; $^{*}p<0.05$ compared with the no sample-treated group.

3.3. Increasing the cytosolic Ca^{2+} level by IO extract in skeletal myotubes

The elevating of Ca^{2+} level activates the signal transduction pathway that helps to increase the glucose uptake by skeletal muscle cells [41,42]. the cytosolic Ca^{2+} level was analyzed by detecting fluorescence changes in myotubes with different concentrations of IO extract (15, 45, 100 μg/ml). IO extract induced the instantly elevation of the cytosolic Ca^{2+} level dose-dependently (Fig. 1-3).

Cytosolic Ca^{2+} levels can be increased via either Ca^{2+} influx by plasma membrane Ca^{2+} channels or Ca^{2+} release from the SR [10]. Thus, we conducted to investigate the change of cytosolic Ca^{2+} level using Fluo-4-AM. Myotubes was exposed to IO extract (100 μg/ml) with the presence/absence of extracellular Ca^{2+}, induced that elevation of the cytosolic Ca^{2+} levels in both Fig. 1-4. Resulting the elevated cytosolic Ca^{2+} level by 100 μg/ml of IO extract treatment for 60 sec was no significantly changed either addition of external Ca^{2+} (Fig. 1-4B). Irrespective of whether there are presence or absence of extracellular Ca^{2+}, myotubes was induced to elevate the cytosolic Ca^{2+} level by IO extract. We can suggest that elevation of the cytosolic Ca^{2+} levels by IO extract is related to release from the SR and not from Ca^{2+} influx by plasma membrane Ca^{2+} channels [10,11]. These data showed that IO extract can induce Ca^{2+} release from SR in myotubes.

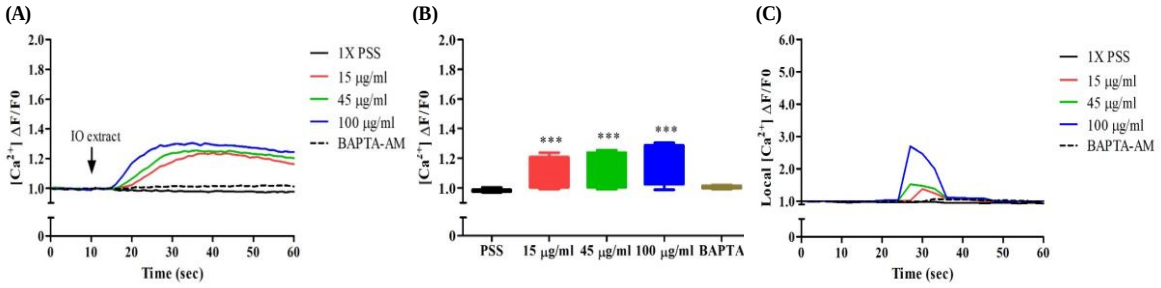

Fig. 1-3. Detection of cytosolic Ca^{2+} levels by IO extract in the absence of extracellular Ca^{2+} using the Fluo-4 Ca^{2+} indicator in the myotubes. (A) Traces and (B) box plot representation of Ca^{2+} levels in response to addition of IO extract (15, 45, and 100 μg/ml) or BAPTA-AM in total myotubes. (C) The fluorescence levels of single myotubes after addition of IO extract or BAPTA-AM was also monitored. $^{***}p<0.001$ compared with the PSS group.

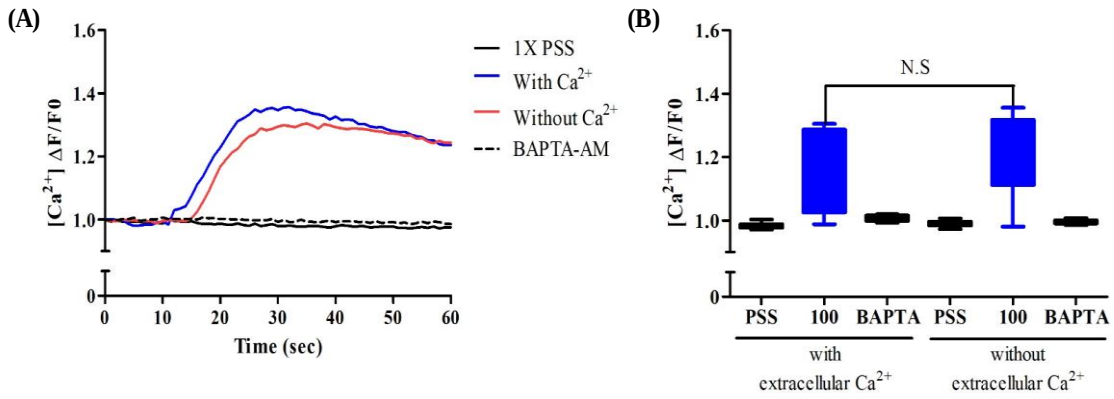

Fig. 1-4. Detection of cytosolic Ca^{2+} levels by IO extract using the Fluo-4 Ca^{2+} indicator in the skeletal myotubes. Myotubes were loaded with Fluo4 in PSS (A) in the presence or absence of Ca^{2+} and treated with control (PSS only), 100 μg/ml of IO extract or BAPTA-AM. (B) Box plots representation of the cytosolic Ca^{2+} levels in myotubes responses after 100 μg/ml of IO extract or BAPTA-AM treatment as presented in (A). No significance; N.S compared with the IO extract in the presence or absence of extracellular Ca^{2+}.

3.4. Measurement of cell viability and glucose uptake by IPA and DPHC in skeletal myotubes

We examined the effect of IPA and DPHC on glucose uptake in skeletal myotubes. Initially the cells were treated with IPA (0.25, 0.75, 2.5, and 7.5 μM) and DPHC (0.1, 2, 10, and 30 μM) for 24 h and cell viability was assessed using an MTT assay. As shown in Fig. 1-5A and C, cells treated with IPA and DPHC did not show a significant difference in cell viability compared to those of the control group. It was therefore confirmed that these concentrations of IPA and DPHC were non-toxic, and were used for further *in vitro* experiments.

Glucose uptake following IPA and DPHC treatment in skeletal myotubes was evaluated without insulin stimulation (Fig. 1-5B and D). Treatment of the skeletal myotubes with IPA and DPHC led to an increase in glucose uptake in a concentration-dependent manner. In particular, 7.5 μM of IPA and 30 μM of DPHC led to a significant increase in glucose uptake compared to that in the control group. These data suggested that IPA and DPHC treatment can induce glucose uptake in the absence of insulin in skeletal myotubes.

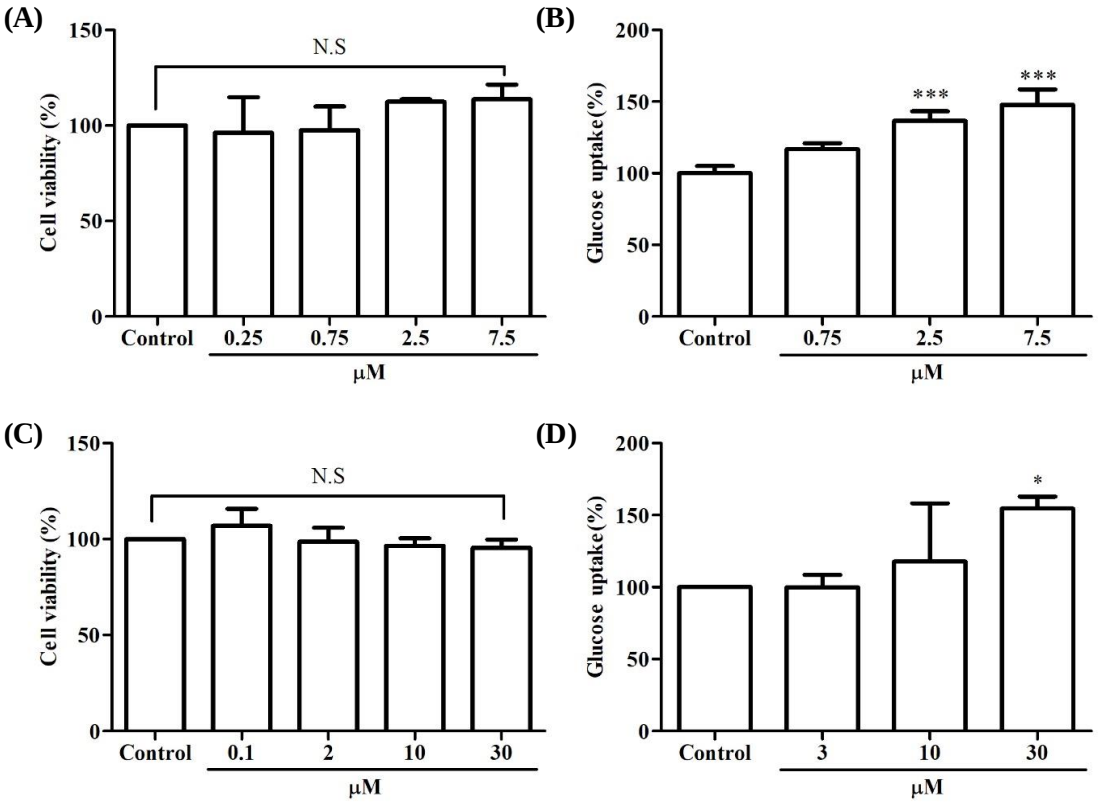

Fig. 1-5. Determination of cell viability by the MTT assay and glucose uptake by 2-NBDG in the skeletal myotubes. The skeletal muscle cells were incubated with the indicated concentrations of (A) IPA and (C) DPHC for 24. Differentiated skeletal muscle cells were starved in low glucose media and incubated for 24 h with (B) IPA (0.75, 2.5, and 7.5 μM), (D) DPHC (3, 10, and 30 μM) and 2-NBDG (50 μM). Data are expressed as the mean ± SE (n = 3 for each group). * Values having different superscript are significantly different at $^{*}p<0.05$ and $^{***}p<0.001$ compared with the non-treated group. No significance; N.S.

3.5. Increasing the cytosolic Ca^{2+} level by IPA and DPHC in skeletal myotubes

In order to identify how the IPA and DPHC in IO extract affects blood glucose level, it was evaluated the change of cytosolic Ca^{2+} by IPA and DPHC using Fluo-4-AM. The level of cytosolic Ca^{2+} with different concentrations of IPA (0.75, 2.5, and 7.5 μM) and DPHC (3, 10, and 30 μM) was analyzed by measuring fluorescence changes in skeletal myotubes in the absence of extracellular Ca^{2+}. IPA induced the instantly elevation of the cytosolic Ca^{2+} level dose-dependently (Fig. 1-6A, B,and C). Also, DPHC induced the instantly elevation of the cytosolic Ca^{2+} level dose-dependently (Fig. 1-6D, E,and F). These data showed that IPA and DPHC can elevate cytosolic Ca^{2+} level in myotubes.

As shown in Fig. 1-7A, myotubes was treated with increasing concentrations of 7.5 μM IPA in the presence/absence of extracellular Ca^{2+}, resulted in elevation of the cytosolic Ca^{2+} levels for 60 sec. Elevation of cytosolic Ca^{2+} level by 7.5 μM IPA treatment was no significantly changed either addition of external Ca^{2+} (Fig. 1-7B). In Fig. 1-7C, myotubes was treated with increasing concentrations of 30 μM DPHC in the presence/absence of extracellular Ca^{2+}, resulted in elevation of the cytosolic Ca^{2+} levels for 60 sec. Elevation of cytosolic Ca^{2+} level by 30 μM DPHC treatment was no significantly changed either addition of external Ca^{2+} (Fig. 1-7D). Irrespective of whether there are presence or absence of extracellular Ca^{2+}, myotubes was induced to elevate the cytosolic Ca^{2+} level by IPA and DPHC. We can suggest that elevation of the cytosolic Ca^{2+} levels by IPA and DPHC is related to release from the SR and not from Ca^{2+} influx by plasma membrane Ca^{2+} channels [10,11].

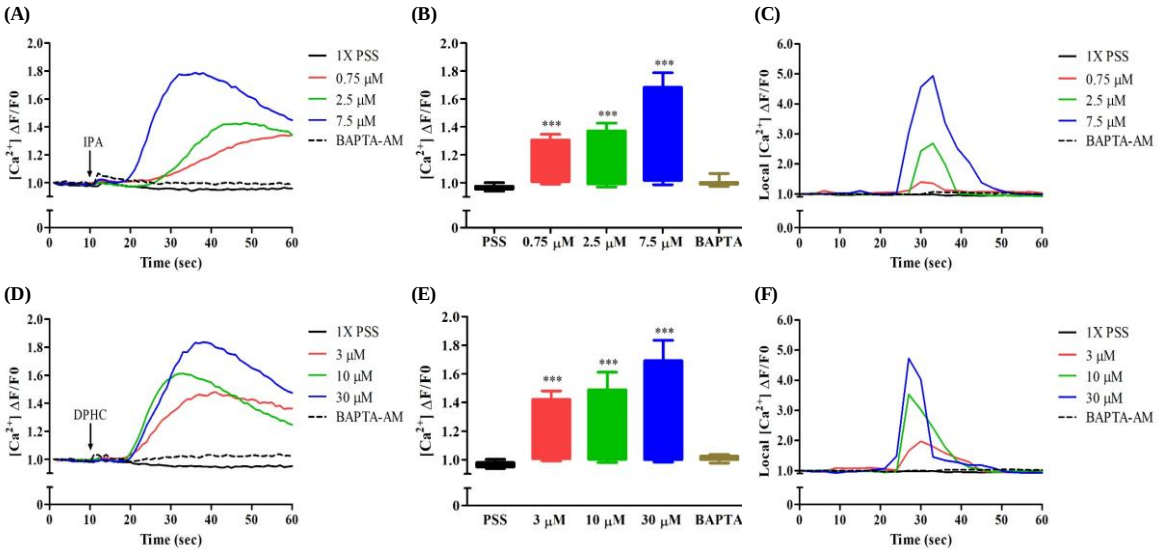

Fig. 1-6. Detection of cytosolic Ca^{2+} levels by IPA and DPHC in the absence of extracellular Ca^{2+} using the Fluo-4 Ca^{2+} indicator in the myotubes. (A) Traces and (B) box plot representation of Ca^{2+} levels in response to addition of IPA (0.75, 2.5, and 7.5 μM) or BAPTA-AM in myotubes. (D) Traces and (E) box plot representation of Ca^{2+} levels in response to addition of DPHC (3, 10, and 30 μM) or BAPTA-AM in myotubes. The fluorescence levels of single myotubes after addition of (C) IPA or (F) DPHC or BAPTA-AM was also monitored. $^{***}p<0.001$ compared with the PSS group.

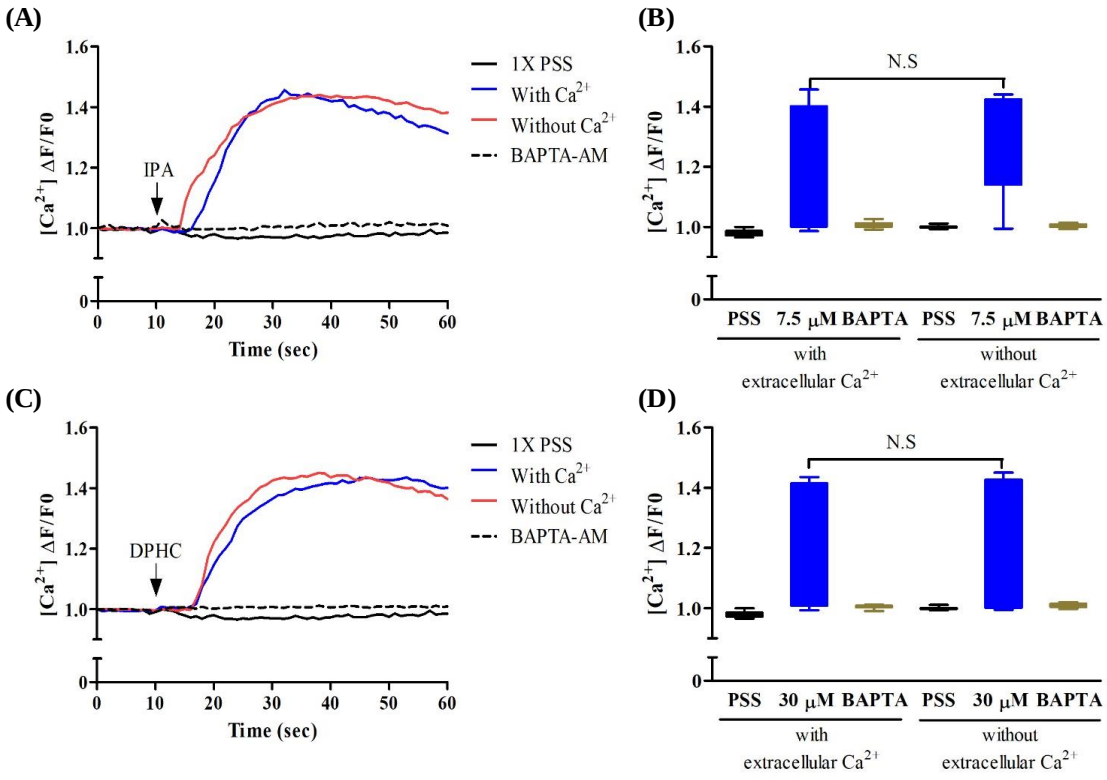

Fig. 1-7. Detection of cytosolic Ca^{2+} levels by IPA and DPHC using the Fluo-4 Ca^{2+} indicator in the skeletal myotubes. Myotubes were loaded with Fluo4 in PSS in the presence or absence of Ca^{2+} and treated with control (PSS only), (A) 7.5 μM of IPA or (C) 30 μM of DPHC or BAPTA-AM. (B) and (D) Box plots representation of the cytosolic Ca^{2+} levels in myotubes responses after 7.5 μM of IPA or 30 μM of DPHC or BAPTA-AM treatment as presented in (A) and (C). No significance; N.S compared with the IPA or DPHC in the presence or absence of extracellular Ca^{2+}.

3.6. Regulation of blood glucose level by IPA and DPHC in hyperglycemic zebrafish model

We have confirmed that the effect of regulation blood glucose level by IO extract in hyperglycemic zebrafish. Therefore, we conducted to evaluate the glucose transport pathway between regulation blood glucose level and glucose homeostasis by IPA and DPHC as component of IO extract. Initially, to evaluate the toxicity of IPA and DPHC, zebrafish embryos were exposed to IPA (0.3, 1.5, 3, and 5 μM) and DPHC (1.2, 6, 12, and 20 μM) in the embryo media for 168 hpf. After treatment with 0.3, 1.5, and 3 μM IPA, the survival rate of zebrafish was showed as 93%, 93%, and 87% (Fig. 1-8A). Whereas 5 μM of IPA treatment showed a significant decrease in survival to 77 ± 4.71% compared to the control group. As shown in Fig. 1-8B, 90%, 90%, and 80% of the zebrafish survived after treatment with 1.2, 6, and 12 μM DPHC, respectively, whereas 20 μM DPHC treatment showed a significant decrease in survival to 70 ± 4.71% compared to that observed in the control group. Therefore, the subsequent zebrafish experiments were conducted with concentrations that permitted ≥ 80% survival (Fig. 1-8).

In order to evaluate the effect of the equivalent content of IPA and DPHC in IO extract on hyperglycemic zebrafish, it was injected with saline (control), or IPA (0.03, 0.1, and 0.3 μg/g body weight) of DPHC (0.03, 0.1, and 0.3 μg/g body weight), or Metformin (5 μg/g body weight) for 90 min. In Fig. 1-9A, IPA- and Metformin-injected groups were observed the levels to 203%, 182%, and 175% of IPA and 151% Metformin as a positive control with known blood glucose level-controlling activity [40] compared with control group. IPA treatment was significantly exhibited reductions in high blood glucose level less metformin treatment. As shown in Fig. 1-9B, injection with increasing concentrations of DPHC (0.03, 0.1, and 0.3 μg/g) in 0.6% glucose to zebrafish decreased blood glucose levels by 245, 203, and 188%,

respectively, whereas metformin (3 μg/g) led to a 160% decrease in blood glucose levels. As a results, we suggest that the IPA and DPHC can reduce blood glucose levels in a hyperglycemic zebrafish model.

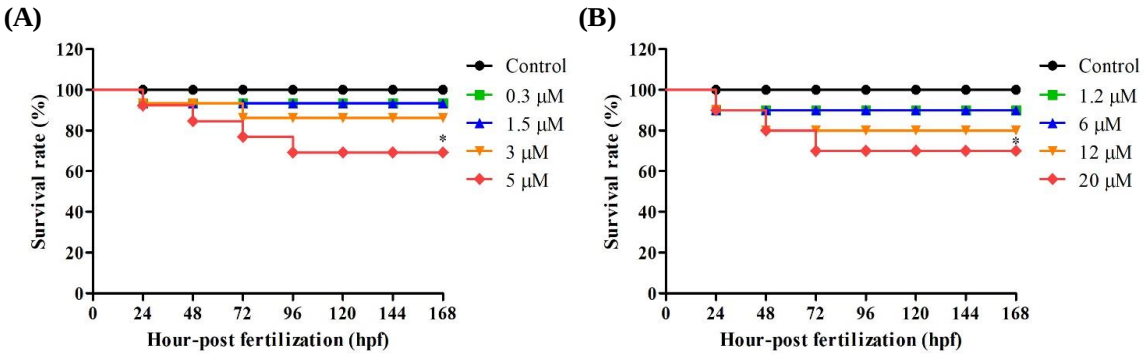

Fig. 1-8. Toxicity of IPA and DPHC by assessment of survival rate in zebrafish. The zebrafish were treated with various of concentrations of IPA and DPHC. (A) Survival curves of zebrafish embryos after exposure to (A) IPA (0.3, 1.5, 3, and 5 μM) and (B) DPHC (1.2, 6, 12, and 20 μM) (n = 15 for each group). Data are expressed as the mean ± SE (n = 4 for each group). * Values having different superscript are significantly different at $^{*}p<0.05$ compared with the no sample-treated group.

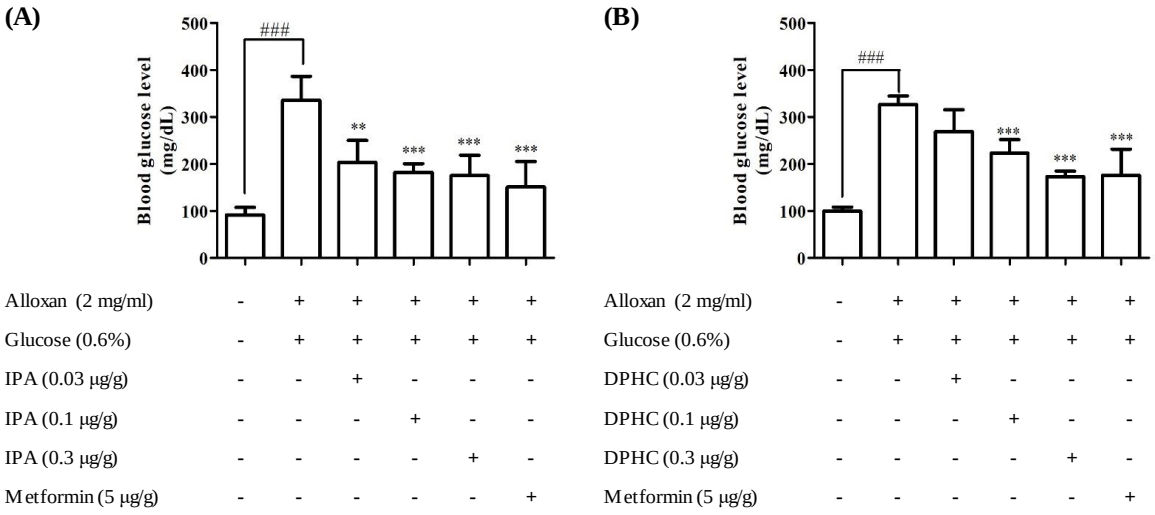

Fig. 1-9. Regulation of blood glucose level by IPA and DPHC in hyperglycemic zebrafish model. The zebrafish exposed to 0.6% glucose and then injected with (A) IPA (0.03, 0.1, and 0.3 μg/g body weight), or DPHC (0.03, 0.1, and 0.3 μg/g), or Metformin (5 μg/g) for 90 min. Data are expressed as the mean ± SE, $n = 4$ per group. * and $^{\#}$ Values having different superscript are significantly different at $^{\#\#\#}p<0.001$ compared with the non-treated group; $^{**}p<0.01$ and $^{***}p<0.001$ compared with the no sample-treated group.

3.7. Increasing the cytosolic Ca^{2+} level by IPA and DPHC in zebrafish

We hypothesized that the blood glucose level can be regulated by increasing cytosolic Ca^{2+} level in zebrafish muscle. To test this, we performed Ca^{2+} imaging studies in 3 dpf zebrafish embryos using Fluo-4 dye in the absence of external Ca^{2+} following exposure to IPA and DPHC. Initially, we confirmed that no significant fluorescence was induced by treatment with different concentrations of IPA alone (without Fluo-4) compared to that in the controls (N, no Fluo-4 and no drugs exposed, and F, only Fluo-4 exposed) (Fig. 1-10A). Moreover, fluorescence in the zebrafish in the Fluo-4 alone (F) sample increased 1.52 fold compared to that in the normal (N) control. These data showed that the cytosolic Ca^{2+} in zebrafish embryos was detected by Fluo-4. Next, the effect of IPA in Fluo-4-exposed embryos was assessed. Zebrafish embryos exposed to IPA and Fluo-4 had a rapid rise in cytosolic Ca^{2+}, however this increase was abolished with pre-incubation of the 3 μM IPA treated zebrafish embryos with 0.1 mM BAPTA-AM for 1 h (Fig. 1-10B). As shown Fig. 1-10C, fluorescence was no induced by treatment with different concentrations of DPHC alone (without Fluo-4) compared to that in the controls (N, no Fluo-4 and no drugs exposed, and F, only Fluo-4 exposed). Treatment with Fluo-4 and DPHC showed changes of fluorescence intensity that were significantly increased, compared to the Normal (Fig. 1-10D). However, this increase was abolished with pre-incubation of the 12 μM DPHC treated zebrafish embryos with 0.1 mM BAPTA-AM for 1 h (Fig. 1-10D). This finding suggests that IPA and DPHC can induce cytosolic Ca^{2+} elevation in zebrafish embryos.

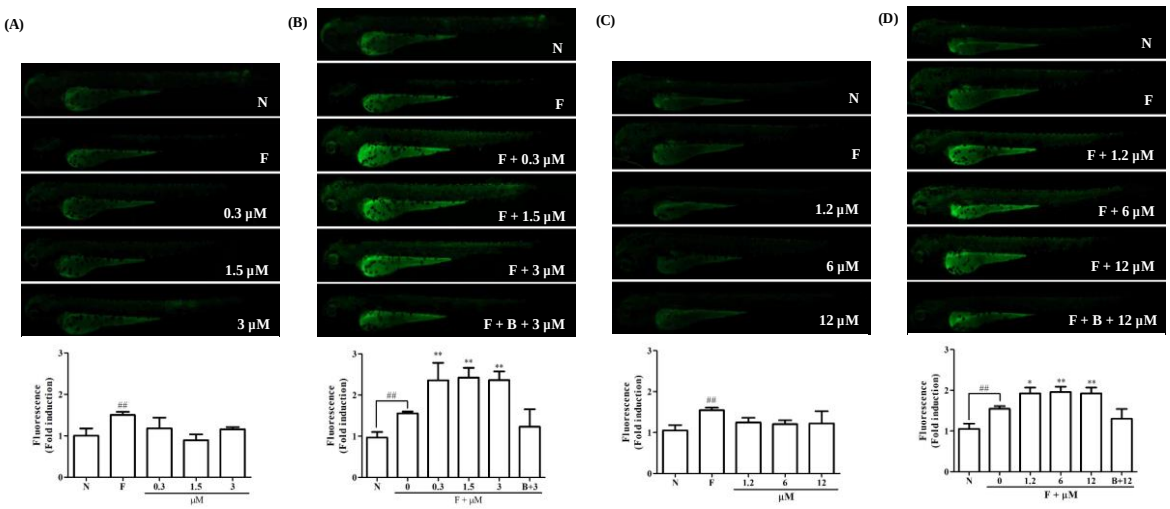

Fig. 1-10. Detection of cytosolic Ca^{2+} images by IPA and DPHC using the Fluo-4 in zebrafish larvae. Zebrafish larvae were stimulated with only (A) IPA (0.3, 1.5, and 3 μM) and (C) DPHC (1.2, 6, and 12 μM), compared with Fluo-4 exposed group (F). Zebrafish larvae were stimulated with (B) IPA or (D) DPHC in Fluo-4 and compared with/without Fluo-4 groups. Changes in cytosolic Ca^{2+} levels were measured by changes in fluorescence intensity of Fluo-4 using Image J. Experiments were performed in triplicate and the data are expressed as the mean ± SE, n = 4 per group. * and $^{\#}$ Values having different superscript are significantly different at $^{\#\#}p<0.01$ compared with the non-treated group; $^{**}p<0.01$ compared with the no sample-treated group.

3.8. Regulation of blood glucose level by IPA and DPHC through increasing cytosolic Ca^{2+} level in hyperglycemic zebrafish model

The important role of Ca^{2+} in increasing glucose transport in muscle as previously reported by Clausen et al [43]. To examine whether Ca^{2+} is required for the blood glucose-lowering effect of IPA and DPHC, we treated alloxan-induced hyperglycemic zebrafish with IPA and DPHC, and measured blood glucose level. Hyperglycemic zebrafish was injected with saline (control), or IPA (0.3 μg/g body weight) or DPHC (0.3 μg/g body weight) or Metformin (5 μg/g body weight), or BAPTA-AM (3 μg/g body weight) with/without IPA or DPHC. As shown Fig. 1-11A, the blood glucose level is significantly increase to 3-fold of normal group. When injected IPA, and Metformin, the blood glucose level decreased to 187% and 183% of control group. In particular, BAPTA-AM injected groups with/without IPA was no significantly observed the levels to 350% and 361%, compared with control group. While blood glucose level of BAPTA-AM injected group was no change, IPA injected group can control in hyperglycemic zebrafish as much as metformin injected group.

As shown in Fig. 1-11B, the alloxan-treated group had blood glucose levels of up to 3-fold, while they were significantly lower in the DPHC (0.3 μg/g) and metformin (3 μg/g) (180% and 174% respectively) treatment groups and the blank group (first column, saline only injected group). Importantly, this blood glucose-lowering effect of DPHC was significantly attenuated with BAPTA-AM treatment, resulting in blood glucose being at the same level as in the non-DPHC treated zebrafish. These data suggest that IPA and DPHC can stimulate glucose homeostasis through an increasing cytosolic Ca^{2+} levels in hyperglycemic zebrafish.

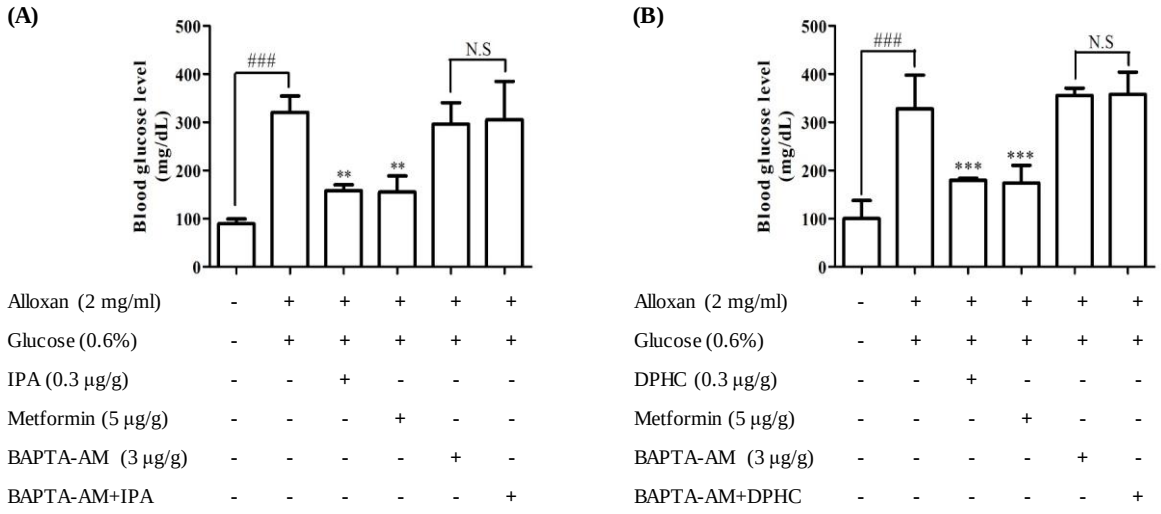

Fig. 1-11. Regulation of blood glucose level by IPA and DPHC in hyperglycemic zebrafish model. Zebrafish were injected with BAPTA-AM (3 µg/g body weight) for 1 h, after which the zebrafish were injected with (A) IPA (0.3 µg/g body weight) or (B) DPHC (0.3 µg/g body weight) for 90 min. Experiments were performed in triplicate and the data are expressed as mean ± SE, n = 4 per group. * and $^{\#}$ Values having different superscript are significantly different at $^{\#\#\#}p<0.001$ compared with non-treated group; $^{**}p<0.05$, and $^{***}p<0.001$ compared with the no sample-treated group. No significance; N.S compared with BAPTA-AM treated group.

3.9. Effect of IPA and DPHC on glucose translocation by increasing cytosolic Ca^{2+} level in zebrafish muscle tissue

Glucose uptake is mediated by a family of glucose transporter proteins, Glut4 being the major isoform present in skeletal muscle [44]. Diabetes is characterized by reduced insulin-mediated glucose uptake associated with reduced Glut4 expression [45]. Alloxan-induced diabetic mouse model was reported to affect expression of Glut4 [46]. Therefore, we examined the effect of IPA and DPHC on the translocation of Glut4 in the membrane of muscles in hyperglycemic zebrafish by using immunofluorescence, as shown in Fig. 1-12.

Hyperglycemic zebrafish was injected with saline (control), or IPA (0.3 μg/g body weight) or DPHC (0.3 μg/g body weight) or Metformin (5 μg/g body weight), or BAPTA-AM (3 μg/g body weight) with/without IPA or DPHC. As shown Fig. 1-12B, Glut4 intensity is significantly decrease to 0.5-fold of normal group. When injected IPA, and Metformin, the Glut4 intensity increased to 0.87- and 0.86-fold of control group. The DPHC (0.3 μg/g) and metformin (3 μg/g) (0.87- and 0.90-fold respectively) treatment groups and the blank group (first column, saline only injected group) in Fig. 1-12D. In particular, BAPTA-AM injected groups with/without IPA or DPHC was no significantly observed the intensity 0.57- and 0.57-fold, compared with control group. While blood glucose level of BAPTA-AM injected group was no change, the increase in Glut4 by IPA or DPHC could improve glucose metabolism through an increasing cytosolic Ca^{2+} levels in the skeletal muscle of hyperglycemic zebrafish.

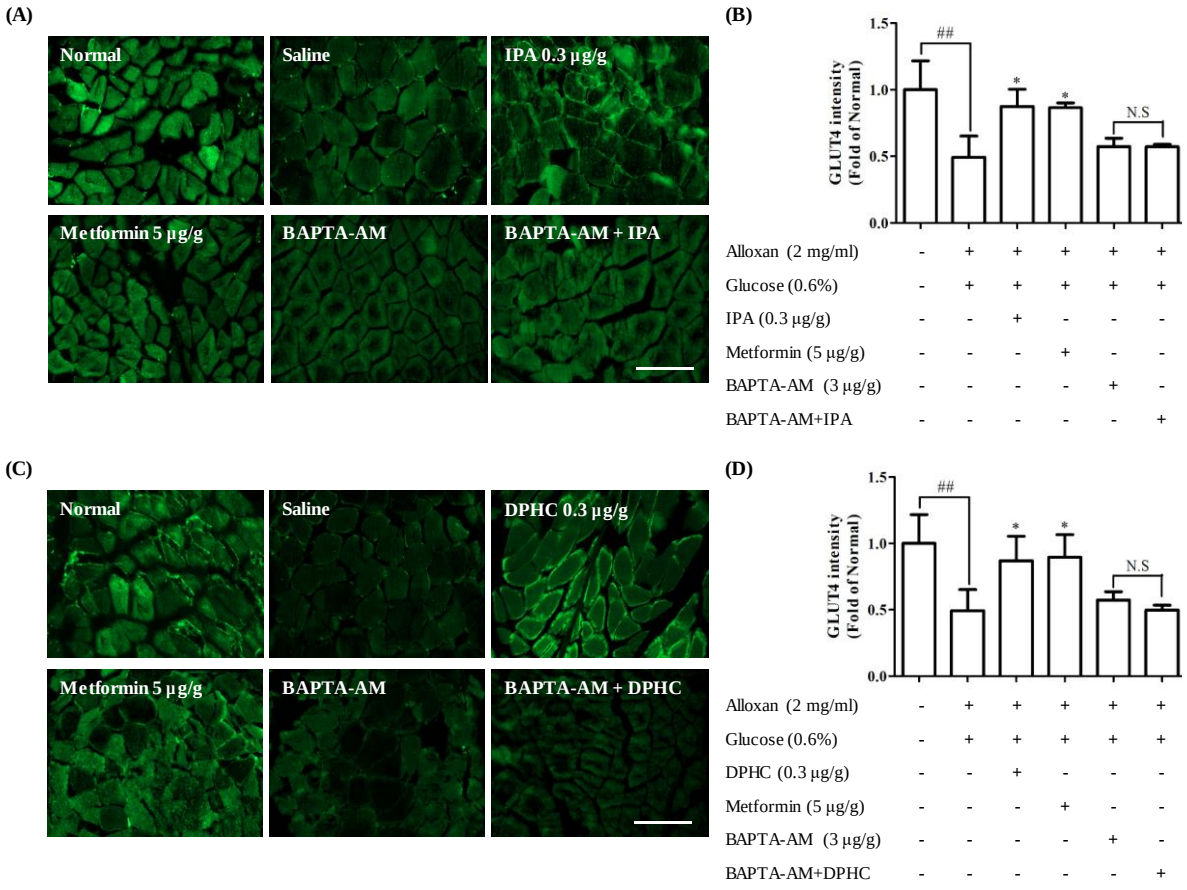

Fig. 1-12. Effect of IPA on Glut4 expression increase of skeletal muscle in hyperglycemic zebrafish model. Representative Glut4 immunofluorescence images by (A) IPA and (C) DPHC in skeletal muscle of hyperglycemic zebrafish model. Quantitative graph was show level of Glut4 expression by (B) IPA and (D) DPHC from representative images and Image J software was used for measurement. Scale bar = 100 μm, Data are expressed as mean ± SE. * and # Values having different superscript are significantly different at $^{\#\#}p$ <0.01 compared with non-treated group; $^{*}p$<0.05, compared with the no sample-treated group. No significance; N.S compared with BAPTA-AM treated group.

3.10. Assessment of the expression of glucose transport pathway components by IPA and DPHC in zebrafish muscle tissue

Increased cytosolic Ca^{2+} levels in the skeletal muscle leads to the initiation of contraction to provide the signal to activate Glut4 translocation [47,48]. Glucose uptake in the skeletal muscle tissue is achieved by mechanisms; activation of AMPK by muscle contraction due to exercise in order to maintain the energy balance [49]. Activation of AMPK plays a key role in maintaining cellular energy levels and stimulation of glucose uptake. Furthermore, the AMPK-independent pathway may regulate glucose transport in the contracting muscle [50].

To evaluate the molecular components that are involved in the regulation of glucose uptake by IPA and DPHC, the protein levels of membrane-associated Glut4 and phosphorylation of AMPK in the muscle of alloxan-induced hyperglycemic zebrafish was analyzed by western blotting. We conducted protein expression levels by western blot. In the muscle of hyperglycemic zebrafish, protein expression levels of AMPK, and Glut4 were significantly decreased (Fig. 1-13A, and B). Whereas treatment of IPA and Metformin resulted in significant stimulation in this decreased AMPK and Glut4 by hyperglycemic zebrafish. In contrast, upon hyperglycemic condition, BAPTA-injected group was inactivated these proteins and unchanged in the presence of IPA.

As shown in Fig. 1-13C, and D, phosphorylation levels of AMPK and the membrane localization of Glut4 significantly decreased in the muscle of alloxan-induced hyperglycemic zebrafish compared to those in the blank-treated animals. However, DPHC and metformin promoted Glut4 translocation to the membrane and phosphorylation of AMPK, indicating that DPHC can stimulate the glucose transport pathway in hyperglycemic zebrafish. These data suggest that IPA and DPHC can promote the glucose homeostasis which means the controlling metabolism by breaking the mechanisms.

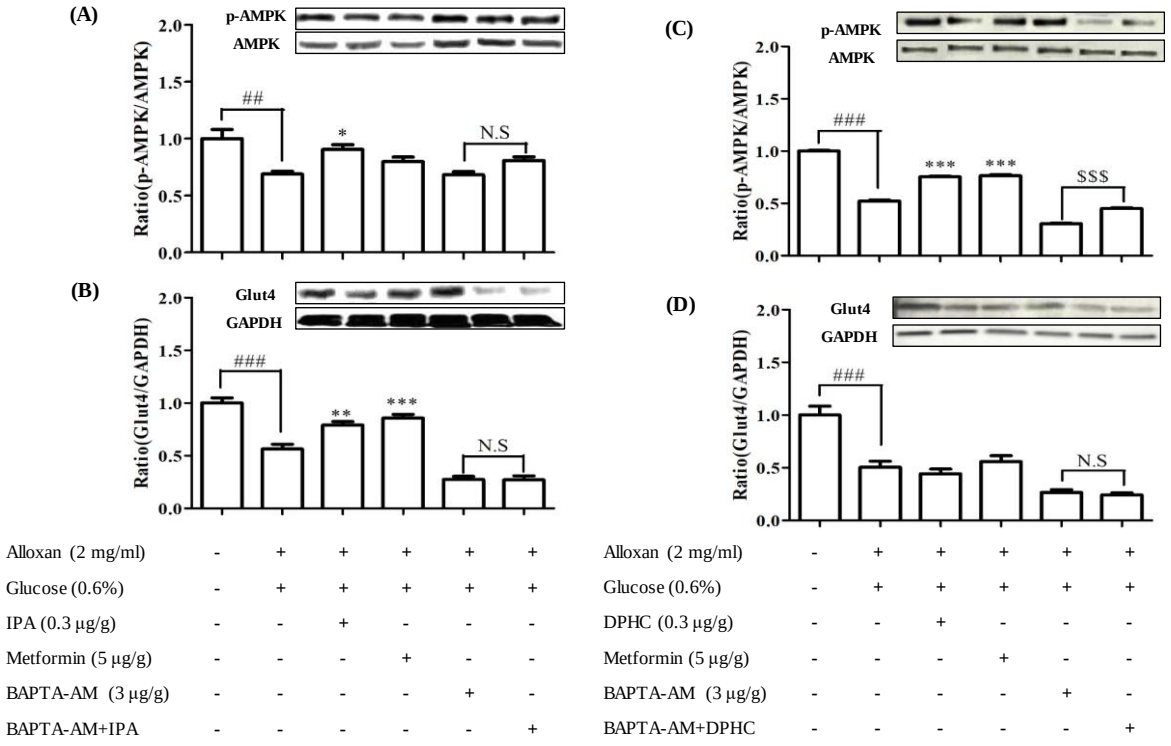

Fig. 1-13. Improvement of glucose transport pathway by IPA and DPHC in zebrafish muscle tissues. The zebrafish exposed to 0.6% glucose and then injected with IPA (0.3 μg/g) or DPHC (0.3 μg/g) or Metformin (5 μg/g) for 90 min. Zebrafish were pre-injected with BAPTA-AM (3 μg/g) for 1 h. Tissues were analyzed (A) AMPK, and (B) Glut4 by western blotting and signal intensity were evaluated by the Fusion FX7 acquisition system (Vibert Lourmat, Eberhardzell, Germany). Data expressed as the mean ± SE, n = 4 per group. $^{\#\#}p$ <0.01 and $^{\#\#\#}p$ <0.001; compared to non-treated group, $^{*}p$<0.05, $^{**}p$ <0.01, and $^{***}p$ <0.001; compared to control.

4. DISCUSSION

Skeletal muscle which is part of the body, as a fundamentally important role, is maintain the glucose homeostasis and regulate the whole-body carbohydrate metabolism [51,52]. In addition, upon physiological conditions, glucose uptake is the rate limiting step in glucose homeostasis in skeletal muscle by the cell membrane [53], and is independently stimulated by Ca^{2+}/contraction-dependent process [54,55]. In this study, we demonstrate relation to the cytosolic Ca^{2+} release by IO extract and its component (2.45% IPA and 2.4% DPHC) in skeletal myotubes and it anti-diabetes activity through hyperglycemic zebrafish model. Myotubes was induced to significantly elevate the cytosolic Ca^{2+} level by IO extract containing 2.45% and 2.4% regardless of the presence of extracellular Ca^{2+}. We suggest that IPA and DPHC has role of the cytosolic Ca^{2+} levels elevation, it is associated to release from the sarcoplasmic reticulum and not from Ca^{2+} influx by plasma membrane Ca^{2+} channels.

This observation was further assessed the glucose uptake by IPA and DPHC, cells were analyzed by staining with 2-NBDG. The percentage of glucose uptake was increased by 7.5 μM IPA and 30 μM DPHC from by PBS only, resulting in suggested stimulating of glucose uptake by muscle contraction upon insulin-independent state [54]. In our study, cytosolic Ca^{2+} release by IPA and DPHC treatment can induce glucose uptake resulting in the regulation of blood glucose level through hyperglycemic zebrafish model, suggesting that cytosolic Ca^{2+} in skeletal myotubes can improve glucose homeostasis. Increased cytosolic Ca^{2+} levels, even at low concentrations to induce contractions, provide the signal to activate Glut4 translocation to the cell surface in skeletal muscle, independently of insulin [5].

We confirmed that DPHC and IPA can activate Glut4 translocation to the cell surface in skeletal muscle tissue of hyperglycemic zebrafish model by immunofluorescence staining assay.

Depending on the coordination and integration of several physiological systems, the blood glucose homeostasis is maintained. Moreover, during exercise increased need for glucose by contracting muscle results in glucose uptake from blood into the working skeletal muscles [56]. This study suggest, glucose homeostasis in muscle can be suggested an important strategy for diabetes therapy [57], and can improve insulin sensitivity and reduce postprandial hyperglycemia [58-60].

We further examined the Ca^{2+}-induced protein expression of AMPK, and Glut4 through hyperglycemic zebrafish muscle. Glucose transport pathway are regulated mainly through insulin-dependent activation of PI3-K/Akt and insulin-independent activation of AMPK mechanism [61]. AMPK activation promotes Glut4 translocation and increases glucose uptake directly in skeletal muscle [33]. Our result showed that the protein expression of AMPK, and Glut4 stimulated by IPA regardless of the presence of insulin. DPHC can stimulate Glut4 translocation and phosphorylation of AMPK. The cytosolic Ca^{2+} regulation by DPHC treatment in myotubes can reinforce Glut4/AMPK pathways for the propound effect on glucose uptake metabolism. Our data further indicated that IPA and DPHC can normalize metabolic disturbances in diabetes and improves glucose homeostasis in skeletal muscle. Therefore, findings from this study employ a mechanistic and integrative approach linking upregulation of the cytosolic Ca^{2+} by IPA and DPHC in skeletal muscle as a potential therapeutic mechanism to improve glucose metabolism during hyperglycemia.

5. CONCLUSION

In this study, we identified that IO extract can stimulate to increase cytosolic Ca^{2+} level from SR in myotubes. Furthermore, IPA and DPHC as composition of IO extract can maintain glucose homeostasis by elevating the cytosolic Ca^{2+} level resulting in controlling the blood glucose level. IPA and DPHC may help to prevent the diabetes as potential nutraceutical application.

Part II.

Improved glucose intolerance by *Ishige okamurae* and its components in high cholesterol diet zebrafish model

1. ABSTRACT

The lipids in intramyocellular of skeletal muscle is closely related to glucose intolerance by dietary intake of cholesterol. In addition, a state insulin resistance reduced muscle glucose uptake all contribute to elevated blood glucose levels. Here, Zebrafish were fed 4% high cholesterol diet (HCD) for 5 weeks to induce glucose intolerance resulting in disruption of glucose transporter. In this study, we investigated IO extract, IPA, and DPHC supplementation improved glucose intolerance in HCD zebrafish. In addition, these supplementations can translocate glucose transporter 4 (Glut4) in skeletal muscle of HCD zebrafish. Our results suggested that IPA and DPHC, which are components of IO, can improve glucose tolerance via Glut4 in the muscles of HCD zebrafish. IO extract including IPA and DPHC might be used as marine-derived nutraceuticals on maintenance of glucose tolerance for the prevention of diabetes.

2. MATERIALS AND METHODS

2.1. Chemicals and reagents

Cholesterol, D-(+)-Glucose (Glucose) and 1,1-Dimethylbiguanide hydrochloride (Metformin) were purchased from Sigma-Aldrich (St. Louis, MO, USA). Antibodies against phospho-AMP-activated protein kinase (Thr172), AMPK and p-Akt (Ser473), Akt, Glut4, and GAPDH were obtained from Cell Signaling Technology (Bedford, MA, USA) and anti-rabbit secondary antibodies were purchased from Santa Cruz Biotechnology (Santa Cruz, CA, USA).

2.2. Maintenance of parental zebrafish

Adult zebrafish was obtained from a commercial dealer (Jeju aquarium, Jeju, Korea). Fifteen fishes were kept in 3.5 L acrylic tank according to the conditions; 28.5 ± 1 ˚C, fed two times a day (Tetra GmgH D-49304 Melle Made in Germany) with a 14/10 light/dark cycle. The zebrafish experiment received approval from the Animal Care and Use Committee of the Jeju National University (Approval No. 2017-0001).

2.3. High cholesterol diet-fed zebrafish model

Zebrafish were acclimated for 1 week. After acclimation, the zebrafish were fed a 4% high cholesterol diet (HCD) for 3 weeks, except for the normal group. And then, the zebrafish group were randomly assigned into 12 treatment groups: NCD/saline, HCD/saline, HCD/IO extract (1, 3, and 5%), HCD/IPA (0.0003, 0.001, and 0.003%), HCD/DPHC (0.0003, 0.001, and

0.003%), and HCD/Met (1%). After 3 weeks, each group of zebrafish was fed a 4% cholesterol with or without IO extract, IPA, DPHC, and Met supplementation for 2 weeks. After 5 weeks, all zebrafish were measured fasting and postprandial blood glucose level and sacrificed on 0.0006% MS-222 and muscle was isolated from zebrafish for immunofluorescence and western blot.

2.4. Glucose tolerance test (IPGTT)

Zebrafish were fasted for 8 h before performing intraperitoneal glucose tolerance test (IPGTT). After fasting, glucose (0.3 mg/g body weight) were injected intraperitoneally and blood was collected at different time points (15, 30, 45, and 60 mins). Blood glucose level was measured using blood glucose meter (AccuChek Advantage; Roche Diagnostics Corp, USA). The data were analyzed through the calculation of the area under curve (AUC).

2.5. Tissue preparation

Zebrafish muscle tissue was fixed in Bouin's solution for approximately 24 h and subsequently transferred to 70% ethanol for storage. After dehydration and embedding in paraffin, the tissue block was sliced to 7 μm.

2.6. Immunofluorescence staining assay

Paraffin-sectioned slides were deparaffinized twice with xylene for 5 min, and hydrated in graded ethanol, and then incubated in antigen-retrieval solution for 5 min in the microscope.

The slides were washed in running water for 5 min and then incubated in blocking solution for 1 h. After three washes in phosphate-buffered saline (PBS), the slides were incubated for overnight at 4 °C with primary antibody; glucose transporter type 4 (GLUT4). The primary antibody was diluted to 1:400 with blocking solution. The slides were washed with PBS, and then incubated with 488-fluorescent anti-rabbit secondary antibody for 2 h. The secondary antibody was diluted to 1:200 with blocking solution. After incubation for 2 h, the slides were washed with PBS, and mounted by mounting medium. The images were captured using the microscope (Gen 5 version 3.03, BioTek, Winooski, Vermont, U.S.). The intensity of the immunofluorescence staining, Image J software was used.

2.7. Statistical analysis

All of data were presented as means ± standard deviation (S.D). The mean values were calculated based on data from at least three independent experiments which were conducted on separate days using freshly prepared reagents. All the experiments were statistically analyzed using one-way analysis of variance (one-way ANOVA) and Dunnet (in GraphPad Prism Version 5.03). A p-value of less than 0.05 ($^{\#}p<0.05$, $^{\#\#}p<0.01$, and $^{\#\#\#}p<0.001$) was considered statistically significant and compared with non-treated group. A p-value of less than 0.05 ($^{*}p<0.05$, $^{**}p<0.01$, and $^{***}p<0.001$) was considered statistically significant and compared with no sample-treated group.

3. RESULTS

3.1. Examination of impaired glucose tolerance in HCD zebrafish

Dietary intake of cholesterol increased the total body cholesterol and induced deposited the lipids in hepatocytes of liver and intramyocellular of skeletal muscle which is closely related to insulin resistance [62,63]. In order to assess whether the glucose tolerance in zebrafish are impaired by HCD for 5 weeks, we investigated glucose tolerance, fasting and postprandial glucose levels in HCD zebrafish every week. For 5 weeks, intraperitoneal glucose tolerance test (0.3 mg/g, IPGTT) was conducted at different time points (15, 30, 45, and 60 mins). As shown in Fig. 2-1A, HCD group showed the lower glucose tolerance with higher glucose level, at each time point compare to NCD group. The area under the curve (AUC) of IPGTT suggest to evaluate the degree of the glucose tolerance impairment in each groups. The consistent result with Fig. 2-1, the AUC of IPGTT in HCD group was significantly increased except 1 week, compared to the NCD group at each time point.

Maintaining fasting and postprandial glucose levels are an important therapeutic goal in diabetes [64]. As shown in Fig. 2-2A and B, fasting and postprandial glucose levels were time-dependently increased in the HCD group compared to the NCD group. These data suggest that zebrafish was impaired glucose tolerance by HCD. We further examined the glucose homeostasis in skeletal muscle of HCD zebrafish at each time point.

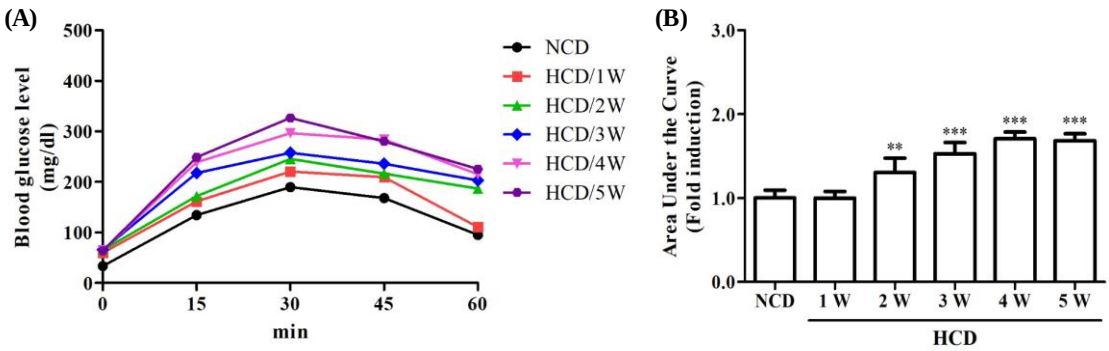

Fig. 2-1. Change of blood glucose level in HCD zebrafish for 5 weeks. Zebrafish receiving HCD for 5 weeks and induced impaired glucose tolerance. (A) intraperitoneal glucose tolerance tests (IPGTT) were performed and calculated (B) area under the curve (AUC) from the GTT in all zebrafish groups at each time point. Data are expressed as the mean ± SE (*n* = 4 for each group). * Values having different superscript are significantly different at $^{**}p<0.01$ and $^{***}p<0.001$ compared with the NCD group.

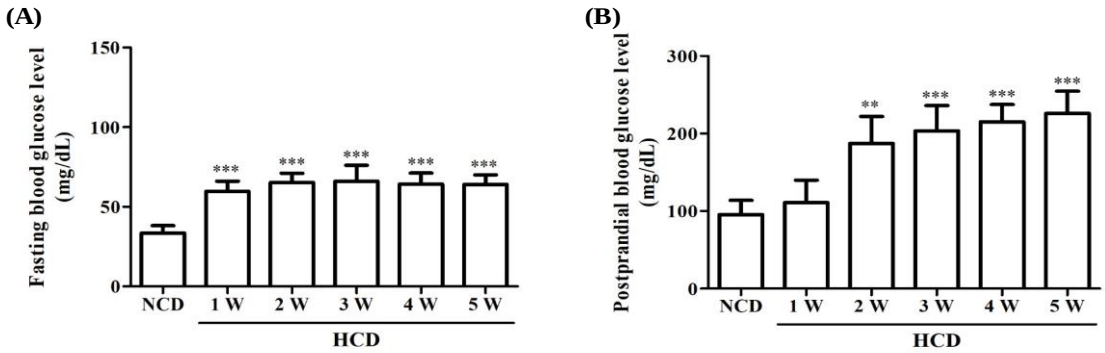

Fig. 2-2. Fasting and postprandial glucose levels in HCD zebrafish for 5 weeks. Zebrafish receiving HCD for 5 weeks measured (A) fasting and (B) postprandial glucose levels at each point time point. Data are expressed as the mean ± SE (n = 4 for each group). * Values having different superscript are significantly different at $^{**}p<0.01$ and $^{***}p<0.001$ compared with the NCD group.

3.2. Evaluation of glucose translocation in skeletal muscle of HCD zebrafish

The glucose transporter (Glut4) in skeletal muscle is essential to the maintenance of normal glucose homeostasis [65]. Diabetes is characterized by reduced insulin-mediated glucose uptake associated with reduced Glut4 expression [45]. HCD rat model was reported to affects of Glut4 translocation [66]. Therefore, we evaluated the Glut4 translocation in skeletal muscle of HCD zebrafish by using immunofluorescence. As shown Fig. 2-3, Glut4 intensity time-dependently decreased to 0.8-, 0.71-, 0.63-, 0.45-, and 0.39-fold of NCD group. These data showed that decreased Glut4 intensity was induced imbalance of glucose metabolism by HCD group.

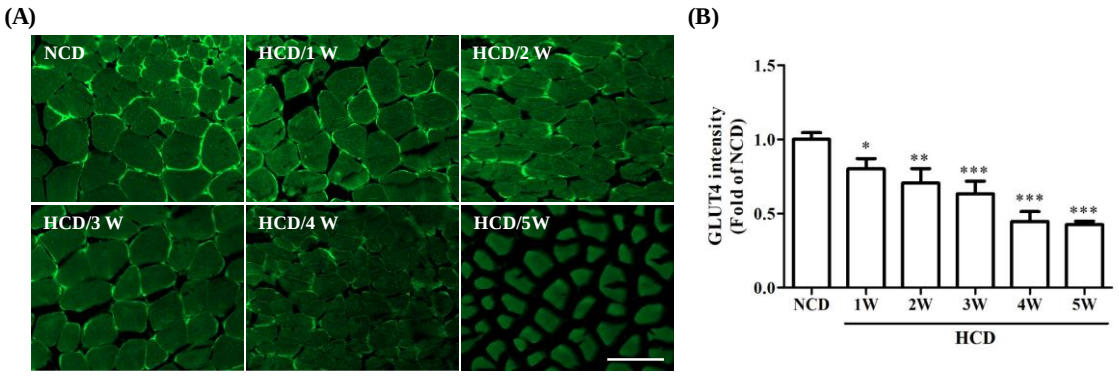

Fig. 2-3. Evaluation of Glut4 expression level in skeletal muscle of HCD zebrafish at each time point. (A) Representative Glut4 immunofluorescence images of skeletal muscle in HCD zebrafish at each point time. (B) Quantitative graph was show level of Glut4 expression by HCD from representative images and Image J software was used for measurement. Scale bar = 100 μm, Data are expressed as mean ± SE. * Values having different superscript are significantly different at $^{*}p<0.05$, $^{**}p<0.01$, and $^{***}p<0.001$ compared with the NCD group.

3.3. Improvement of glucose intolerance by IO extract supplementation in HCD zebrafish

To examine whether the increased the imbalance of glucose tolerance in HCD zebrafish were improved by IO extract, we evaluated glucose tolerance, fasting and postprandial glucose levels in HCD zebrafish. We fed zebrafish HCD supplemented IO extract (1, 3, and 5%, HCD/IO) and Metformin (1%, HCD/Met), used as positive control for regulation of blood glucose level in diabetes [40], for 2 weeks followed by additional 3 weeks of HCD. After 2 weeks of HCD/IO and HCD/Met intraperitoneal glucose tolerance test (0.3 mg/g, IPGTT) was conducted at different time points (15, 30, 45, and 60 mins). As shown in Fig. 2-4A, HCD group showed the glucose intolerance with higher glucose level, at each time point compare to NCD group. The area under the curve (AUC) of IPGTT suggest to measure the degree of the glucose intolerance in each groups. Resulting the increased blood glucose level by HCD at each time point was significantly decreased by IO extract and Metformin supplementation compare to HCD/saline group (Fig. 2-4B).

Maintaining fasting and postprandial glucose levels are an important therapeutic goal in diabetes [64]. As shown in Fig. 2-5A and 5B, fasting and postprandial glucose levels were significantly increased in the HCD group compared with that in the NCD group. Increased fasting glucose levels were significantly decreased by HCD/IO and HCD/Met. However, increased postprandial glucose levels were significantly decreased by HCD/IO (3% and 5%) and HCD/Met, except HCD/1%IO group which was no significantly changed. These data suggested that IO extract can improve glucose tolerance in HCD mice. We further assessed the balance of glucose homeostasis in skeletal muscle of HCD zebrafish as a means to regulate blood glucose level.

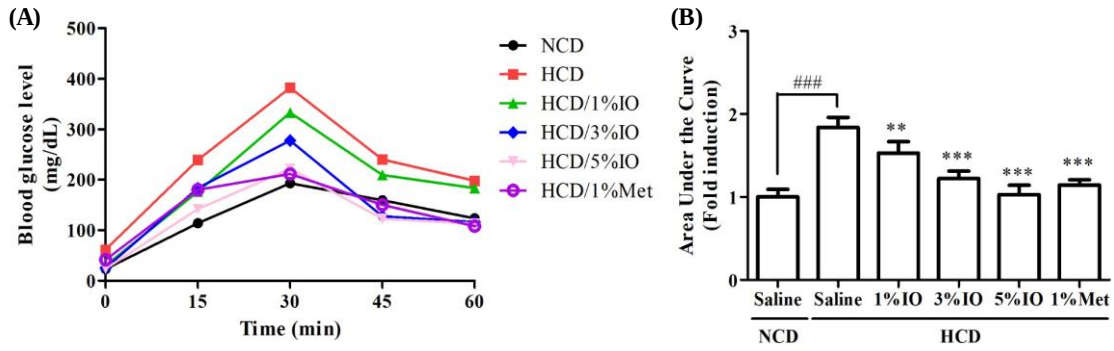

Fig. 2-4. Effect of IO extract supplementation on glucose intolerance in HCD zebrafish. Zebrafish were fed HCD supplemented IO extract (1, 3, and 5%, HCD/IO) and Metformin (1%, HCD/Met) for 2 weeks followed by additional 3 weeks of HCD. After 5 weeks, zebrafish were intraperitoneally injected with glucose (0.3 mg/g body weight). (A) intraperitoneal glucose tolerance tests (IPGTT) were performed and calculated (B) area under the curve (AUC) from the GTT in all zebrafish group at each time point. Data are expressed as the mean ± SE ($n = 4$ for each group). * and $^{\#}$ Values having different superscript are significantly different at $^{\#\#\#}p<0.001$ compared with the NCD group; $^{**}p<0.01$ and $^{***}p<0.001$ compared with the HCD/Saline group.

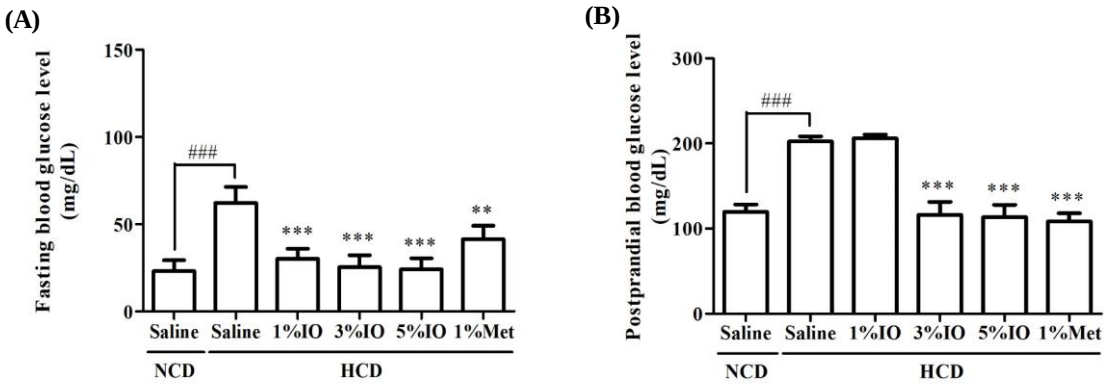

Fig. 2-5. Effect of IO extract supplementation on fasting and postprandial glucose levels in HCD zebrafish. After 5 weeks, zebrafish were intraperitoneally injected with glucose (0.3 mg/g body weight), and then measured (A) fasting and (B) postprandial glucose levels in all zebrafish group. Data are expressed as the mean ± SE (n = 4 for each group). * and $^{\#}$ Values having different superscript are significantly different at $^{\#\#\#}p<0.001$ compared with the NCD group; $^{**}p<0.01$ and $^{***}p<0.001$ compared with the HCD/Saline group.

3.4. Effect of IO extract supplementation on glucose translocation in skeletal muscle of HCD zebrafish

Previous study reported that the defects of Glut4 translocation were caused by impairment of glucose metabolism in HCD rat model [66]. To evaluate whether the defects of Glut4 translocation in HCD zebrafish was increased by IO extract for glucose tolerance, we investigated the effect of IO extract on glucose translocation in HCD zebrafish by using immunofluorescence. As shown Fig. 2-6, we measured the intensity of Glut4 in representative images to quantify the effect of IO extract on glucose translocation in skeletal muscle of HCD zebrafish. The Glut4 intensity in HCD zebrafish was significantly lower than in NCD zebrafish. However, the decreased Glut4 intensity was significantly increased in the HFD/IO and HFD/Met groups. These data suggested that IO extract could protect against defects of Glut4 translocation that occurs in HCD-induced diabetes.

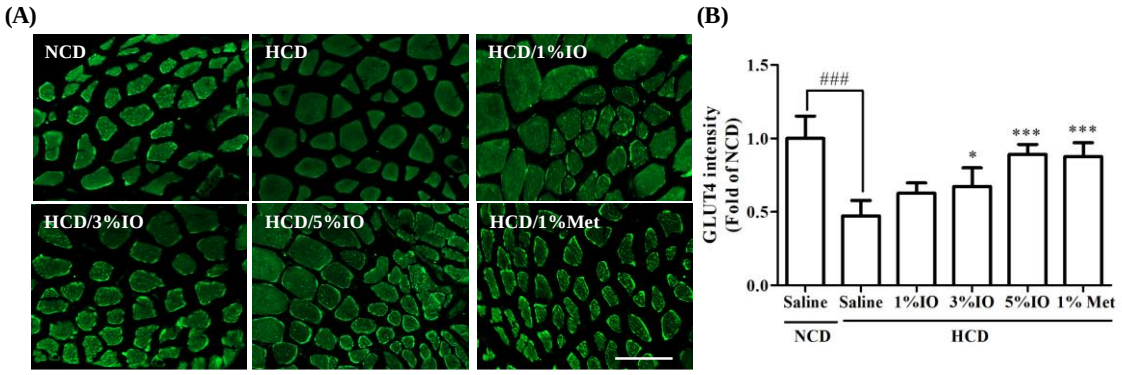

Fig. 2-6. Evaluation of Glut4 expression level by IO extract supplementation in skeletal muscle of HCD zebrafish. (A) Representative Glut4 immunofluorescence images of skeletal muscle in all zebrafish groups after 5 weeks. (B) Quantitative graph was show level of Glut4 expression by IO extract from representative images and Image J software was used for measurement. Scale bar = 100 μm, Data are expressed as mean ± SE. * and $^{\#}$ Values having different superscript are significantly different at $^{\#\#\#}p<0.001$ compared with the NCD group; $^{*}p<0.05$ and *** $p<0.001$ compared with the HCD/Saline group.

3.5. Improvement of glucose intolerance by IPA and DPHC supplementation in HCD zebrafish

To examine whether the increased the imbalance of glucose tolerance in HCD zebrafish were improved by IPA and DPHC, we evaluated glucose tolerance, fasting and postprandial glucose levels in HCD zebrafish. We fed zebrafish HCD supplemented IPA (0.0003%, 0.001%, and 0.003%, HCD/IPA), DPHC (0.0003%, 0.001%, and 0.003%, HCD/DPHC) and Metformin (1%, HCD/Met), used as positive control for regulation of blood glucose level in diabetes [40], for 2 weeks followed by additional 3 weeks of HCD. After 2 weeks of HCD/IPA, HCD/DPHC, and HCD/Met intraperitoneal glucose tolerance test (0.3 mg/g, IPGTT) was conducted at different time points (15, 30, 45, and 60 mins). As shown in Fig. 2-7 and 2-8, HCD group showed the glucose intolerance with higher glucose level, at each time point compare to NCD group. The area under the curve (AUC) of IPGTT suggest to measure the degree of the glucose intolerance in each groups. Resulting the increased blood glucose level by HCD at each time point was significantly decreased by IPA and DPHC supplementation compare to HCD group. Maintaining fasting and postprandial glucose levels are an important therapeutic goal in diabetes [64]. As shown in Fig. 2-7 (C and D) and 2-8 (C and D), fasting and postprandial glucose levels were significantly increased in the HCD group compared with that in the NCD group. Increased fasting glucose levels were significantly decreased by HCD/IPA and HCD/DPHC. However, increased postprandial glucose levels were significantly decreased by HCD/IPA and HCD/DPHC. These data suggested that IPA and DPHC can improve glucose tolerance in HCD mice. We further assessed the balance of glucose homeostasis in skeletal muscle of HCD zebrafish as a means to regulate blood glucose level.

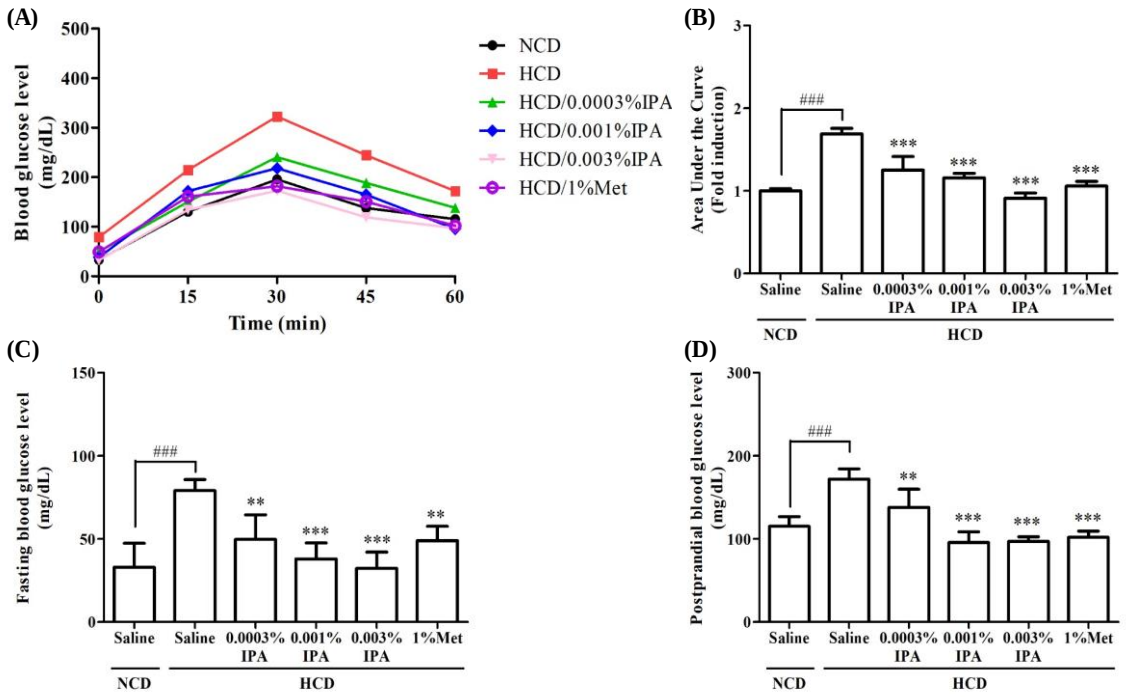

Fig. 2-7. Effect of IPA supplementation on glucose intolerance in HCD zebrafish. Zebrafish were fed HCD supplemented IPA (0.0003, 0.001, and 0.003%, HCD/IPA) and Metformin (1%, HCD/Met) for 2 weeks followed by additional 3 weeks of HCD. After 5 weeks, zebrafish were intraperitoneally injected with glucose (0.3 mg/g body weight). (A) intraperitoneal glucose tolerance tests (IPGTT) were performed and calculated (B) area under the curve (AUC) from the GTT in all zebrafish group at each time point. (C) fasting and (D) postprandial glucose levels were in all zebrafish group. Data are expressed as the mean ± SE ($n = 4$ for each group). * and $^{\#}$ Values having different superscript are significantly different at $^{\#\#\#}p<0.001$ compared with the NCD group; $^{**}p<0.01$ and $^{***}p<0.001$ compared with the HCD/Saline group.

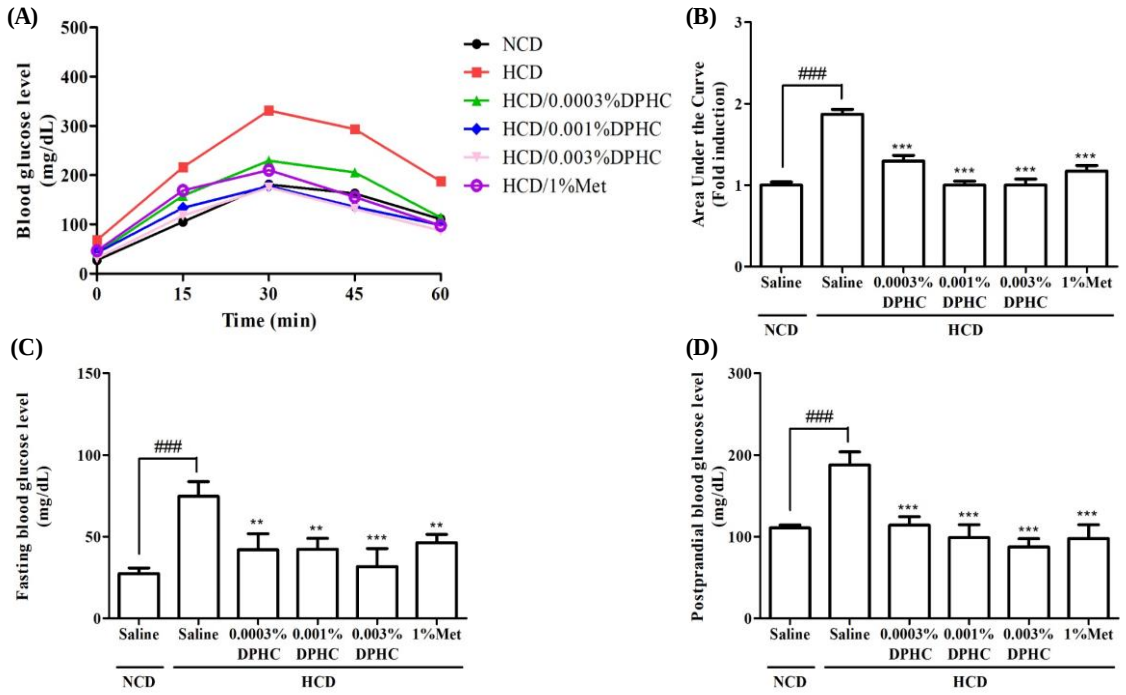

Fig. 2-8. Effect of DPHC supplementation on glucose intolerance in HCD zebrafish. Zebrafish were fed HCD supplemented DPHC (0.0003, 0.001, and 0.003%, HCD/DPHC) and Metformin (1%, HCD/Met) for 2 weeks followed by additional 3 weeks of HCD. After 5 weeks, zebrafish were intraperitoneally injected with glucose (0.3 mg/g body weight). (A) intraperitoneal glucose tolerance tests (IPGTT) were performed and calculated (B) area under the curve (AUC) from the GTT in all zebrafish group at each time point. (C) fasting and (D) postprandial glucose levels were in all zebrafish group. Data are expressed as the mean ± SE ($n = 4$ for each group). * and $^{\#}$ Values having different superscript are significantly different at $^{\#\#\#}p<0.001$ compared with the NCD group; $^{**}p<0.01$ and $^{***}p<0.001$ compared with the HCD/Saline group.

3.6. Effect of IPA and DPHC supplementation on glucose translocation in skeletal muscle of HCD zebrafish

Previous study reported that the defects of Glut4 translocation were caused by impairment of glucose metabolism in HCD rat model [66]. To evaluate whether the defects of Glut4 translocation in HCD zebrafish was increased by IPA and DPHC as a components of IO for glucose tolerance, we investigated the effect of IPA and DPHC on glucose translocation in HCD zebrafish by using immunofluorescence. As shown Fig. 2-9, we measured the intensity of Glut4 in representative images to quantify the effect of IPA and DPHC on glucose translocation in skeletal muscle of HCD zebrafish. The Glut4 intensity in HCD zebrafish was significantly lower than in NCD zebrafish. However, the decreased Glut4 intensity was significantly increased in the HCD/IPA, HCD/DPHC and HCD/Met groups. These data suggested that IPA and DPHC could protect against defects of Glut4 translocation that occurs in HCD-induced diabetes.

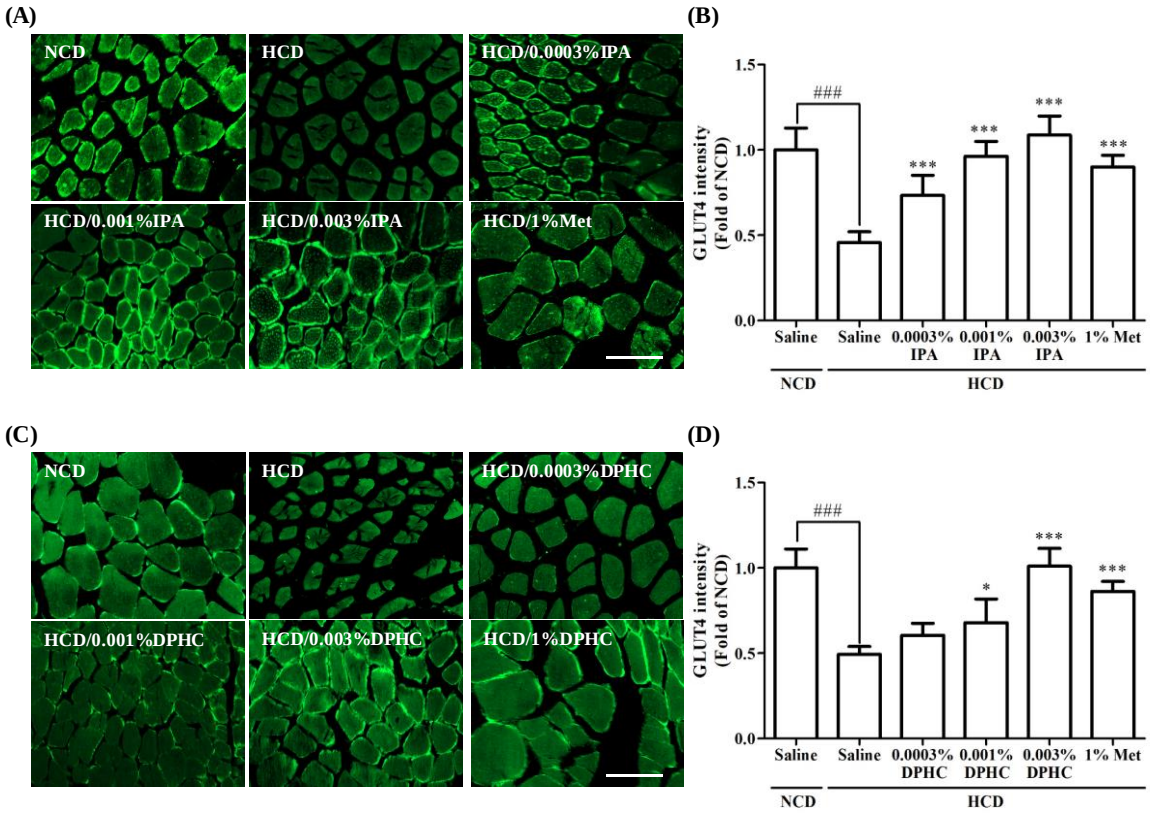

Fig. 2-9. Evaluation of Glut4 expression level by IPA and DPHC supplementation in skeletal muscle of HCD zebrafish. Zebrafish were fed HCD supplemented IPA (0.0003, 0.001, and 0.003%, HCD/IPA), DPHC (0.0003, 0.001, and 0.003%, HCD/DPHC) and Metformin (1%, HCD/Met) for 2 weeks followed by additional 3 weeks of HCD. Representative Glut4 immunofluorescence images of (A) IPA and (C) DPHC in skeletal muscle of all zebrafish groups after 5 weeks. Quantitative graph was show level of Glut4 expression by (B) IPA and (D) DPHC from representative images and Image J software was used for measurement. Scale bar = 100 μm, Data are expressed as mean ± SE. * and $^{\#}$ Values having different superscript are significantly different at $^{\#\#\#}p<0.001$ compared with the NCD group; $^{*}p<0.05$ and $^{***}p<0.001$ compared with the HCD group.

4. DISCUSSION

A previous study reported that IO extract and its components (IPA and DPHC) showed an antidiabetic activity in diabetic mice [67,68]. However, the effect of IO extract, including IPA and DPHC as an agent for diabetes prevention has not yet been assessed on glucose homeostasis in skeletal muscle of HCD zebrafish. The enriched cholesterol diet increased blood glucose level, resulting in impairment of glucose tolerance [63,69]. Diabetes mellitus is defined clinically by fasting and postprandial glucose levels in response to a defined glucose load [70]. In this study, our data suggest that HCD can induce impairment of glucose tolerance in skeletal muscle of zebrafish via deregulation of glucose transport pathway. In particular, intensity of Glut4, as glucose transporters, time-dependently decreased in skeletal muscle of HCD zebrafish for 5 weeks. We confirmed that the HCD zebrafish model can be used for studying diabetes and its complications.

We further assessed the maintenance of glucose homeostasis by IO extract and its components (IPA and DPHC) supplementation, zebrafish were fed HCD supplemented IO extract, IPA, DPHC, and Metformin for 2 weeks, followed additional 3 weeks of HCD. Previous studies reported that muscle and adipose may sense glucose and communicate changes of glucose flux to other tissues to maintain glucose homeostasis [70]. Glut4, as a key glucose transporter, plays a predominant role in maintenance of glucose homeostasis by translocation of Glut4 and expression in muscle [71]. The plasma membrane Glut4 protein was lower in skeletal muscles in mice with glucose intolerance [72]. IO extract and its components significantly increased the intensity of Glut4 in skeletal muscle of HCD zebrafish, suggesting the effect of IO extract and its components supplementation against decreased Glut4 translocation in HCD-induced glucose intolerance.

Glucose transport pathway maintained glucose homeostasis via insulin-dependent activation of PI3-K/Akt and insulin-independent activation of AMPK pathway [73]. Increased the protein expression level of AMPK was promoted glucose uptake via enhancing the translocation of Glut4 in skeletal muscle [74].

5. CONCLUSION

In summary, we indicated that HCD induced imbalance of glucose homeostasis in zebrafish via deactivation of glucose transport, resulting in the rise of blood glucose levels. We confirmed that IO extract, IPA and DPHC supplementation can stimulate to regulate glucose homeostasis in skeletal muscle of HCD zebrafish. IO extract including IPA and DPHC may help to improve the glucose tolerance and metabolism as potential nutraceutical application in prediabetes.

Part III.

Energy metabolism and its regulation by Ishophloroglucin A and Diphlorethohydroxycarmalol in zebrafish muscle tissue

1. ABSTRACT

Ishige okamurae (IO) has been reported to prevent diabetes through glucose metabolism. However, how glucose metabolism exerts a correlation with muscle contraction in skeletal muscle to maintain energy homeostasis remains largely unexplored. This study was investigated to evaluate the effects of an IPA and DPHC, as components of IO, on energy homeostasis through muscle contraction in zebrafish which is type 1 and type2 diabetes model. The results showed that CaMKII and AMPK activation by IPA and DPHC treatment can induce glucose uptake resulting in the regulation of homeostasis via energy expenditure in diabetes zebrafish model. Furthermore, IPA and DPHC stimulated muscle contraction, which induced to change expression level Troponin C and I. Overall, IPA and DPHC can maintain energy homeostasis through muscle contraction in skeletal muscle of diabetes zebrafish model. IO including IPA and DPHC might be used as marine-derived nutraceuticals for glucose and energy homeostasis promoting effects in diabetes.

2. MATERIALS AND METHODS

2.1. Chemicals and reagents

Troponin I, Troponin C, 488-fluorescent anti-rabbit secondary antibody and ATP assay kit were obtained from Abcam (Cambridge, London, England). Perchloric acid (PCA), Potassium hydroxide (KOH), D-(+)-Glucose (Glucose), 1,2-Bis(2-aminophenoxy)ethane-N,N,N′,N′-tetraacetic acid tetrakis(acetoxymethyl ester) (BAPTA-AM), 2,4,5,6(1H,3H)-Pyrimidinetetrone (Alloxan monohydrate), and 1,1-Dimethylbiguanide hydrochloride (Metformin) were purchased from Sigma-Aldrich (St. Louis, MO, USA). Alamar Blue were purchased from Thermo Fisher Scientific (Waltham, MA, USA). Antibodies against Ca^{2+}/calmodulin-dependent protein kinase II (CAMK2) and GAPDH were obtained from Cell Signaling Technology (Bedford, MA, USA) and anti-rabbit secondary antibodies were purchased from Santa Cruz Biotechnology (Santa Cruz, CA, USA).

2.2. Maintenance of parental zebrafish and collection of embryos

Adult zebrafish was obtained from a commercial dealer (Jeju aquarium, Jeju, Korea). Fifteen fishes were kept in 3.5 L acrylic tank according to the conditions; 28.5 ± 1 ˚C, fed two times a day (Tetra GmgH D-49304 Melle Made in Germany) with a 14/10 light/dark cycle. Embryos were mated, and spawning was stimulated by setting of light, after breeding 1 female and 2 males interbreed. Embryos were collected within 30 min and transferred to Petri dishes containing embryo media. The zebrafish experiment received approval from the Animal Care and Use Committee of the Jeju National University (Approval No. 2017-0001).

2.3. Hyperglycemic zebrafish model

Wild-type zebrafish were exposed to 2 mg/ml alloxan for 1 h and transferred to 1% glucose for another 1 h. The media was then changed to water for 1 h, and zebrafish were injected with saline, IO extract, or IPA, or DPHC, or Metformin, with or without BAPTA-AM for 90 min. Adult zebrafish were divided into six groups: normal, alloxan-treated group, IO extract (10, 30, and 100 μg/g body weight), IPA (0.03, 0.1, and 0.3 μg/g body weight), DPHC (0.03, 0.1, and 0.3 μg/g body weight), Metformin (5 μg/g body weight), BAPTA-AM (3 μg/g body weight), and BAPTA-AM (3 μg/g body weight) with IPA or DPHC (0.3 μg/g body weight).

2.4. High cholesterol diet-fed zebrafish model

Zebrafish were acclimated for 1 week. After acclimation, the zebrafish were fed a 4% high cholesterol diet (HCD) for 3 weeks, except for the normal group. And then, the zebrafish group were randomly assigned into 12 treatment groups: NCD/saline, HCD/saline, HCD/IO extract (1, 3, and 5%), HCD/IPA (0.0003, 0.001, and 0.003%), HCD/DPHC (0.0003, 0.001, and 0.003%), and HCD/Met (1%). After 3 weeks, each group of zebrafish was fed a 4% cholesterol with or without IO extract, IPA, DPHC, and Met supplementation for 2 weeks. After 5 weeks, all zebrafish were measured fasting and postprandial blood glucose level and sacrificed on 0.0006% MS-222 and muscle was isolated from zebrafish for immunofluorescence and western blot.

2.5. Tissue preparation

Zebrafish muscle tissue was fixed in Bouin's solution for approximately 24 h and subsequently transferred to 70% ethanol for storage. After dehydration and embedding in paraffin, the tissue block was sliced to 7 μm.

2.6. Immunofluorescence staining assay

Paraffin-sectioned slides were deparaffinized twice with xylene for 5 min, and hydrated in graded ethanol, and then incubated in antigen-retrieval solution for 5 min in the microscope. The slides were washed in running water for 5 min and then incubated in blocking solution for 1 h. After three washes in phosphate-buffered saline (PBS), the slides were incubated for overnight at 4 °C with primary antibody; Troponin I and Troponin C. The primary antibody was diluted to 1:400 with blocking solution. The slides were washed with PBS, and then incubated with 488-fluorescent anti-rabbit secondary antibody for 2 h. The secondary antibody was diluted to 1:200 with blocking solution. After incubation for 2 h, the slides were washed with PBS, and mounted by mounting medium. The images were captured using the microscope (Gen 5 version 3.03, BioTek, Winooski, Vermont, U.S.). The intensity of the immunofluorescence staining, Image J software was used.

2.7. Hematoxylin and Eosin staining

Paraffin-sectioned slides were deparaffinized twice with xylene for 5 min. After serial incubation in EtOH and running water to rehydrate, the slides were stained with hematoxylin (DAKO, Carpinteria, CA, USA) for 2 min at room temperature. The slides were washed with running water for 5 min, stained with eosin (Sigma-Aldrich) for 30 s, and washed with running

water for 5 min. The slides were mounted by mounting medium. The images were captured using the microscope (Gen 5 version 3.03, BioTek, Winooski, Vermont, U.S.). The intensity of the immunofluorescence staining, Image J software was used.

2.8. Western blot analysis

Zebrafish muscle tissue were homogenized in lysis buffer using a homogenizer and then incubated for 10 min at 4 °C. The homogenates were centrifuged at 14,000 rpm for 15 min at 4 °C. The protein was quantified by using BCA^{TM} protein assay kit and equal amount of proteins (30 μg) were separated using 10% SDS-polyacrylamide gel. The separated proteins were transferred to nitrocellulose membranes (GE Healthcare Life Science) and blocked for 3 h with nonfat dry milk at room temperature. Membranes were incubated for overnight at 4 °C with primary antibodies; Ca^{2+}/calmodulin-dependent protein kinase type II (CaMKII) and Glyceraldehyde 3-phosphate dehydrogenase (GAPDH). And then, membranes incubated with the secondary antibodies at 1:3000 dilutions for 2 h, protein bands were detected with chemiluminescence reagent (Maximum sensitivity substrate, Thermo Scientific). The images were captured using Fusion Solo apparatus (Vilber Lourmat) and measured using image J software.

2.9. ATP assay

Using 0.1 mM ATP standard dilution, a standard curve was generated following the ATP assay kit protocol (ab83355, Abcam, America). 10 mg of muscle tissue was harvested for each assay and washed in cold PBS. Tissue was homogenized in ice cold 2 N PCA with 10-15 passes.

Following maintaining on ice for 30-45 min, samples were centrifuged at 13,000 g for 3 min at 4 °C, and supernatant were collected. Samples were adjusted to pH between 6.5 and 8 to neutralize the samples and precipitate the excess PCA. Samples were centrifuged at 13,000 g for 15 min at 4 °C, and supernatants were collected. The supernatants were transferred to individual wells of 96-well plates mixed with same volume of ATP reaction mix and incubated at room temperature for 30 min, protected from light. ATP levels in each sample was determined by measuring optical density (OD) at 570 nm using a microplate reader (Gen5 version 2.05, BioTek, Winooski, Vermont, U.S.). The amount of ATP in the samples was calculated according to the standard curve.

2.10. Alamar blue metabolic rate assay

At 4 hours post-fertilization (hpf), 1 larva was transferred to the individual wells of 96 well plate with E3 embryo medium containing of 34.8 g NaCl, 1.6 g KCl, 5.8 g $CaCl_2$•$2H_2O$, and 9.78 g $MgCl_2$•$6H_2O$ in 1.95 L distilled water (DW) [75]. The metabolic rate of zebrafish larvae was measured by Alamar blue assay buffer. The assay buffer is supplemented to contain 1.667% E3 embryo medium, 96.233% DW, 0.1% dimethyl sulfoxide (DMSO; Sigma-Aldrich, Corp., St. Louis, MO), 1% (10×) Alamar Blue, and 400 mM sodium hydroxide. The IO extract (1, 3, and 10 μg/ml), IPA (0.3, 1.5, and 3 μM), DPHC (1.2, 6, and 12 μM), and Metformin (1, 3, and 10 μg/ml) were tested for their effects on metabolic rate were added to the assay buffer at 28 °C. From 0 to 24 h, the metabolic rate in each sample was determined by excitation at 530 nm and emission at 590 nm using a microplate reader (Gen5 version 2.05, BioTek, Winooski, Vermont, U.S.) The metabolic rate of zebrafish larvae in the samples was calculate as follows: Relative change in fluorescence = change in fluorescence (each well) / Average change in fluorescence

(control).

2.11. Statistical analysis

All of data were presented as means ± standard deviation (S.D). The mean values were calculated based on data from at least three independent experiments which were conducted on separate days using freshly prepared reagents. All the experiments were statistically analyzed using one-way analysis of variance (one-way ANOVA) and Dunnet (in GraphPad Prism Version 5.03). A p-value of less than 0.05 ($^{\#}p<0.05$, $^{\#\#}p<0.01$, and $^{\#\#\#}p<0.001$) was considered statistically significant and compared with non-treated group. A p-value of less than 0.05 ($^{*}p<0.05$, $^{**}p<0.01$, and $^{***}p<0.001$) was considered statistically significant and compared with no sample-treated group.

3. RESULTS

3.1. Examination of Troponin C and I intensity in skeletal muscle of HCD zebrafish

Muscle contraction in skeletal muscle is regulated by Ca^{2+} through specific regulatory proteins, tropomyosin and troponin [76]. Troponin C is Ca^{2+}-binding component for muscle contraction. Troponin I is an inhibitory components of contractile interaction between myosin and actin in the presence of tropomyosin [77]. In order to assess whether the muscle contraction in skeletal muscle of zebrafish are affected by high cholesterol diet (HCD) for 5 weeks, we examined Troponin C and I intensity in HCD zebrafish every week using immunofluorescence. As shown in Fig. 3-1A and B, Troponin C intensity in skeletal muscle of HCD zebrafish time-dependently decreased to 0.87-, 0.75-, 0.75-, 0.56-, and 0.42-fold of NCD group. In addition, Troponin I intensity time-dependently increased to 1.39-, 1.51-, 1.70-, 1.78-, and 1.87-fold of NCD group (Fig. 3-2C and D). These data suggest that zebrafish was affected muscle contraction by HCD. We further examined the muscle contraction in skeletal muscle of HCD zebrafish with/without IPA and DPHC supplementation.

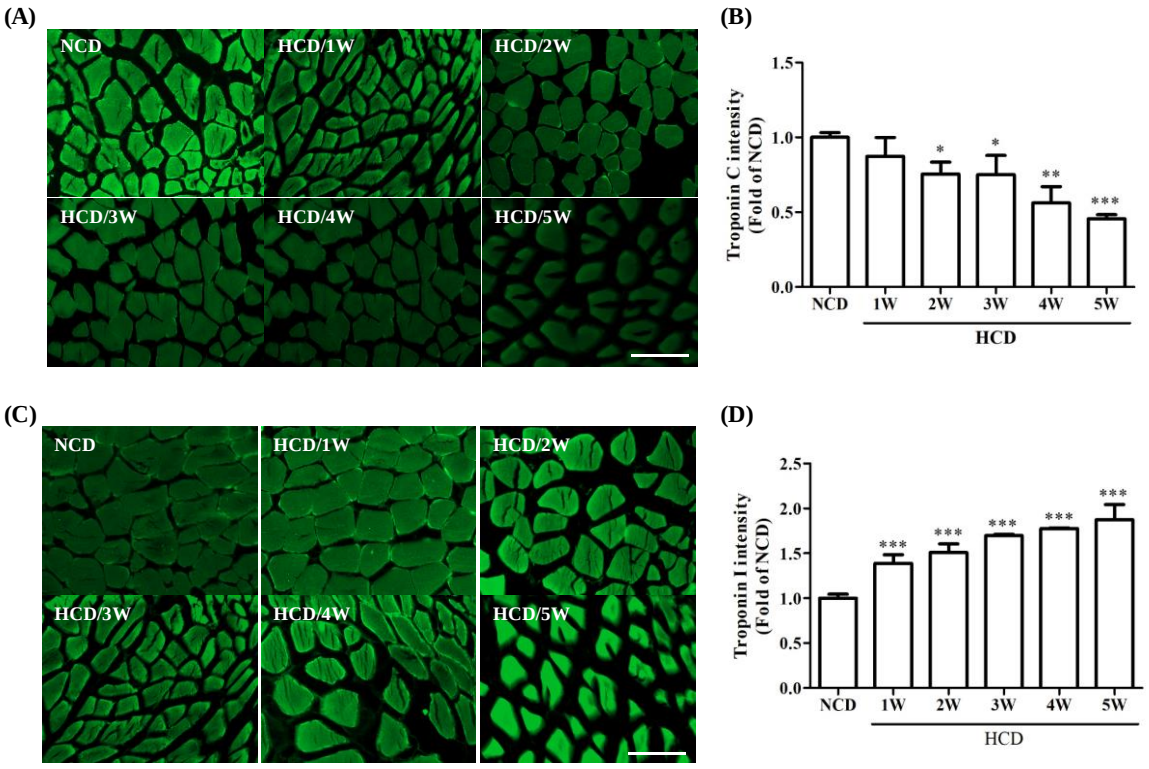

Fig. 3-1. Measurement of Troponin C & I intensity in skeletal muscle of HCD zebrafish. Zebrafish were fed HCD for 5 weeks. Representative (A) Troponin C and (C) Troponin I immunofluorescence images of skeletal muscle in HCD zebrafish at each time point. Quantitative graph was show level of (B) Troponin C and (D) Troponin I intensity from representative images and Image J software was used for measurement at each time point. Scale bar = 100 μm, Data are expressed as mean ± SE. * Values having different superscript are significantly different at $^{*}p<0.05$, $^{**}p<0.01$ and $^{***}p<0.001$ compared with NCD group.

3.2. Changes of Troponin C and I intensity by IPA supplementation on muscle contraction in HCD zebrafish

To assess whether the dysfunction of muscle contraction in HCD zebrafish were improved by IPA, we evaluated Troponin C and I intensity in skeletal muscle of HCD zebrafish using immunofluorescence. The zebrafish were fed a 4% HCD for 3 weeks, except for the normal group. After 3 weeks, zebrafish was fed a 4% HCD with or without IPA (0.0003, 0.001, and 0.003%), and Metformin (1%) supplementation for 2 weeks. As shown in Fig. 3-3, Troponin C intensity significantly decreased to 0.49-fold of NCD group. The IPA supplementation was significantly increased to 0.84-, 0.94, and 0.98-fold of HCD group. In addition, Troponin I intensity significantly increased to 1.6-fold of NCD group (Fig. 3-2). However, the IPA supplementation was significantly decreased to 1.27-, 1.16-, and 0.96-fold of HCD group. As a results, we suggest that the increased troponin C and I intensity by IPA could improve energy metabolism through an increasing cytosolic Ca^{2+} levels in the skeletal muscle of HCD zebrafish.

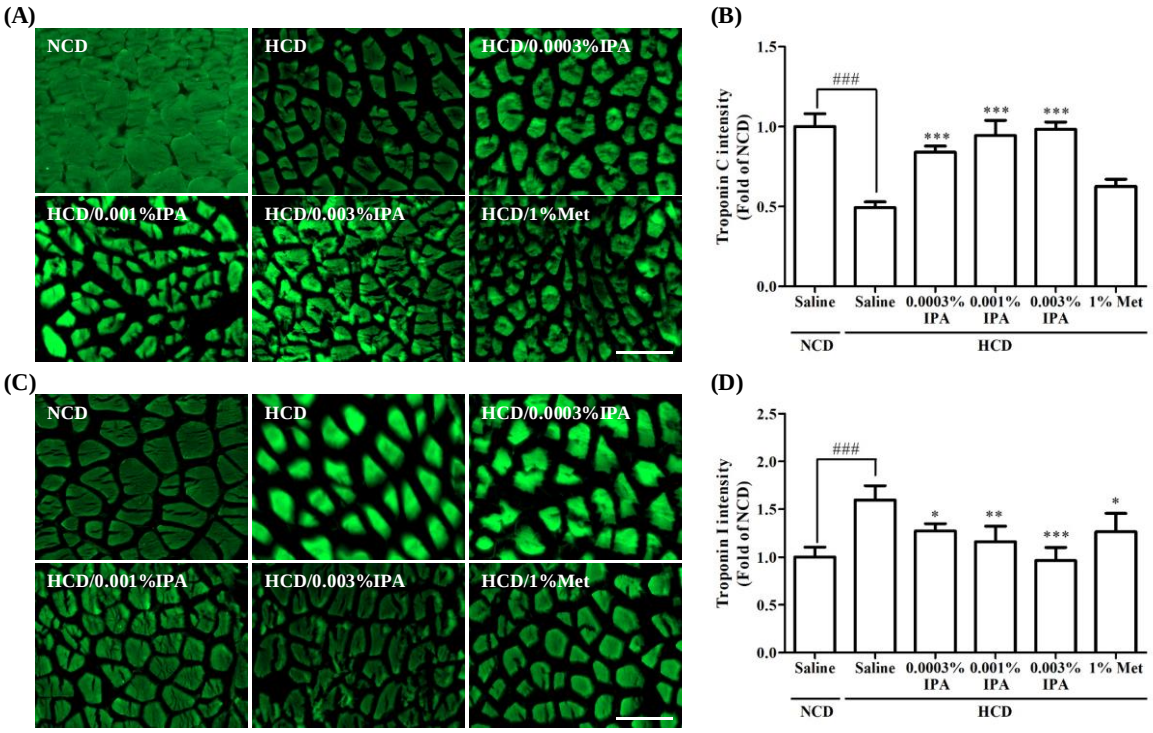

Fig. 3-2. Effect of IPA on Troponin C and I intensity increase of skeletal muscle in HCD zebrafish. Representative (A) Troponin C and (C) Troponin I immunofluorescence images of skeletal muscle in HCD zebrafish model. Quantitative graph was show level of (B) Troponin C and (D) Troponin I intensity by IPA from representative images and Image J software was used for measurement. Scale bar = 100 μm, Data are expressed as mean ± SE. * and $^{\#}$ Values having different superscript are significantly different at $^{\#\#\#}p<0.001$ compared with NCD group; * $p<0.05$, and ** $p<0.01$, and *** $p<0.001$ compared with HCD group.

3.3. Histological changes of skeletal muscle by IPA supplementation

To examine whether the histological changed skeletal muscle in HCD zebrafish was affected by IPA supplementation for protection of skeletal muscle, we investigated the effect of IPA on the change in morphology by using hematoxylin and eosin (H&E) staining. As shown in Fig. 3-3, the size of skeletal muscle from the histological changes in HCD zebrafish was decreased compared with that in NCD zebrafish, whereas the size of skeletal muscle was increased in the HCD/IPA and HCD/1%Met. This data suggested that IPA supplementation could protect against histological changed skeletal muscle that occurs in HCD-induced imbalance of energy metabolism.

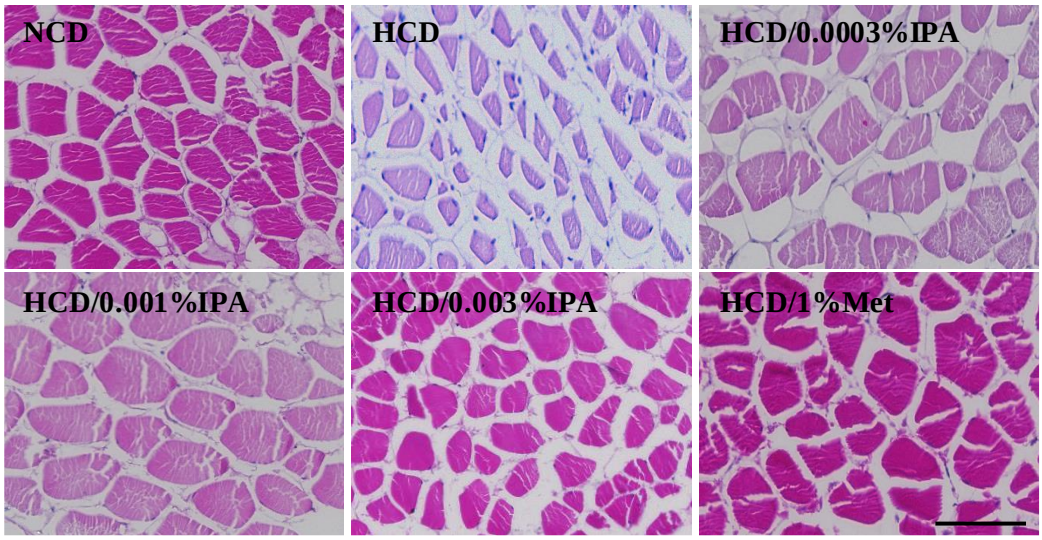

Fig. 3-3. Histological changes of skeletal muscle by IPA supplementation in HCD zebrafish. Representative histological changes of skeletal muscle by IPA supplementation in HCD zebrafish model using H&E staining. Scale bar = 100 μm.

3.4. Changes of Troponin C and I intensity by DPHC supplementation on muscle contraction in HCD zebrafish

To assess whether the dysfunction of muscle contraction in HCD zebrafish were improved by DPHC, we evaluated Troponin C and I intensity in skeletal muscle of HCD zebrafish using immunofluorescence. The zebrafish were fed a 4% HCD for 3 weeks, except for the normal group. After 3 weeks, zebrafish was fed a 4% HCD with or without DPHC (0.0003, 0.001, and 0.003%), and Metformin (1%) supplementation for 2 weeks. As shown in Fig. 3-4A and B, Troponin C intensity significantly decreased to 0.48-fold of NCD group. The DPHC supplementation was significantly increased to 0.53-, 0.94, and 1.01-fold of HCD group. In addition, Troponin I intensity significantly increased to 1.58-fold of NCD group (Fig. 3-4C and D). However, the DPHC supplementation was significantly decreased to 1.62-, 1.09-, and 0.98-fold of HCD group. As a results, we suggest that the increased troponin C and I intensity by DPHC could improve energy metabolism through an increasing cytosolic Ca^{2+} levels in the skeletal muscle of HCD zebrafish.

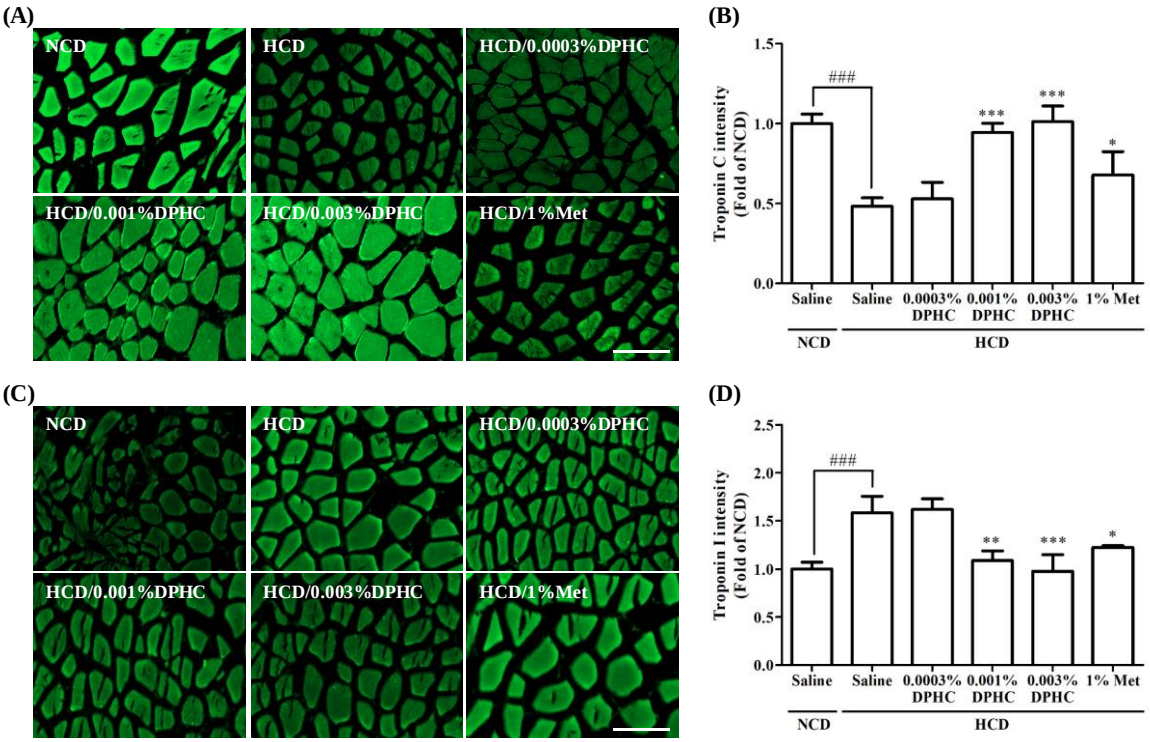

Fig. 3-4. Effect of DPHC on Troponin C and I intensity increase of skeletal muscle in HCD zebrafish. Representative (A) Troponin C and (C) Troponin I immunofluorescence images of skeletal muscle in HCD zebrafish model. Quantitative graph was show level of (B) Troponin C and (D) Troponin I intensity by DPHC from representative images and Image J software was used for measurement. Scale bar = 100 μm, Data are expressed as mean ± SE. * and $^{\#}$ Values having different superscript are significantly different at $^{\#\#\#}p$ <0.001 compared with NCD group; $^{*}p$ <0.05, $^{**}p$ <0.01, and $^{***}p$ <0.001 compared with HCD group.

3.5. Histological changes of skeletal muscle by DPHC supplementation

To examine whether the histological changed skeletal muscle in HCD zebrafish was affected by DPHC supplementation for protection of skeletal muscle, we investigated the effect of DPHC on the change in morphology by using hematoxylin and eosin (H&E) staining. As shown in Fig. 3-5, the size of skeletal muscle from the histological changes in HCD zebrafish was decreased compared with that in NCD zebrafish, whereas the size of skeletal muscle was increased in the HCD/DPHC and HCD/1%Met. This data suggested that DPHC supplementation could protect against histological changed skeletal muscle that occurs in HCD-induced imbalance of energy metabolism.

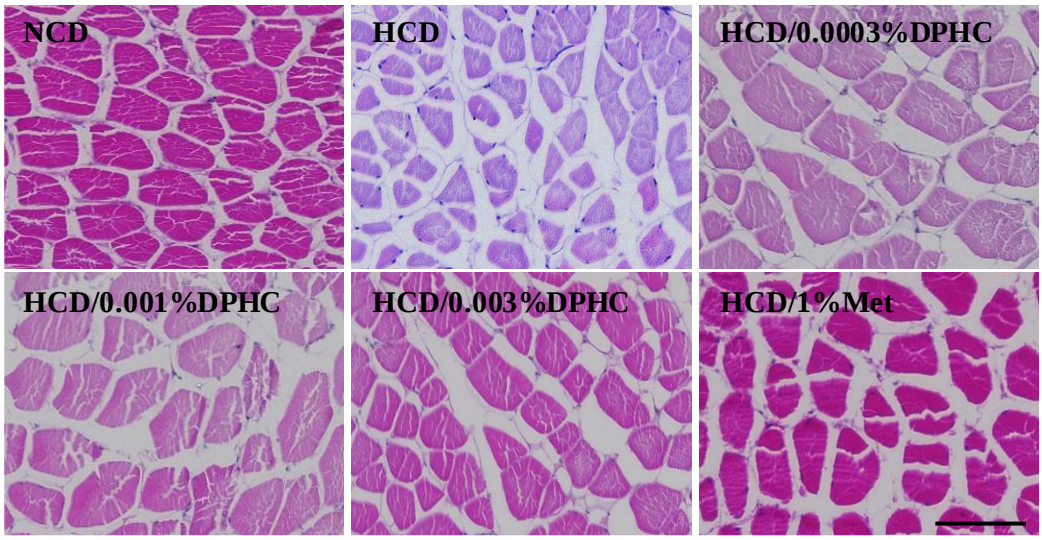

Fig. 3-5. Histological changes of skeletal muscle by DPHC supplementation in HCD zebrafish. Representative histological changes of skeletal muscle by DPHC supplementation in HCD zebrafish model using H&E staining. Scale bar = 100 μm.

3.6. Change of the CaMKII expression level by IPA and DPHC in zebrafish muscle tissue

To examine the CaMKII that are involved in the improvement of glucose tolerance by IPA and DPHC in the muscle of alloxan-induced hyperglycemic zebrafish as type 1 diabetes model and HCD zebrafish as type 2 diabetes model. As shown in Fig. 3-6A, IPA-injected group significantly increased the CaMKII level reduction in hyperglycemic zebrafish muscle. Whereas BAPTA-injected group was inactivated these proteins and unchanged in the presence of IPA. In addition, DPHC-injected group significantly increased the reduced CaMKII level of muscle in hyperglycemic zebrafish, whilst this increase was abolished with BAPTA-injected group (Fig. 3-6B).

As shown in Fig. 3-7, the CaMKII level of muscle was significantly decreased by HCD. However, IPA and DPHC supplementation significantly increased the CaMKII level reduction in muscle of HCD zebrafish. Also, the CaMKII level was significantly increased by Metformin supplementation. These data suggest that IPA and DPHC can improve the glucose homeostasis by muscle contraction in type 1 and type 2 diabetes model.

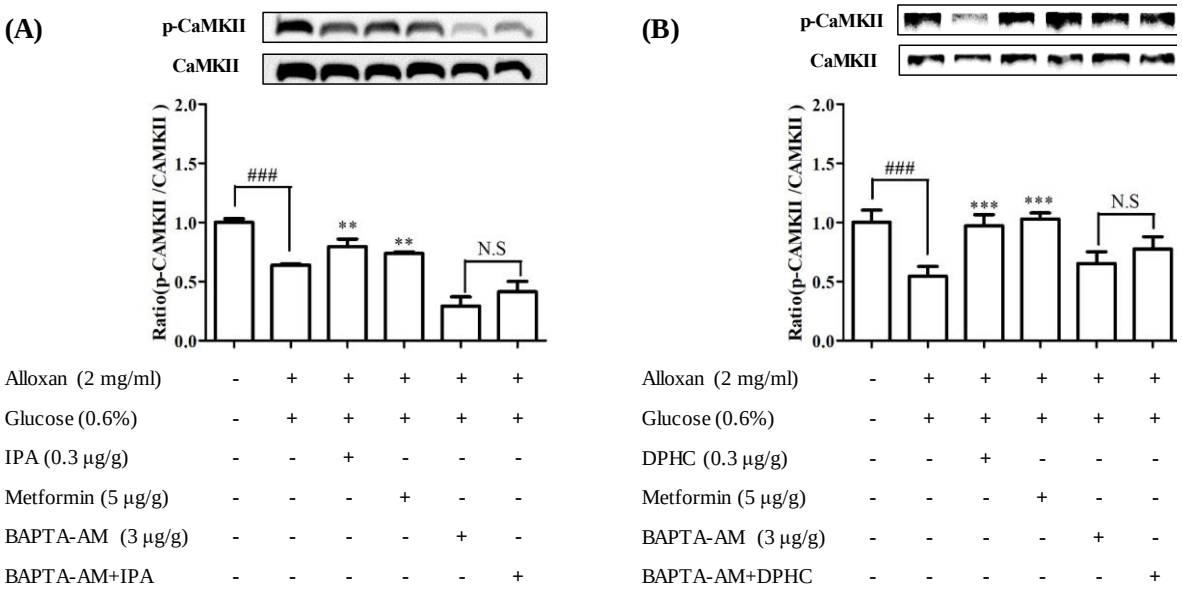

Fig. 3-6. The CaMKII expression level by IPA and DPHC in hyperglycemic zebrafish muscle tissues. The zebrafish exposed to 0.6% glucose and then injected with (A) IPA (0.3 μg/g) or (B) DPHC (0.3 μg/g) or Metformin (5 μg/g) for 90 min. Zebrafish were pre-injected with BAPTA-AM (3 μg/g) for 1 h. Tissues were analyzed CaMKII by western blotting and signal intensity were evaluated by the Fusion FX7 acquisition system (Vibert Lourmat, Eberhardzell, Germany). Data expressed as the mean ± SE, n = 4 per group. $^{###}p<0.001$; compared to non-treated group, $^{**}p<0.01$, and $^{***}p<0.001$; compared to control. N.S; No Significant.

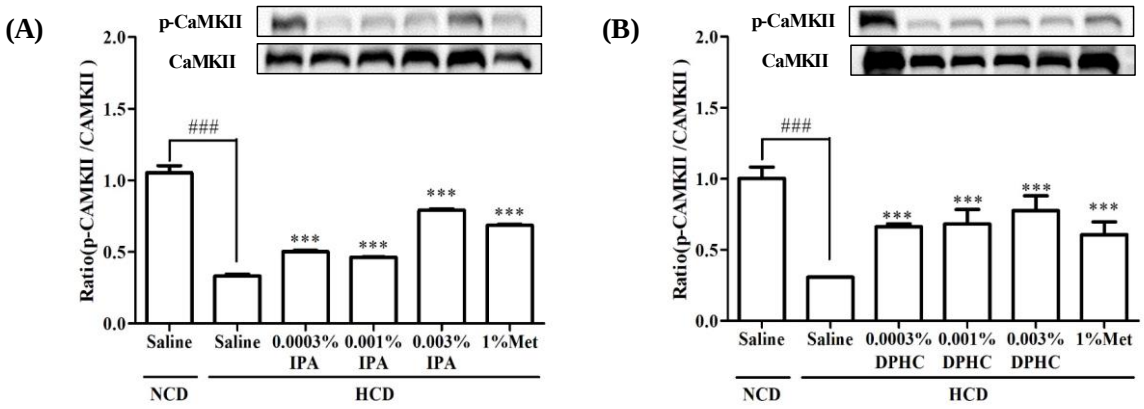

Fig. 3-7. The CaMKII expression level by IPA and DPHC in HCD zebrafish muscle tissues. Zebrafish were fed HCD supplemented (A) IPA (0.0003, 0.001, and 0.003%, HCD/IPA), (B) DPHC (0.0003, 0.001, and 0.003%, HCD/DPHC) and Metformin (1%, HCD/Met) for 2 weeks followed by additional 3 weeks of HCD. Tissues were analyzed CaMKII by western blotting and signal intensity were evaluated by the Fusion FX7 acquisition system (Vibert Lourmat, Eberhardzell, Germany). Data are expressed as mean ± SE. * and $^{\#}$ Values having different superscript are significantly different at $^{\#\#\#}p<0.001$ compared with the NCD group; $^{***}p<0.001$ compared with the HCD/Saline group. N.S; No Significant.

3.7. Measurement of ATP level by IPA and DPHC in zebrafish muscle tissue

The Ca^{2+} release into the myofibril induced to initiate the muscle contraction resulting in the increasing ATP demand via the activity of the myosin and Ca^{2+} ATPases [50]. In addition, AMPK modulate between reduction of ATP consumption and increasing of ATP production as energy sensor [61]. To assess the ATP level through energy homeostasis, we used an alloxan-induced hyperglycemia zebrafish as type 1 diabetes model and High cholesterol diet (HCD) zebrafish as type 2 diabetes model. As shown in Fig. 3-8A, IPA significantly increased the ATP level reduction in hyperglycemic zebrafish muscle. However, upon ATP reduction, BAPTA-injected group was unchanged regardless of IPA treatment. Additionally, DPHC treatment modestly increased the reduced ATP level of skeletal muscle in hyperglycemia zebrafish, whilst this increase was abolished with BAPTA-AM treatment (Fig. 3-8B). This result showed that the cytosolic Ca^{2+} release from SR by IPA and DPHC is indispensable for its effect of glucose and energy homeostasis in hyperglycemic zebrafish upon suppression of insulin secretion.

In Fig. 3-9, the ATP level of skeletal muscle was significantly decreased by HCD. However, IPA supplementation significantly increased the ATP level reduction in HCD zebrafish muscle (Fig. 3-9A). Also, DPHC supplementation significantly increased the ATP level reduction in HCD zebrafish muscle (Fig. 3-9B). In addition, the ATP level was significantly increased by Metformin. As a result, we suggest that IPA and DPHC can induce ATP production through improved glucose tolerance in HCD zebrafish.

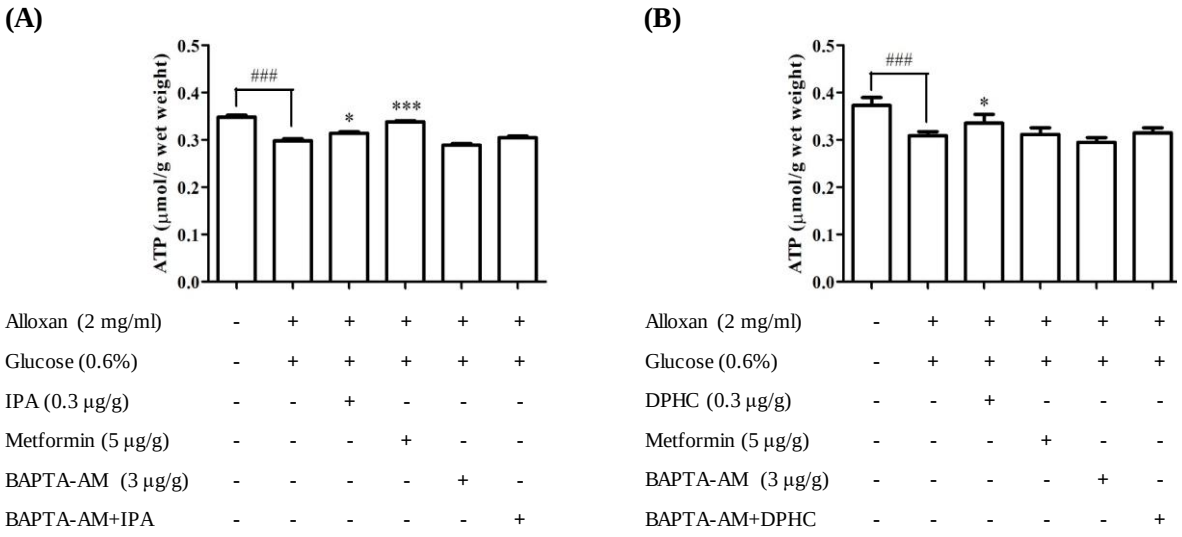

Fig. 3-8. Measurement of ATP levels in an alloxan-induced hyperglycemia zebrafish muscle tissues. Zebrafish were injected with BAPTA-AM (3 μg/g body weight) for 1 h, after which the zebrafish were injected with (A) IPA (0.3 μg/g body weight) or (B) DPHC (0.3 μg/g body weight) for 90 min. Experiments were performed in triplicate and the data are expressed as mean ± SE, n = 3 per group. * and $^{\#}$ Values having different superscript are significantly different at *p<0.05 compared with the no sample-treated group; $^{\#\#\#}$ p<0.0001 compared with the non-treated group.

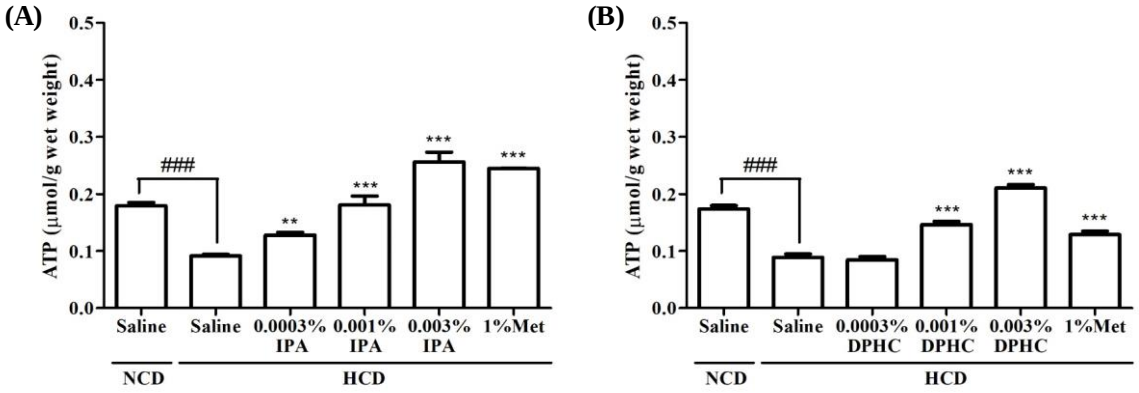

Fig. 3-9. Measurement of ATP levels in HCD zebrafish muscle tissues. Zebrafish were fed 4% HCD supplemented (A) IPA (0.3 μg/g body weight) or (B) DPHC (0.3 μg/g body weight) for 2 weeks followed by additional 3 weeks of HCD. Experiments were performed in triplicate and the data are expressed as mean ± SE, n = 3 per group. * and $^{\#}$ Values having different superscript are significantly different at $^{**}p<0.01$ and $^{***}p<0.001$ compared with HCD group; $^{\#\#\#}p<0.001$ compared with NCD group.

3.8. Improvement of energy expenditure from IPA and DPHC

We examined the effect of IPA and DPHC energy expenditure in zebrafish larvae. The larvae were exposed IPA (0.3, 1.5, and 3 μM) and DPHC (1.2, 6, and 12 μM) for 24 h and energy expenditure was assessed using an Alamar blue assay. As shown in Fig. 3-10A and C, IPA and DPHC showed the energy expenditure with increasing fluorescence, at each time point compare to the control group. The area under the curve (AUC) of fluorescence change suggest to evaluate the degree of the energy expenditure in IPA and DPHC treatment (Fig. 3-10B and D). The AUC of fluorescence change in IPA and DPHC treatment was significantly increased, compared to the control group. These data suggest that IPA and DPHC can induce energy expenditure for homeostasis.

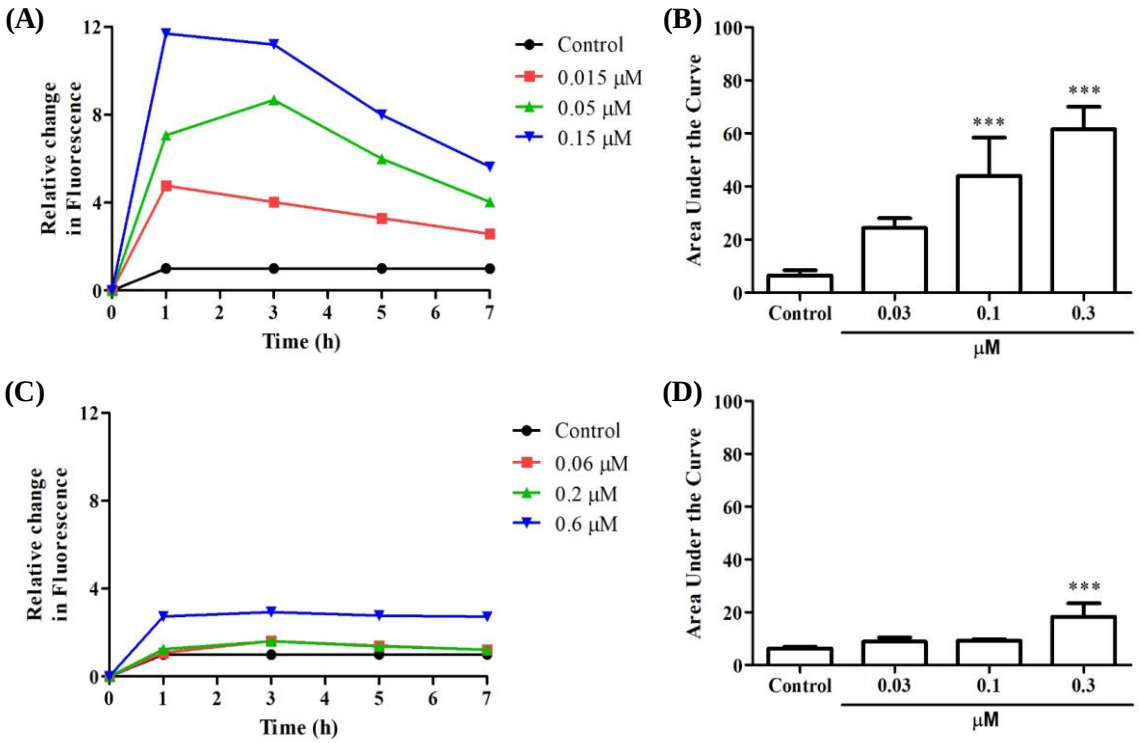

Fig. 3-10. Detection of energy expenditure IPA and DPHC using Alamar blue. The larvae were exposed to IPA (0.3, 1.5, and 3 μM), and DPHC (1.2, 6, and 12 μM) with Alamar blue. Energy expenditure was measured from relative change in Fluorescence in response to addition of (A) IPA and (C) DPHC. Area under the curve (AUC) from the energy expenditure in all zebrafish groups at each time point. Data are expressed as the mean ± SE (n = 4 for each group). * Values having different superscript are significantly different at $^{***}p<0.001$ compared with the non-treated group.

4. DISCUSSION

Homeostasis is the maintenance of stable internal environment which means regulating many parameters including blood glucose level and energy status in human [78,79]. In skeletal muscle, the efficient energy expenditure is decreased in diabetes mellitus including type1 and type2 [17,18]. In addition, muscle contraction in skeletal muscle is a highly effective prophylactic against the hyperglycemia associated with the diabetes mellitus and induce glucose uptake by signaling pathways [6,7]. Moreover, during muscle contraction, energy expenditure is conducted by the molecular components including AMPK and CaMKII [16,80].

AMPK, an important cellular energy sensor, regulates metabolic energy balance at the whole-body level [81]. Previous study reported that activation of AMPK increased the NAD^+/NADH ratio in skeletal muscle cells resulting in energy expenditure [82]. In our study, AMPK activation by IPA and DPHC treatment can induce energy expenditure resulting in the regulation of homeostasis in diabetes zebrafish model.

In addition, AMPK and CaMKII activation promotes Glut4 translocation and increases glucose uptake directly in skeletal muscle [9,33]. Previous study showed that caffeine treatment was induced the activation of CaMKII by muscle contraction via release of Ca^{2+} from the SR in rat muscle [83]. We confirmed that IPA and DPHC can activate CaMKII in skeletal muscle tissue of diabetes zebrafish by western blot analysis. Our result showed that IPA and DPHC can stimulate the activation of CaMKII which was intermediated by cytosolic Ca^{2+} in skeletal muscle of diabetes zebrafish.

The major energy-consuming processes are release and uptake of by the SR and the actomyosin interaction [84]. The energy source during the muscle contraction is provided by adenosine 5'-triphosphate (ATP) [15]. ATP is produced from glucose through the glycolytic pathway. In

addition, AMPK could regulate the reduced ATP consumption and increase ATP production in skeletal muscle [14]. Cells were known to cause metabolic disease such as obesity and diabetes by breaking the mechanisms involved in controlling metabolism by suppressing energy consumption when energy is lacking [85]. We suggest that IPA and DPHC can stimulate the activation of AMPK, it is associated to reduce ATP consumption and increase ATP production through glycolytic pathway resulting in the maintenance of energy homeostasis in diabetes zebrafish.

We further examined the Ca^{2+}-induced Troponin C and I intensity in skeletal muscle of diabetes zebrafish. Muscle contraction is switched on and off by the troponin and tropomyosin reacting in concert to changes in cytosolic Ca^{2+} levels. Troponin C initiate structural changes between the thin filaments and thick filaments in response to cytosolic Ca^{2+} level. Troponin I is an inhibitor of the contractile ATPase in muscle [86]. In our study, IPA and DPHC can stimulate muscle contraction via increasing cytosolic Ca2+ level in skeletal muscle of diabetes zebrafish. Therefore, findings from this study applicate a mechanistic and integrative approach linking muscle contraction by IPA and DPHC in skeletal muscle as a potential therapeutic mechanism to improve energy metabolism without distinguishing type 1 and type 2.

5. CONCLUSION

In conclusion, the present study demonstrates that IPA and DPHC can stimulate muscle contraction resulting in the maintenance of energy homeostasis in muscle of diabetes zebrafish. We expect *Ishige okamurae* including IPA and DPHC to become a useful ingredient in processed foods and dietary supplements that will have glucose and energy homeostasis promoting effects in diabetes.

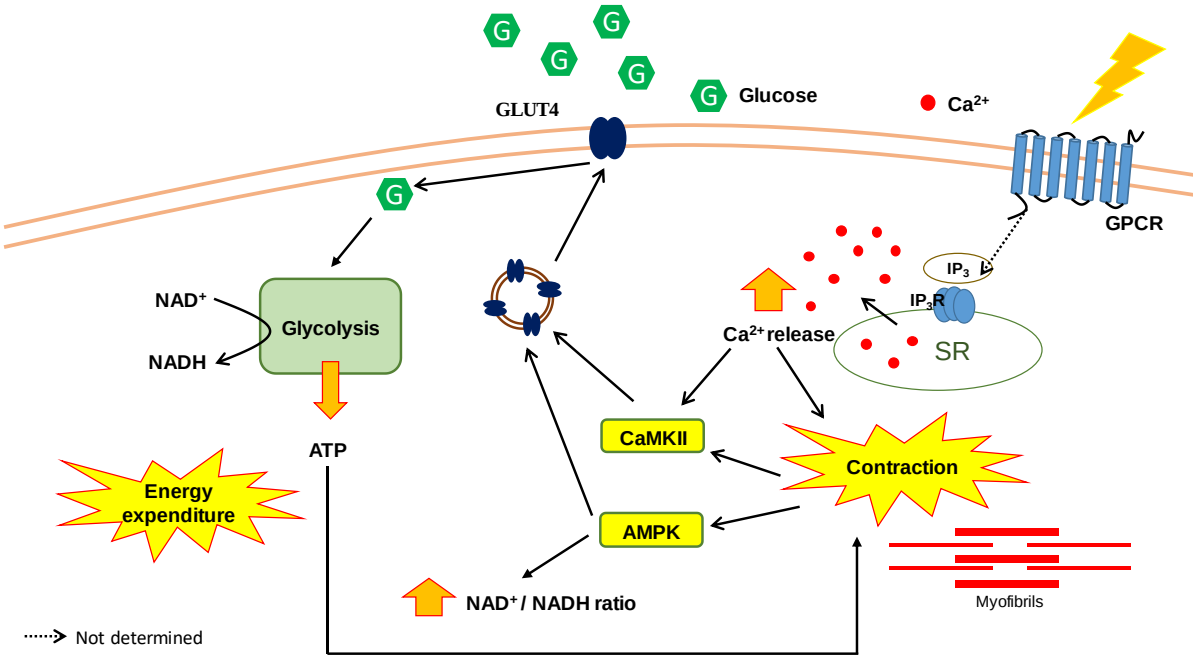

Fig. 3-11. Mechanism of glucose homeostasis in skeletal muscle

References

1. Rudkowska, I. Functional foods for health: focus on diabetes. *Maturitas* **2009**, *62*, 263-269.
2. Koolman, J.; Röhm, K.-H.; Wirth, J.; Robertson, M. *Color atlas of biochemistry*; Thieme Stuttgart: 2005; Vol. 2.
3. Meng, Z.-X.; Li, S.; Wang, L.; Ko, H.J.; Lee, Y.; Jung, D.Y.; Okutsu, M.; Yan, Z.; Kim, J.K.; Lin, J.D. Baf60c drives glycolytic metabolism in the muscle and improves systemic glucose homeostasis through Deptor-mediated Akt activation. *Nature medicine* **2013**, *19*, 640.
4. Meng, Z.-X.; Gong, J.; Chen, Z.; Sun, J.; Xiao, Y.; Wang, L.; Li, Y.; Liu, J.; Xu, X.S.; Lin, J.D. Glucose sensing by skeletal myocytes couples nutrient signaling to systemic homeostasis. *Molecular cell* **2017**, *66*, 332-344. e334.
5. Richter, E.A.; Hargreaves, M. Exercise, GLUT4, and skeletal muscle glucose uptake. *Physiological reviews* **2013**, *93*, 993-1017.
6. Castro, A.J.G.; Frederico, M.J.S.; Cazarolli, L.H.; Mendes, C.P.; Bretanha, L.C.; Schmidt, É.C.; Bouzon, Z.L.; de Medeiros Pinto, V.A.; da Fonte Ramos, C.; Pizzolatti, M.G. The mechanism of action of ursolic acid as insulin secretagogue and insulinomimetic is mediated by cross-talk between calcium and kinases to regulate glucose balance. *Biochimica et Biophysica Acta (BBA)-General Subjects* **2015**, *1850*, 51-61.
7. Goodyear, L.J.; Kahn, B.B. Exercise, glucose transport, and insulin sensitivity. *Annual review of medicine* **1998**, *49*, 235-261.
8. Shepherd, P.R.; Kahn, B.B. Glucose transporters and insulin action—implications for insulin resistance and diabetes mellitus. *New England Journal of Medicine* **1999**, *341*, 248-257.
9. Ojuka, E.O.; Goyaram, V.; Smith, J.A. The role of CaMKII in regulating GLUT4 expression in skeletal muscle. *American Journal of Physiology-Endocrinology and Metabolism* **2012**, *303*, E322-E331.
10. Chin, E.R. Role of Ca2+/calmodulin-dependent kinases in skeletal muscle plasticity. *Journal of applied Physiology* **2005**, *99*, 414-423.
11. Holloszy, J.O.; Narahara, H. Nitrate ions: potentiation of increased permeability to sugar associated with muscle contraction. *Science* **1967**, *155*, 573-575.
12. Berchtold, M.W.; Brinkmeier, H.; Muntener, M. Calcium ion in skeletal muscle: its crucial role for muscle function, plasticity, and disease. *Physiological reviews* **2000**, *80*, 1215-1265.
13. Hansen, P.A.; Gulve, E.A.; Marshall, B.A.; Gao, J.; Pessin, J.E.; Holloszy, J.O.; Mueckler, M. Skeletal muscle glucose transport and metabolism are enhanced in transgenic mice overexpressing the Glut4 glucose transporter. *Journal of Biological Chemistry* **1995**, *270*, 1679-1684.
14. Liu, W.; Zhao, J. Insights into the molecular mechanism of glucose metabolism regulation under stress in chicken skeletal muscle tissues. *Saudi journal of biological sciences* **2014**, *21*, 197-203.

15. Westerblad, H.; Bruton, J.D.; Katz, A. Skeletal muscle: energy metabolism, fiber types, fatigue and adaptability. *Experimental cell research* **2010**, *316*, 3093-3099.
16. Cantó, C.; Auwerx, J. PGC-1alpha, SIRT1 and AMPK, an energy sensing network that controls energy expenditure. *Current opinion in lipidology* **2009**, *20*, 98.
17. Hebert, S.L.; Nair, K.S. Protein and energy metabolism in type 1 diabetes. *Clinical Nutrition* **2010**, *29*, 13-17.
18. He, J.; Watkins, S.; Kelley, D.E. Skeletal muscle lipid content and oxidative enzyme activity in relation to muscle fiber type in type 2 diabetes and obesity. *Diabetes* **2001**, *50*, 817-823.
19. Kawanaka, K. Regulation of glucose transport in skeletal muscle during and after exercise. *The Journal of Physical Fitness and Sports Medicine* **2012**, *1*, 563-572.
20. Homsher, E. Muscle enthalpy production and its relationship to actomyosin ATPase. *Annual Review of Physiology* **1987**, *49*, 673-690.
21. Cohen, N.; Shaw, J. Diabetes: advances in treatment. *Internal medicine journal* **2007**, *37*, 383-388.
22. Nathan, D.M. Diabetes: advances in diagnosis and treatment. *Jama* **2015**, *314*, 1052-1062.
23. Kazeem, M.I.; Davies, T.C. Anti-diabetic functional foods as sources of insulin secreting, insulin sensitizing and insulin mimetic agents. *Journal of Functional Foods* **2016**, *20*, 122-138.
24. Xing, X.-H.; Zhang, Z.-M.; Hu, X.-Z.; Wu, R.-Q.; Xu, C. Antidiabetic effects of Artemisia sphaerocephala Krasch. gum, a novel food additive in China, on streptozotocin-induced type 2 diabetic rats. *Journal of ethnopharmacology* **2009**, *125*, 410-416.
25. Latha, R.C.R.; Daisy, P. Insulin-secretagogue, antihyperlipidemic and other protective effects of gallic acid isolated from Terminalia bellerica Roxb. in streptozotocin-induced diabetic rats. *Chemico-biological interactions* **2011**, *189*, 112-118.
26. Holdt, S.L.; Kraan, S. Bioactive compounds in seaweed: functional food applications and legislation. *Journal of applied phycology* **2011**, *23*, 543-597.
27. Kiuru, P.; D′Auria, M.V.; Muller, C.D.; Tammela, P.; Vuorela, H.; Yli-Kauhaluoma, J. Exploring marine resources for bioactive compounds. *Planta Medica* **2014**, *80*, 1234-1246.
28. Sanjeewa, K.A.; Lee, W.W.; Kim, J.-I.; Jeon, Y.-J. Exploiting biological activities of brown seaweed Ishige okamurae Yendo for potential industrial applications: a review. *Journal of applied phycology* **2017**, *29*, 3109-3119.
29. Heo, S.-J.; Hwang, J.-Y.; Choi, J.-I.; Han, J.-S.; Kim, H.-J.; Jeon, Y.-J. Diphlorethohydroxycarmalol isolated from Ishige okamurae, a brown algae, a potent α-glucosidase and α-amylase inhibitor, alleviates postprandial hyperglycemia in diabetic mice. *European Journal of Pharmacology* **2009**, *615*, 252-256.
30. Min, K.-H.; Kim, H.-J.; Jeon, Y.-J.; Han, J.-S. Ishige okamurae ameliorates hyperglycemia and insulin resistance in C57BL/KsJ-db/db mice. *Diabetes research and clinical practice* **2011**, *93*,

70-76.

31. Seth, A.; Stemple, D.L.; Barroso, I. The emerging use of zebrafish to model metabolic disease. *Disease models & mechanisms* **2013**, *6*, 1080-1088.
32. Capiotti, K.M.; Junior, R.A.; Kist, L.W.; Bogo, M.R.; Bonan, C.D.; Da Silva, R.S. Persistent impaired glucose metabolism in a zebrafish hyperglycemia model. *Comparative Biochemistry and Physiology Part B: Biochemistry and Molecular Biology* **2014**, *171*, 58-65.
33. Kim, E.-A.; Lee, S.-H.; Lee, J.-H.; Kang, N.; Oh, J.-Y.; Ahn, G.; Ko, S.C.; Fernando, S.P.; Kim, S.-Y.; Park, S.-J. A marine algal polyphenol, dieckol, attenuates blood glucose levels by Akt pathway in alloxan induced hyperglycemia zebrafish model. *RSC Advances* **2016**, *6*, 78570-78575.
34. Zang, L.; Shimada, Y.; Nishimura, N. Development of a novel zebrafish model for type 2 diabetes mellitus. *Scientific reports* **2017**, *7*, 1461.
35. Ryu, B.; Jiang, Y.; Kim, H.-S.; Hyun, J.-M.; Lim, S.-B.; Li, Y.; Jeon, Y.-J. Ishophloroglucin A, a novel phlorotannin for standardizing the anti-α-glucosidase activity of Ishige okamurae. *Marine drugs* **2018**, *16*, 436.
36. Heo, S.-J.; Kim, J.-P.; Jung, W.-K.; Lee, N.-H.; Kang, H.-S.; Jun, E.-M.; Park, S.-H.; Kang, S.-M.; Lee, Y.-J.; Park, P.-J. Identification of chemical structure and free radical scavenging activity of diphlorethohydroxycarmalol isolated from a brown alga, Ishige okamurae. *J Microbiol Biotechnol* **2008**, *18*, 676-681.
37. Balasubramanian, R.; Robaye, B.; Boeynaems, J.-M.; Jacobson, K.A. Enhancement of glucose uptake in mouse skeletal muscle cells and adipocytes by P2Y6 receptor agonists. *PloS one* **2014**, *9*, e116203.
38. Shin, E.; Hong, B.N.; Kang, T.H. An optimal establishment of an acute hyperglycemia zebrafish model. *African Journal of Pharmacy and Pharmacology* **2012**, *6*, 2922-2928.
39. Zhang, Y.; Shi, J.; Zhao, Y.; Cui, H.; Cao, C.; Liu, S. An investigation of the anti-diabetic effects of an extract from Cladonia humilis. *Pakistan journal of pharmaceutical sciences* **2012**, *25*, 509-512.
40. Panahi, Y.; Mojtahedzadeh, M.; Zekeri, N.; Beiraghdar, F.; Khajavi, M.-R.; Ahmadi, A. Metformin treatment in hyperglycemic critically ill patients: another challenge on the control of adverse outcomes. *Iranian journal of pharmaceutical research: IJPR* **2011**, *10*, 913.
41. Higaki, Y.; Mikami, T.; Fujii, N.; Hirshman, M.F.; Koyama, K.; Seino, T.; Tanaka, K.; Goodyear, L.J. Oxidative stress stimulates skeletal muscle glucose uptake through a phosphatidylinositol 3-kinase-dependent pathway. *American Journal of Physiology-Endocrinology and Metabolism* **2008**, *294*, E889-E897.
42. Kumar, N.; Shaw, P.; Razzokov, J.; Yusupov, M.; Attri, P.; Uhm, H.S.; Choi, E.H.; Bogaerts, A. Enhancement of cellular glucose uptake by reactive species: a promising approach for diabetes therapy. *RSC advances* **2018**, *8*, 9887-9894.

43. Clausen, T.; Elbrink, J.; Dahl-Hansen, A. The relationship between the transport of glucose and cations across cell membranes in isolated tissues. IX. The role of cellular calcium in the activation of the glucose transport system in rat soleus muscle. *Biochimica et Biophysica Acta (BBA)-Biomembranes* **1975**, *375*, 292-308.
44. Khamaisi, M.; Potashnik, R.; Tirosh, A.; Demshchak, E.; Rudich, A.; Trischler, H.; Wessel, K.; Bashan, N. Lipoic acid reduces glycemia and increases muscle GLUT4 content in streptozotocin-diabetic rats. *Metabolism* **1997**, *46*, 763-768.
45. Berger, J.; Biswas, C.; Vicario, P.P.; Strout, H.V.; Saperstein, R.; Pilch, P.F. Decreased expression of the insulin-responsive glucose transporter in diabetes and fasting. *Nature* **1989**, *340*, 70.
46. Siddiqui, M.R.; Moorthy, K.; Taha, A.; Hussain, M.E.; Baquer, N.Z. Low doses of vanadate and Trigonella synergistically regulate Na+/K+-ATPase activity and GLUT4 translocation in alloxan-diabetic rats. *Molecular and cellular biochemistry* **2006**, *285*, 17-27.
47. Jessen, N.; Goodyear, L.J. Contraction signaling to glucose transport in skeletal muscle. *Journal of Applied Physiology* **2005**, *99*, 330-337.
48. Waller, A.P.; Kalyanasundaram, A.; Hayes, S.; Periasamy, M.; Lacombe, V.A. Sarcoplasmic reticulum Ca2+ ATPase pump is a major regulator of glucose transport in the healthy and diabetic heart. *Biochimica et Biophysica Acta (BBA)-Molecular Basis of Disease* **2015**, *1852*, 873-881.
49. Tsuchiya, Y.; Hatakeyama, H.; Emoto, N.; Wagatsuma, F.; Matsushita, S.; Kanzaki, M. Palmitate-induced down-regulation of sortilin and impaired GLUT4 trafficking in C2C12 myotubes. *Journal of Biological Chemistry* **2010**, *285*, 34371-34381.
50. MacIntosh, B.R.; Holash, R.J.; Renaud, J.-M. Skeletal muscle fatigue–regulation of excitation–contraction coupling to avoid metabolic catastrophe. *J Cell Sci* **2012**, *125*, 2105-2114.
51. Minokoshi, Y.; Toda, C.; Okamoto, S. Regulatory role of leptin in glucose and lipid metabolism in skeletal muscle. *Indian journal of endocrinology and metabolism* **2012**, *16*, S562.
52. Sinacore, D.R.; Gulve, E.A. The role of skeletal muscle in glucose transport, glucose homeostasis, and insulin resistance: implications for physical therapy. *physical therapy* **1993**, *73*, 878-891.
53. Tanner, C.J.; Koves, T.R.; Cortright, R.L.; Pories, W.J.; Kim, Y.-B.; Kahn, B.B.; Dohm, G.L.; Houmard, J.A. Effect of short-term exercise training on insulin-stimulated PI 3-kinase activity in middle-aged men. *American Journal of Physiology-Endocrinology And Metabolism* **2002**, *282*, E147-E153.
54. Röckl, K.S.; Witczak, C.A.; Goodyear, L.J. Signaling mechanisms in skeletal muscle: acute responses and chronic adaptations to exercise. *IUBMB life* **2008**, *60*, 145-153.
55. Kuo, I.Y.; Ehrlich, B.E. Signaling in muscle contraction. *Cold Spring Harbor perspectives in biology* **2015**, *7*, a006023.
56. Suh, S.-H.; Paik, I.-Y.; Jacobs, K. Regulation of blood glucose homeostasis during prolonged.

Mol cells **2007**, *23*, 272-279.

57. Özcan, U.; Yilmaz, E.; Özcan, L.; Furuhashi, M.; Vaillancourt, E.; Smith, R.O.; Görgün, C.Z.; Hotamisligil, G.S. Chemical chaperones reduce ER stress and restore glucose homeostasis in a mouse model of type 2 diabetes. *Science* **2006**, *313*, 1137-1140.
58. Blodgett, A.B.; Kothinti, R.K.; Kamyshko, I.; Petering, D.H.; Kumar, S.; Tabatabai, N.M. A fluorescence method for measurement of glucose transport in kidney cells. *Diabetes technology & therapeutics* **2011**, *13*, 743-751.
59. Ko, S.-C.; Lee, M.; Lee, J.-H.; Lee, S.-H.; Lim, Y.; Jeon, Y.-J. Dieckol, a phlorotannin isolated from a brown seaweed, Ecklonia cava, inhibits adipogenesis through AMP-activated protein kinase (AMPK) activation in 3T3-L1 preadipocytes. *Environmental toxicology and pharmacology* **2013**, *36*, 1253-1260.
60. Braun, B.; Zimmermann, M.B.; Kretchmer, N. Effects of exercise intensity on insulin sensitivity in women with non-insulin-dependent diabetes mellitus. *Journal of Applied Physiology* **1995**, *78*, 300-306.
61. Egawa, T.; Tsuda, S.; Oshima, R.; Goto, A.; Ma, X.; Goto, K.; Hayashi, T. Regulatory mechanism of skeletal muscle glucose transport by phenolic acids. *Phenolic compounds–Biological activities* **2017**, 169-191.
62. Eggen, D.A. Cholesterol metabolism in groups of rhesus monkeys with high or low response of serum cholesterol to an atherogenic diet. *Journal of lipid research* **1976**, *17*, 663-673.
63. Li, X.; Chen, Y.; Liu, J.; Yang, G.; Zhao, J.; Liao, G.; Shi, M.; Yuan, Y.; He, S.; Lu, Y. Serum metabolic variables associated with impaired glucose tolerance induced by high-fat-high-cholesterol diet in Macaca mulatta. *Experimental biology and medicine* **2012**, *237*, 1310-1321.
64. Ratner, R.E. Controlling postprandial hyperglycemia. *The American journal of cardiology* **2001**, *88*, 26-31.
65. Zisman, A.; Peroni, O.D.; Abel, E.D.; Michael, M.D.; Mauvais-Jarvis, F.; Lowell, B.B.; Wojtaszewski, J.F.; Hirshman, M.F.; Virkamaki, A.; Goodyear, L.J. Targeted disruption of the glucose transporter 4 selectively in muscle causes insulin resistance and glucose intolerance. *Nature medicine* **2000**, *6*, 924.
66. Kamel, M.A.; Helmy, M.H.; Hanafi, M.Y.; Mahmoud, S.A.; Elfetooh, H.A.; Badr, M.S. Maternal obesity and malnutrition in rats differentially affect glucose sensing in the muscles and adipose tissues in the offspring. *Int J Biochem Res Rev* **2014**, *4*, 440-469.
67. Yang, H.-W.; Son, M.; Choi, J.; Oh, S.; Jeon, Y.-J.; Byun, K.; Ryu, B. Effect of Ishophloroglucin A, A Component of Ishige okamurae, on Glucose Homeostasis in the Pancreas and Muscle of High Fat Diet-Fed Mice. *Marine Drugs* **2019**, *17*, 608.
68. Lee, S.-H.; Choi, J.-I.; Heo, S.-J.; Park, M.-H.; Park, P.-J.; Jeon, B.-T.; Kim, S.-K.; Han, J.-S.; Jeon, Y.-J. Diphlorethohydroxycarmalol isolated from Pae (Ishige okamurae) protects high glucose-induced damage in RINm5F pancreatic β cells via its antioxidant effects. *Food Science and*

Biotechnology **2012**, *21*, 239-246.

69. Adamopoulos, P.N.; Papamichael, C.M.; Zampelas, A.; Moulopoulos, S.D. Cholesterol and unsaturated fat diets influence lipid and glucose concentrations in rats. *Comparative Biochemistry and Physiology Part B: Biochemistry and Molecular Biology* **1996**, *113*, 659-663.
70. Herman, M.A.; Kahn, B.B. Glucose transport and sensing in the maintenance of glucose homeostasis and metabolic harmony. *The Journal of clinical investigation* **2006**, *116*, 1767-1775.
71. J Morgan, B.; Yeen Chai, S.; L Albiston, A. GLUT4 associated proteins as therapeutic targets for diabetes. *Recent patents on endocrine, metabolic & immune drug discovery* **2011**, *5*, 25-32.
72. Tan, Z.; Zhou, L.-J.; Mu, P.-W.; Liu, S.-P.; Chen, S.-J.; Fu, X.-D.; Wang, T.-H. Caveolin-3 is involved in the protection of resveratrol against high-fat-diet-induced insulin resistance by promoting GLUT4 translocation to the plasma membrane in skeletal muscle of ovariectomized rats. *The Journal of nutritional biochemistry* **2012**, *23*, 1716-1724.
73. Schultze, S.M.; Hemmings, B.A.; Niessen, M.; Tschopp, O. PI3K/AKT, MAPK and AMPK signalling: protein kinases in glucose homeostasis. *Expert reviews in molecular medicine* **2012**, *14*.
74. Takaguri, A.; Inoue, S.; Kubo, T.; Satoh, K. AMPK activation by prolonged stimulation with interleukin-1β contributes to the promotion of GLUT4 translocation in skeletal muscle cells. *Cell biology international* **2016**, *40*, 1204-1211.
75. Williams, S.Y.; Renquist, B.J. High throughput danio rerio energy expenditure assay. *JoVE (Journal of Visualized Experiments)* **2016**, e53297.
76. Ebashi, S.; Endo, M.; Ohtsuki, I. Control of muscle contraction. *Quarterly reviews of biophysics* **1969**, *2*, 351-384.
77. HATAKENAKA, M.; OHTSUKI, I. Effect of removal and reconstitution of troponins C and I on the Ca2+-activated tension development of single glycerinated rabbit skeletal muscle fibers. *European journal of biochemistry* **1992**, *205*, 985-993.
78. Kotas, M.E.; Medzhitov, R. Homeostasis, inflammation, and disease susceptibility. *Cell* **2015**, *160*, 816-827.
79. Keesey, R.E.; Powley, T.L. Body energy homeostasis. *Appetite* **2008**, *51*, 442-445.
80. Raney, M.A.; Turcotte, L.P. Evidence for the involvement of CaMKII and AMPK in Ca2+-dependent signaling pathways regulating FA uptake and oxidation in contracting rodent muscle. *Journal of applied physiology* **2008**, *104*, 1366-1373.
81. Hardie, D.G.; Ross, F.A.; Hawley, S.A. AMPK: a nutrient and energy sensor that maintains energy homeostasis. *Nature reviews Molecular cell biology* **2012**, *13*, 251.
82. Cantó, C.; Gerhart-Hines, Z.; Feige, J.N.; Lagouge, M.; Noriega, L.; Milne, J.C.; Elliott, P.J.;

Puigserver, P.; Auwerx, J. AMPK regulates energy expenditure by modulating NAD+ metabolism and SIRT1 activity. *Nature* **2009**, *458*, 1056.

83. Wright, D.C.; Geiger, P.C.; Holloszy, J.O.; Han, D.-H. Contraction-and hypoxia-stimulated glucose transport is mediated by a Ca2+-dependent mechanism in slow-twitch rat soleus muscle. *American Journal of Physiology-Endocrinology and Metabolism* **2005**, *288*, E1062-E1066.
84. Szentesi, P.; Zaremba, R.; Van Mechelen, W.; Stienen, G. ATP utilization for calcium uptake and force production in different types of human skeletal muscle fibres. *The Journal of Physiology* **2001**, *531*, 393-403.
85. Lee, K.M.; Yang, S.-J.; Kim, Y.D.; Choi, Y.D.; Nam, J.H.; Choi, C.S.; Choi, H.-S.; Park, C.-S. Disruption of the cereblon gene enhances hepatic AMPK activity and prevents high-fat diet–induced obesity and insulin resistance in mice. *Diabetes* **2013**, *62*, 1855-1864.
86. Galińska-Rakoczy, A.; Engel, P.; Xu, C.; Jung, H.; Craig, R.; Tobacman, L.S.; Lehman, W. Structural basis for the regulation of muscle contraction by troponin and tropomyosin. *Journal of molecular biology* **2008**, *379*, 929-935.

ACKNOWLEDGEMENT

석사, 박사 과정을 큰 문제 없이 결실을 얻을 수 있게 도와주신 모든 분의 관심과 도움에 대한 표현을 이 자리를 빌어 감사의 말씀을 드리고자 합니다. 부족한 저에게 관심을 주시고 연구의 길을 걸을 수 있도록 이끌어주셔서 3년이라는 박사 과정을 마치고 본 논문이 있기까지 세심한 가르침과 사랑을 주신 전유진 교수님께 진심으로 감사드립니다. 언제나 긍정적이고 밝은 미소로 맞이해주시는 교수님이 계셔서 제가 자신이 없어 안될 것 같던 일도 교수님이 주시는 관심과 사랑으로 모든 일을 이겨 낼 수 있었습니다. 진심으로 감사드립니다. 그리고 대학원 기간 동안 전공적인 지식과 조언을 해주셔서 논문이 좀 더 나은 방향으로 나갈 수 있게 도와주신 송춘복 교수님, 최광식 교수님, 이제희 교수님, 허문수 교수님, 여인규 교수님, 이경준 교수님, 정준범 교수님, 김기영 교수님, 이승헌 교수님, 정석근 교수님, 박상률 교수님께 감사드립니다.

제가 실험실 생활을 잘 해나갈 수 있게 이끌어주시고 아낌없는 조언과 응원을 해주신 해양생물자원이용공학 연구실, 관심과 격려로 많은 힘을 주시는 허수진 선배님, 연구 관련으로 좋은 결과를 얻을 수 있게 도와주시고 응원해주시는 김길남 선배님, 아낌없는 조언과 언제나 도와주시는 안긴내 선배님, 제브라피쉬 실험에

있어 문제점을 도와주시고 해결해주시는 차선희 선배님, 잘 할 수 있을 것이라고 응원해주시는 이승홍 선배님, 멀리 캐나다에서 응원해주시는 강성명 선배님, 김아름다슬 선배님, 처음 세포실험 가르쳐주시고 여러 조언을 해주시는 고석천 선배님, 항상 제게 도움을 주는 좋은 말과 아낌없는 응원을 해주시는 이원우 선배님, 조언과 격려를 아끼지 않으시는 강민철 선배님, 생소한 분야에 어려움이 있을 때마다 알려주시는 이지혁 선배님, 고주영 선배님, 갑작스런 연락에도 도움을 주시는 고창익 선배님, 아무 말 없이 도와주시는 오재영 선배님, 실험에 고민을 해결해주시고 잘 챙겨주시는 김은아 선배님, 강나래 선배님, 불평없이 도와주는 김현수 선배님, 지칠 때마다 도와주고 제 편이 되어준 김서영 선배님, 연구하고 실험실 생활하는데 있어 언제나 잘하고 있다고 응원해주시는 류보미 박사님, 갑자기 물어봐도 세심하게 도와주시는 김영상 박사님, 사소한 고민도 잘 들어주는 은이언니, 매번 모르게 도와주는 윤택오빠, 언니지만 친구같이 늘 도와주는 히루니, 저를 잘 따라주고 많은 일을 도와주는 고마운 효근이, 준건이, 진이, 예지, 늘 걱정해주시고 도와주시려는 선희선생님, 유경선생님, 한국 생활 잘 적응하며 다방면으로 도움을 주는 왕뢰, 산지와, 위린, 윤페이, 유안, 틸리나, 시닝, 디넷 이 모든 연구실 식구들께 감사드립니다.

매일 늦게 들어가는 날에도 불구하고 뜬 눈으로 기다려주시고 아낌없이 많은 사랑과 쓰러지지 않도록 밀어주시는 우리 아빠, 엄마 사랑합니다. 항상 나를 먼저 생각해주는 나보다 언니 같은 하나뿐인 동생 지원이에게 사랑하는 마음을 전합니다. 다시 한번 저를 지금까지 지켜봐주시고 응원해주신 모든 분들께 감사하고 고마운 마음을 전합니다. 사랑합니다.